REPORT DOCUMENTATION PAGE

Form Approved
OMB No. 0704-0188

1. REPORT DATE *(DD-MM-YYYY)*	**2. REPORT TYPE**	**3. DATES COVERED** *(From - To)*
30 April 2015	Conference Proceedings	30 Sep 2014 – 31 Mar 2015

4. TITLE AND SUBTITLE
Mid-Infrared Optoelectronics: Materials and Devices. MIOMD-XII

5a. CONTRACT NUMBER

5b. GRANT NUMBER
FA9550-14-1-0237

5c. PROGRAM ELEMENT NUMBER
61101F

6. AUTHOR(S)
Dr. Alexei Baranov

5d. PROJECT NUMBER

5e. TASK NUMBER

5f. WORK UNIT NUMBER

7. PERFORMING ORGANIZATION NAME(S) AND ADDRESS(ES)
Centre National de la Recherche Scientifique
CNRS MOY1300
Languedoc Roussillon
1919, route de Mende
Montpellier 34000 France

8. PERFORMING ORGANIZATION REPORT NUMBER
111681

9. SPONSORING / MONITORING AGENCY NAME(S) AND ADDRESS(ES)
EOARD
Unit 4515
APO AE 09421-4515

10. SPONSOR/MONITOR'S ACRONYM(S)
AFRL/AFOSR/IOE (EOARD)

11. SPONSOR/MONITOR'S REPORT NUMBER(S)
AFRL-AFOSR-UK-PC-2015-0009

12. DISTRIBUTION / AVAILABILITY STATEMENT
Distribution A: Approved for public release; distribution is unlimited.

13. SUPPLEMENTARY NOTES

14. ABSTRACT
The international conference on Infrared Optoelectronics: Materials and Devices (MIOMD) has been established in 1996. The MIOMD-XII conference took place in Montpellier (France) on 5-9 October 2014. The scope of the conference included all aspects of infrared technology from the near-IR to THz. The conference was open by a keynote paper devoted to the 20th anniversary of the quantum cascade laser and presented by one of its inventors – Jerome Faist. The main attention was paid to IR and THz emitters - interband and quantum cascade lasers and novel types sources of IR radiation. Recent advances in IR materials, photodetectors, sensors and applications have been discussed in other sessions. The papers were submitted by researchers representing 107 scientific and industrial institutions from 22 countries, 110 delegates participated in the conference. The U.S. have been represented by such scientific centers as AFRL (Albuquerque, NM), NRL (Washington, DC), JPL (Pasadena, CA), NWU (Evanston, IL), as well as a number of other universities and laboratories.

15. SUBJECT TERMS
EOARD, Interband and intersubband physics, of infrared optoelectronic devices, IR Lasers

16. SECURITY CLASSIFICATION OF:			**17. LIMITATION OF ABSTRACT**	**18. NUMBER OF PAGES**	**19a. NAME OF RESPONSIBLE PERSON**
					John Gonglewski
a. REPORT	**b. ABSTRACT**	**c. THIS PAGE**	SAR	130	**19b. TELEPHONE NUMBER** *(include area code)*
UNCLAS	UNCLAS	UNCLAS			011-44-1895616007

Standard Form 298 (Rev. 8-98)
Prescribed by ANSI Std. Z39.18

Foreword

Welcome to the 12th "Mid-Infrared Optoelectronics: Materials and Devices" (MIOMD-XII) conference in Montpellier, France!

The Mid-Infrared Optoelectronics Materials and Devices (MIOMD) conference series has been established in 1996 with a first conference organized in Lancaster. MIOMD is now held on a bi-annual basis and rotates between Europe, America and Asia. The last three conferences were held in Freiburg (2008), Shanghai (2010) and Chicago (2012).

The conference brings together researchers and scientists from all over the World working in the area of mid-infrared optoelectronics, from materials to applications. It covers all aspects of materials (theory, growth, property), optoelectronic devices (lasers, LEDs, photodetectors, modelling, fabrication, characterization) as well as practical applications (sensing, imaging, defense and security applications…). Last years the scope of the conference has been enlarged compared with its first editions and includes now all aspects of infrared technology from near-IR to THz.

This issue of MIOMD is a very special one. Indeed, exactly 20 years ago, in 1994, a new mid-infrared semiconductor laser, the quantum cascade laser (QCL), was invented in the group of F. Capasso at Bell labs. One of the co-inventors, **Prof. Jérôme Faist**, now with ETH Zurich, will open the scientific sessions of MIOMD-XII with a keynote presentation on "20 years of Quantum-Cascade Lasers".

In addition, a total of 16 invited talks, ~40 contributed oral papers and ~30 posters will be presented during the three days of the conference, from Monday 6th October to Wednesday 8th October. We are confident that you will find a lot of interesting papers and that active discussion will take place as usual. We wish to express our sincere gratitude to the members of Scientific Committee for their support. They invested an important amount of their time selecting invited speakers and reviewing abstracts.

Several social events have also been planned. A welcome reception will be offered on Sunday 5th October evening while the conference dinner will take place on Tuesday 7th October in a superb estate. In addition, guided visits of Montpellier or of a vineyard will be possible on Wednesday 8th October afternoon. Finally, a special full-day excursion will be proposed on Thursday 9th October. It will take you to the Pont du Gard, a stunning Roman aqueduct, and to Nîmes, a rich heritage city.

We want to particularly thank the *Agglomération de Montpellier, Région Languedoc-Roussillon, the OPTITEC cluster, the French National Research Agency* and the European Union for their support, as well as our sponsors and exhibitors. Last but not least, we also wish to thank our colleagues of the local-arrangement committee who made it possible to practically happen.

We hope you have a very rewarding and enjoyable conference in the shiny city of Montpellier!

Alexei N. Baranov
Conference Chair

Eric Tournié
Conference Chair

Thierry Taliercio
Program Chair

Aurore Vicet
Local Committee Chair

General information

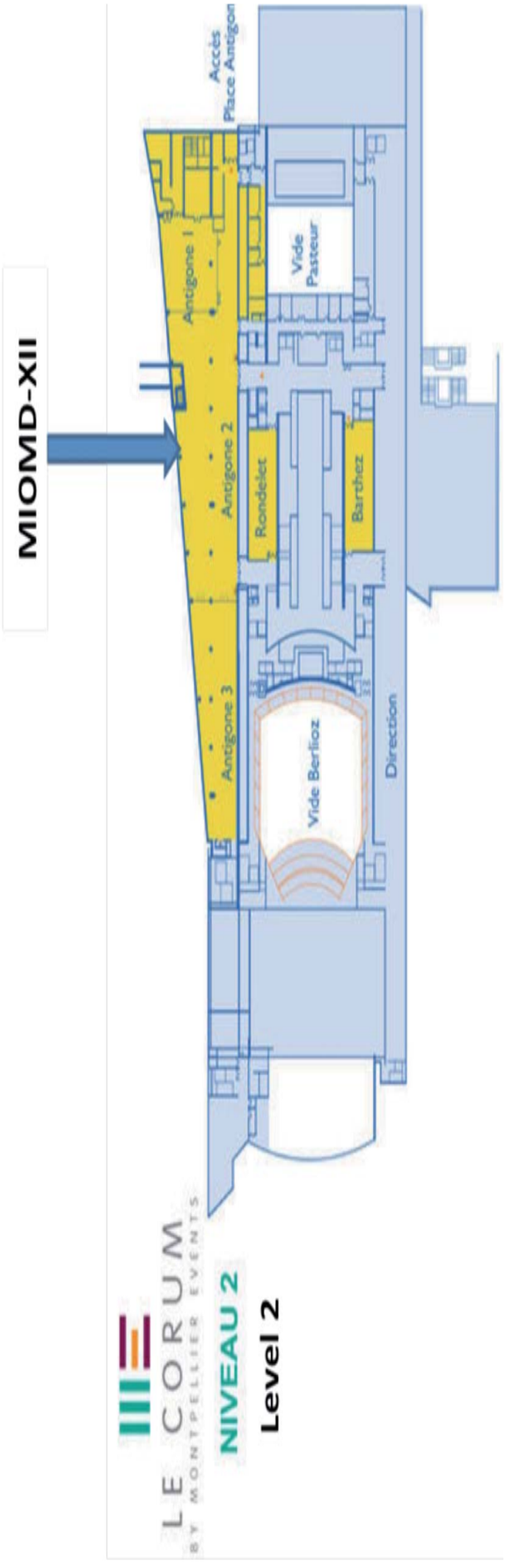

The conference will take place in Corum, the congress center of Montpellier. The entrance to *Corum* is on the side of the building (on the left side when coming from *"Place de la Comédie"*, on the right side when coming from tramway stop *"Corum"*). The entrance is on level 1 of *Corum*.

All MIOMD-XII events (Welcome reception, coffee breaks, lunches, oral sessions, poster session) will take place in ***Espace Antigone***, located on level 2 of Corum.

Instruction to authors

ORAL PRESENTATIONS

The time allotted to each oral presentation will be:

- **Keynote presentation: 1 hour (including discussion)**
- **Invited talks : 30 min. (including discussion)**
- **Contributed papers : 20 min. (including discussion)**

LCD projectors and conference PCs (OS: Windows 7) are available in each room. PowerPoint 2010, and Acrobat Reader are installed on the PCs. Therefore, presenters are recommended to bring a Windows 7 compatible Adobe pdf file or a power point file on memory stick or CD. Please upload in a folder labeled your session number and check your presentation on the conference PC in advance, preferably the day before your session. Please use your program number and your family name as the presentation file name.

It is also possible to connect your own PC to the projector, however it may not project your slide properly on the screen if the screen resolution of your PC does not match to the conference projector. We recommend you to connect your PC and check your presentation on the screen in advance, preferably the day before your session. Do not forget to bring your own conversion cable if you use PC with HDMI interface, Apple PC, and so on.

POSTER PRESENTATIONS

The poster session will take place on Monday 6th October, from 17:20 to 19:30. The posters have to be displayed before Monday 6th October, 17:00. They can be left on display till Tuesday 7th October.

The poster boards are consecutively numbered, and presenters are requested to post their poster according to the allotted number given in the poster session part of the program.

The size of the posters should not exceed 1.18 m x 0. 96 m.

Conference Chairs

ALEXEI BARANOV AND ERIC TOURNIÉ

• University Montpellier 2, France

PROGRAM CHAIR:

• Thierry Taliercio (University Montpellier 2, France)

PROGRAM VICE-CHAIR:

• Roland Teissier (CNRS, University Montpellier 2, France)

CONFERENCE SECRETARY:

• Anne Triaire-Pontier (University Montpellier 2, France)

SCIENTIFIC COMMITTEE

• Alf Adams (University of Surrey, UK)
• Markus-C. Amann (Technical University of Munich, Germany)
• Alexei Baranov (CNRS, University Montpellier 2, France)
• Mathieu Carras (3-5 Lab, France)
• Stephanie Haywood (University of Hull, UK)
• Eduard Hulicius (Czech Academy of Sciences)
• Ron Kaspi (Air Force Research Laboratory, USA)
• Abraham Katzir (Tel Aviv University, Israel)
• Anthony Krier (Lancaster University, UK)
• Aizhen Li (SIMIT Shanghai, P.R.China)
• Hao-Hsiung Lin (National Taiwan University)
• Tariq Manzur (NAVAIR, USA)
• Jerry Meyer (Naval Research Laboratory, USA)
• Maya Mikhailova (Ioffe Institute, Russia)
• Manabu Mitsuhara (NTT, Japan)
• Konstantin Moiseev (Ioffe Institute, Russia)
• Manijeh Razeghi (Northwestern University, USA)
• Stephen Sweeney (University of Surrey, UK)
• Carlo Sirtori (University Paris Diderot, France)
• Gunther Springholz (University of Linz, Austria)
• Robert Suris (Ioffe Institute, Russia)
• Frank Tittel (Rice University, USA)
• Eric Tournié (University Montpellier 2, France)
• Joachim Wagner (Fraunhofer-Institut für Angewandte Festkörperphysik, Germany)
• Yury P. Yakovlev (Ioffe Institute, Russia)
• Yong-Gang Zhang (SIMIT of CAS, Shanghai, China)

LOCAL ORGANIZING COMMITTEE

• Aurore Vicet (University Montpellier 2, France) - Chair
• Jean-Marc Aniel (CNRS, University Montpellier 2, France)
• Michael Bahriz (University Montpellier 2, France)
• Laurent Cerutti (University Montpellier 2, France)
• Jean-Baptiste Rodriguez (CNRS, University Montpellier 2, France)

Sponsors and exhibitors

• RIBER

RIBER is the world's leading supplier of MBE equipment to the compound semiconductor Industry and Research Laboratories. RIBER offers the largest range of MBE reactor platforms and components adapted to the advanced compounds semiconductors and on the forefront innovative ones. Our success is enabled by our long and constant collaborations with the world leading research laboratories and institutions.

• IQE

IQE is the leading global supplier of advanced wafer products that cover a diverse range of applications. The group offers the industry's broadest product portfolio, with a choice of technology platforms from multiple, global manufacturing facilities across Europe, Asia and the USA. With a pedigree dating back more than twenty years, IQE offers unparalleled experience in the production and supply of substrates and epiwafers across a number of key market areas including visible and infrared optoelectronic materials, multi-junction CPV solar cells and RF components for wireless applications.

The Company is able to provide a 'one stop shop' for the wafer needs of the world's leading compound semiconductor manufacturers, who in turn use these wafers to make the devices which form the key components of virtually every high technology system.

IQE has established a leading position in the global wireless sector for applications including: mobile handsets (smartphones); wifi devices; global positioning; and satellite communications. The group also boasts extensive experience in optoelectronic applications including: visible and infrared materials for sensing; communications; optical storage; printing and imaging; high efficiency LEDs; and advanced solar cells (CPV: concentrator photovoltaics).

• Norsk Elektro Optikk

The company's wide expertise in electro optics allows us to undertake a wide range of research and development tasks. Our main areas of interest are, however, applications involving various spectroscopic techniques, the use of lasers, in particular diode lasers, and the use of digital (CCD) cameras, both single line and two dimensional cameras.

Sponsors and exhibitors

• MIRIFISENS

MIRIFISENS is a FP7 Integrated project funded by the European Commission addressing the main bottlenecks in the development of mid-infrared (MIR) sources, being the range of tuneability, the footprint, power consumption and wallplug efficiency, taking in consideration cost and versatility. These aspects are covered bringing major technological advancements in the field of miniaturisation, process development, heterogeneous integration and co-integration of MOEMS functionalities applied to Quantum Cascade Laser (QCL) devices.

In the MIR region, the availability of Quantum Cascade Lasers (QCL) covering a broad portion of the spectral range (MIR, 3-12 µm), where many chemicals of interest for Safety & Security have their strongest absorption lines, has recently pushed forward the commercialisation of TDLS-based detection units. The final goal is to develop QCL-based sources enabling Tunable Diode Laser Spectroscopy (TDLS) technique, which has been identified to be the most attractive sensing solution due to the unique adsorption spectrum of chemicals, allowing their unambiguous detection. The major technologic achievements proposed will address the issues of sensitivity & selectivity, multi-gas capabilities, compactness, efficiency and cost effectiveness as specified by a number of selected Safety & Security applications. These achievements will be tested and validated for these applications. MIRIFISENS will deliver a new class of sensors with superior tuneability, better portability and extended detection capabilities, changing radically the current landscape of MIR chemical sensing spectroscopy.

Sponsors and exhibitors

• OPTITEC

OPTITEC The OPTITEC Competiveness Cluster has historically been focused on complex systems in optics and imaging, in particular for applications in hazardous environments. The Cluster's strategy has a three-fold aim:

- To predict and support technological breakthroughs in the sector with the aim of acquiring markets with high potential in the medium and long term.
- To increase the economic development of the sector, by opening towards other fields and attracting new competencies.
- To achieve recognition as a major cluster at European and international level

• ANR

• Université Montpellier 2

• Institut d'Electronique

• Union Européenne

• Région LR

• Direction Générale de l'Armement

• Air Force Office of Scientific Research

• École Nationale Supérieure de Techniques Avancées

PROGRAM

Monday, 6 October

Mo-A

Mid-IR sources: QCL & QWs

8:00-10:00

20 years of quantum cascade lasers (keynote)

Jerome Faist[1]*

[1] Institute for Quantum Electronics,ETH Zürich,8093 Zürich, Switzerland
*corresponding author: Jerome.faist@phys.ethz.ch

20 years after its first demonstration[1] and more than 40 years after the first proposal of Kazarinov and Suris[2], the quantum cascade laser has established itself both scientifically and technologically. A large body of research aims at improving the high power operation (5 W and more), low dissipation (<1W electrical) as well as attempts a leveraging on the possibilities broadband gain offers for spectroscopy of multicomponent species.

Recently, we have shown that such broadband devices, when operated in continuous wave, emit as a coherent optical comb[3] in which the phase relation between the comb modes corresponds approximately to a FM modulated laser. By combining a Maxwell-Bloch equations and a modal decomposition, the nature of this mode-locking has been elucidated, and traced back to the combination of four-wave mixing with the ultrafast non-linearities of the active medium4. These new comb lasers enables the fabrication of a dual comb spectrometer based on a quantum cascade laser that offers a broadband, all solid-state spectrometer with no moving parts and a ultrafast acquisition time. We demonstrate a spectrometer with a frequency span of 15cm^{-1} and a resolution better than 80MHz by a fine tuning of the combs and its first proof-of-principle applications on the measurement of water vapor[5]. We discuss also the extension of these ideas to the THz, where mode-locking[6] as well as comb operation[7] has been recently reported, as well as recent spectroscopy and noise characterisations of the combs. In particular, we recently demonstrated optical gain over more than a decade of frequency[8], opening the potential of fully self-referenced combs in the THz.

[1] J. FAIST, F. CAPASSO, D. SIVCO, C. SIRTORI, A. HUTCHINSON AND A. CHO, SCIENCE 264 (5158), 553-556 (1994).
[2] R. KAZARINOV AND R. SURIS, SOVIET PHYSICS - SEMICONDUCTORS 6 (1), 120-134 (1972).
[3] A. HUGI, G. VILLARES, S. BLASER, H. C. LIU AND J. FAIST, NATURE 492 (7428), 229-233 (2012).
[4] J. B. KHURGIN, Y. DIKMELIK, A. HUGI AND J. FAIST, APPLIED PHYSICS LETTERS 104 (8), 081118 (2014).
[5] G. VILLARES, A. HUGI, J. FAIST AND S. BLASER, NATURE COMMUNICATIONS (IN PRINT) (2014).
[6] S. BARBIERI, M. RAVARO, P. GELLIE, G. SANTARELLI, C. MANQUEST, C. SIRTORI, S. P. KHANNA, E. H. LINFIELD AND
A. G. DAVIES, NATURE PHOTONICS 5 (5), 306-313 (2011).
[7] D. BURGHOFF, T.-Y. KAO, N. HAN, C. W. I. CHAN, X. CAI, Y. YANG, D. J. HAYTON, J.-R. GAO, J. L. RENO AND
Q. HU, NATURE PHOTONICS, 1-6 (2014).
[8] M. RÖSCH, G. SCALARI, M. BECK AND J. FAIST, ARXIV.ORG PHYSICS.OPTICS (2014).

RT THz sources by DFG in mid-IR QCLs (invited)

S. Slivken[1], Q. Y. Lu[1], Y. Bai[1], N. Bandyopadhyay[1], M. Razeghi[1]*

[1] Center for Quantum Devices, Electrical Engineering and Computer Science Department, Northwestern University, Evanston, IL, USA

*corresponding author: s-slivken@northwestern.edu

The quantum cascade laser (QCL) platform provides a pretty amazing toolbox for realizing novel physics and device capabilities. Band structure engineering allows control over electron transport, the electron-phonon interaction, and linear/ non-linear optical gain. It seems that every year there are exciting new demonstrations in such areas as mode locking, beam shaping, electrical tuning of emission, and even room temperature (RT) terahertz (THz) emission.

THz sources can be very useful for a variety of applications in physics, astronomy, materials engineering, chemistry, and life sciences. Though such devices have been around for a very long time, they have not been very convenient, requiring either large systems, cryogenic cooling, and/or very high speed components. Applications requiring narrow linewidths (like heterodyne detection) add further system overhead.

To overcome these obstacles and maintain a compact and convenient device, we are concentrating on mechanisms for RT THz emission using the QCL platform. The current design utilizes a high power, dual wavelength QCL with an engineered giant nonlinear susceptibility which enables difference frequency generation (DFG) within the laser cavity. THz generation occurs with proper transverse mode control and phase matching conditions, which can lead to very large THz powers. In pulsed mode, up to 1.6 mW at RT has been demonstrated at a frequency of 3.6 THz. Additionally, by focusing effort on mid-IR efficiency and heat dissipation, we have recently obtained the first continuous wave (CW) THz emission at RT with power output up to 3 µW.[1] We are currently looking for new ways to increase device efficiency and increase the collected output power.

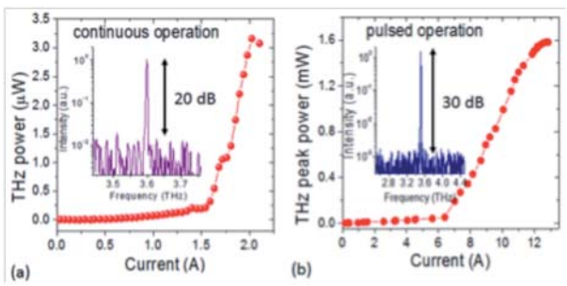

Fig.1. (a) Power-current relationship for a THz source in continuous operation at room temperature. (b) Power-current relationship for a high peak power THz source at room temperature. Inset of both figures shows the emitting spectrum and background-limited side mode suppression ratio.

While these demonstrations were done at a single wavelength, we previously demonstrated very wide THz (1- 4.6 THz) spectral coverage by altering the mid-IR pump laser frequency discretely.[2] Recent efforts by our group to develop tunable mid-IR lasers [3] indicate that a similar architecture may be used to dynamically adjust the THz source pump frequencies and create large shifts in the THz emission. This can enable electrical tuning over several THz at RT.

[1] Q. Y. LU, N. BANDYOPADHYAY, S. SLIVKEN, Y. BAI, AND M. RAZEGHI, APPL. PHYS. LETT. 104, 221105 (2014)

[2] Q. Y. LU, N. BANDYOPADHYAY, S. SLIVKEN, Y. BAI, AND M. RAZEGHI, APPL. PHYS. LETT. 101, 251121 (2012)

[3] S. SLIVKEN, N. BANDYOPADHYAY, Y. BAI, Q. Y. LU, AND M. RAZEGHI, APPL. PHYS. LETT. 103, 231110 (2013)

Mid-IR Semiconductor Lasers for Space (invited)

S. Forouhar,[1] C. Borgentun,[1] C. Frez,[1] R. Briggs,[1] M. Bagheri[1], C. R. Webster, C. L. Canedy,[2] C. S. Kim,[2] M. Kim,[3] W. W. Bewley,[2] C. D. Merritt,[2] J. Abell,[2] I. Vurgaftman,[2] and J. R. Meyer[2]*

[1] Jet Propulsion Laboratory, California Institute of Technology, Pasadena, California 91109, USA.

[2] Naval Research Laboratory, Washington, DC 20375, USA.

[3] Sotera Defense Solutions, Inc., Columbia MD 21046 USA.

*corresponding author: siamak.forouhar@jpl.nasa.gov

Infrared tunable laser spectroscopy is a direct, non-invasive, high sensitivity, ultra high resolution method of measuring molecular gas abundances and isotope ratios, determined by measuring the light absorption in a fixed path-length in a sample cell of measured pressure and temperature. Because the IR laser scans over several rotational-vibrational lines of the target gas, a unique fingerprint pattern is observed to unambiguously identify the molecular gas responsible for the absorption lines. Laser sources are chosen that can scan a small region of a molecular vibrational band chosen to have well-separated lines of multiple isotopic species.

Following the success of the Tunable Laser Spectrometer (TLS) [1-2] aboard the Mars Science Laboratory (MSL) Curiosity rover, laser-based spectroscopy instruments are likely to play an important role in future planetary science missions. The TLS is a powerful instrument that can make precise measurements of gas abundances and their isotope ratios not only in planetary atmospheres but also in gases evolved from in-situ processing of rock or soil samples – as demonstrated on MSL's Curiosity rover.

The availability of low power consumption mid-IR semiconductor lasers enable the generation of compact, mid-infrared (mid-IR) TLS with reduced complexity, and significantly reduced development cost compared to the current system on MSL. These performance improvements will enable the instrument to have more measurement channels and allowing more target gases of interest to be studied. In particular these advances will open a pathway for use of mid-IR TLSs in power-limited platforms such as payloads on landers and balloons.

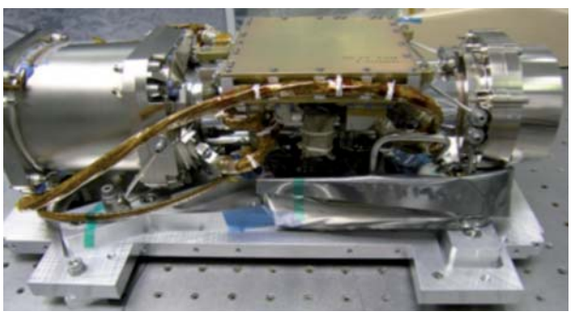

Fig. 1: Photograph of TLS flight hardware as implemented on SAM-MSL

In this presentation, we report on our accomplishments developing high wall plug efficiency diode, interband and quantum cascade lasers operating above room temperature in the mid-IR spectral region enabling the next generation of miniature, low-power TDLs for planetary, earth atmosphere and environmental monitoring within the spacecraft.

[1] CHRISTOPHER R. WEBSTER, SCIENCE 19 JULY 2013: VOL. 341 NO. 6143 PP. 260-263

[2] CHRISTOPHER R. WEBSTER , PAUL R. MAHAFFY, SUSHIL K. ATREYA, GREGORY J. FLESCH, KENNETH A. FARLEY, SCIENCE 18 OCTOBER 2013: VOL. 342 NO. 6156 PP. 355-357

Monday, 6 October

Mo-B

Mid-IR sources: Lasers I

10:30-12:40

Mid-IR laser sources for spectroscopic sensing – from research to market (invited)

J. Koeth[1], M. von Edlinger[1], J. Scheuermann[1], L. Nähle[1], M. Fischer[1], R. Weih[2], M. Kamp[2]*

[1]nanoplus GmbH, Nanosystems and Technologies
97218 Gerbrunn, Germany
[2] Technische Physik and Wilhelm-Konrad-Röntgen-Research-Center for Complex Material Systems, Universität Würzburg 97074 Würzburg, Germany
*corresponding author: koeth@nanoplus.com

The use of laser sources in gas sensing applications has been increasing continuously in recent years. Tunable laser absorption spectroscopy (TLAS) has proven to be a versatile tool in a variety of sectors including industry, health & security and modern environmental analysis. The mid-infrared wavelength region, especially between 3 and 6 µm, is of high interest for spectroscopic sensing applications. Interband Cascade Lasers (ICL) can provide continuous wave operation throughout this wavelength range. This paper reviews the history of this laser concept and presents recent developments. Application examples in industry and research are highlighted.

In recent years the importance of tunable laser sources for spectroscopic sensing applications has been increasing continuously. TLAS offers several advantages compared to other gas sensing concepts, as for example detection limits down to the parts per billion level and the possibility for real-time analysis. Many industrially relevant gas species have their fundamental absorption bands in the mid-infrared wavelength region, especially between 3 and 6 µm. These include important hydrocarbons (like methane) as well as nitric oxide or formaldehyde. Thus, this area is of high interest for spectroscopic sensing applications. The ICL concept [1-2] is a particular promising approach providing application grade laser performance in this wavelength range. Being in some ways a hybrid technology between the interband-transition diode laser and the intraband-transition quantum cascade laser, this concept combines high efficiency through cascading of optically active areas with uncomplicated adjustment of the emission wavelength while retaining low operating voltages.

Mono mode laser sources are crucial for TLAS based sensors. We fabricated distributed feedback (DFB) ICLs operating CW up to 80 °C with wavelength tuning ranges around 22 nm. These devices can e.g. be used in industrial process control like combustion monitoring or on-line detection of toxic gases. The low power consumption of ICL based devices makes them especially favorable for battery-powered or portable sensors.

[1] R. Q. YANG, SUPERLATT. MICROSTRUCT. 17(1), 77-83 (1995).
[2] I. VURGAFTMAN, W. W. BEWLEY C. L. CANEDY, ET AL., NATURE COMMUNICATIONS 2, 585 (2011).

Highly Strained (2.2%) 3.2µm GaSb QW Lasers

T.C. Newell[1], R. Kaspi[1], C. Lu[1], C. Yang[1], S. Luong[1] and D. Gianardi[1]*

[1]Air Force Research Laboratory/ Directed Energy Directorate Albuquerque, New Mexico, 87117 USA
*corresponding author: tcnewell@iCloud.com

It is a challenge to develop >3µm GaSb-based Type-I quantum well diode lasers due to the diminishing hole confinement barrier. Laser power decreases rapidly once the wavelength exceeds 3µm. Two approaches have been investigated to mitigate this loss. The first is to utilize quinary AlGaInAsSb barriers, which improves the hole offset due to the addition of InAs which decreases the valence band energy [1,2]. A second approach is to compressively strain the QWs by adding Antimony into the InGaAsSb QW [2]. The valence band offset increases with the strain.Compressive strain also splits the degeneracy between the heavy and light holes modifying the density of states to reduce the carrier density required to reach transparency.

We push the strain limit beyond that found in the literature by developing highly strained InGaAsSb QWs with AlGaInAsSb quinary barriers. QW lasers with up to 2.2% compressive strain have been grown and tested. Such devices would ordinarily relax because they will exceed the Matthews-Blakesee limit[3]. To prevent this from occurring we incorporate a small tensile strain in the portion of the quinary waveguide prior to the growth of the QWs to provide strain compensation to the QWs.

The general laser design incorporates three $In_{0.56}Ga_{0.44}As_{1-y}Sb_y$ QWs grown in a $Al_{0.2}Ga_{0.55}In_{0.25}As_{1-y}Sb_y$ waveguide that is clad with $Al_{0.9}Ga_{0.1}As_{0.07}Sb_{0.93}$. The composition of the QW and waveguide/barrier is adjusted to create compressive or tensile strain. X-ray diffraction (004 Ω/2θ) analysis shows that QWs are coherently strained with up to ~1.9% without strain compensation, while strain relaxation occurs in wellswith additional antimony. In contrast, tensile strain compensation in the quinarywaveguide can be used to maintain higher compressive strain in the quantum wells, as shown in the x-ray spectra in Figure 1.

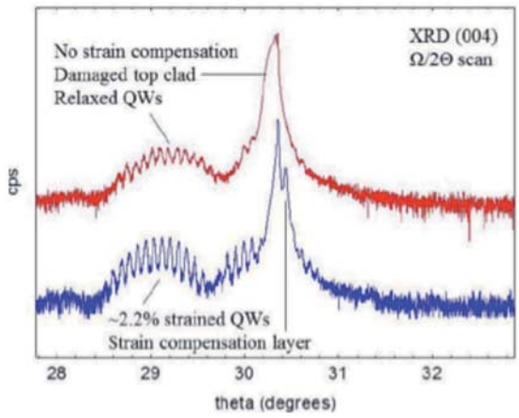

Fig. 1. Rocking curves of a 2.2% coherently strained 3-QW structure (lower trace) with tensile compensated barriers and a relaxed structure (upper trace) that did not incorporate strain compensation.

Material is processed into broad area lasers and initially tested epitaxial-side-up in short pulse (400ns) low duty cycle (<1.5%) mode. Figure 2 shows the total power of three different as-cleaved lasers with 1.5% strain, 1.9% strain and 2.2% strained QWs grown with strain compensation. The lasing wavelength is near 3.2µm. There is an improvement in both threshold and slope efficiency as the strain increases. We attribute this improvement to the increase in hole QW depth. In the talk we will present our exploration of strain, quinary barriers, and digital alloy growth on the pulse and CW lasing performance of λ>3.2µm lasers.

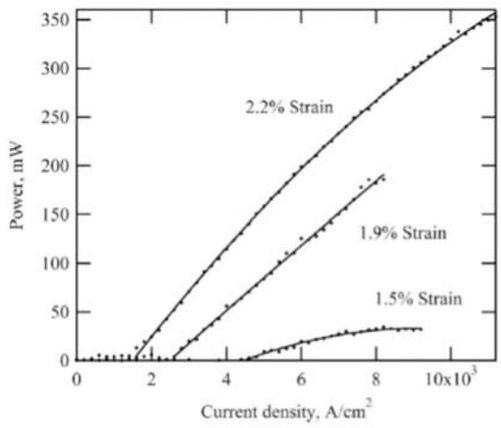

Fig. 2. Total peak power from as-cleaved broad area lasers each possessing different coherent strain. Test conditions are 400ns pulses and 0.4% duty cycle at 5C.

[1] M. GRAU, C. LIN, O. DIER, C. LAUER, AND M.-C.AMANN, APPL. PHYS. LETT. 87, 241104 (2005).

[2]G. BELENKY, L SHTERENGAS, G. KIPSHIDZE, AND T. HOSODA, IEEE J. SELECT. TOP. QUANT. ELECTRON, VOL. 17(5), PP. 1426-1434 (2011).

[3] J.W. MATTHEWS AND A.E. BLAKESLEE, J. CRYST. GROWTH 27, 118 (1974).

InP-based type-II heterostructure lasers for 2.7 µm wavelength

S. Sprengel[1], G. K. Veerabathran[1], A. Koeninger[1], G. Boehm[1] and M.-C. Amann[1]*

[1]Walter Schottky Institut, Technische Universitaet Muenchen, Am Coulombwall 4, 85748 Garching, Germany
*corresponding author: Stephan.Sprengel@wsi.tum.de

Type-II light sources on InP substrate are an innovative concept for wavelengths ranging from 2 µm to the mid-IR. The concept is using the type-II band alignment between GaInAs and GaAsSb to exceed the limitation of type-I devices (2.3µm). First InP type-II heterostructure lasers with increased wavelength were demonstrated in 2012 with lasing wavelengths up to 2.5 µm. Here we report InP-based type-II lasers at 2.7 µm with threshold current densities extrapolated to infinite length of 223 A/cm^2 per quantum well in pulsed mode at 15°C. Lasers could be operated up to 70°C in pulsed mode. Semiconductor lasers for the wavelength range from 2 to 4 µm are up to now mainly type-I lasers on GaSb substrate and interband cascade lasers based on GaSb or InAs. For a long time the technologically more mature InP-based lasers were limited to 2.3 µm [1] due to epitaxial strain limitations. The type-II concept overcomes this limitation by using the type-II band alignment between GaInAs and GaAsSb (see Figure 1).

Fig.1. Photoluminescence spectra of different InP-based W-shaped QWs. Room temperature emission up to 3.9 µm is demonstrated. Spectra show a full width half

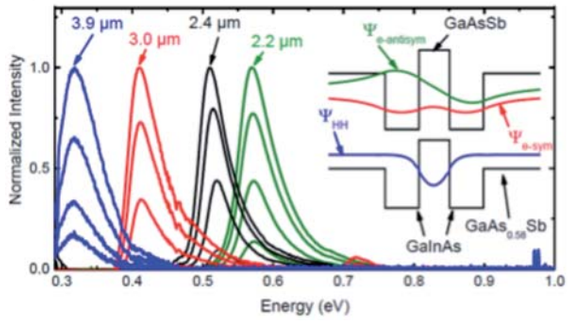

maximum of only 30 to 50 meV. Insert shows W-shaped band structure. Wave functions are indicated.

These materials are arranged in a way that they form a W-shaped band alignment, permitting transition energies lower than the bandgap of both layers and a narrow gain spectrum [2]. We demonstrate up to 3.9 µm emission wavelength using W-shaped quantum wells (QW) grown on InP substrate, (see Figure 1). In 2012 first InP-based type-II lasers exceeding 2.3 µm have been demonstrated [3] with a wavelength of 2.5 µm.

Lasers demonstrated here have a symmetric waveguide, made of Al0.2GaAsSb, in which three W-shaped QWs are implemented, together with electron and hole blocking layers on p- and n-side, respectively. The schematic band structure is

depicted in Figure 2. The emission wavelength of the lasers is 2.7 µm, which is to our knowledge the longest wavelength demonstrated for interband lasing on InP up to now. The threshold current density extrapolated to infinite length at 15°C is 223 A/cm^2.

Fig. 2. Left: Schematic band structure of an InP type-II laser, injection directions for electrons and holes are indicated. Right: Threshold current densities plotted against

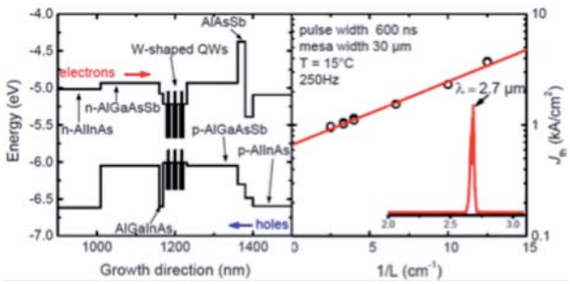

inverse laser length. Threshold current density extrapolated to infinite length is 668 A/cm2 corresponding to 223 A/cm2 per QW. Insert shows laser spectrum at 2.7 µm measured at 17°C in pulsed mode.

Lasers could even be operated up to 70°C in pulsed mode, which is a considerable improvement compared 42°C demonstrated previously [3]. Due to the good laser results and the mature process technology of InP, W-shaped QWs are becoming a more and more promising concept for edge and surface emitting lasers further in the infrared.

[1] G. BÖHM, M. GRAU, ET AL., J. CRYST. GROWTH, 301, 941 (2007).
[2] S. SPRENGEL, C. GRASSE, ET AL., IEEE J. SELECT. TOP. QUANTUM. ELECTRON., 19 1900909 (2013).
[3] S. SPRENGEL, A. ANDREJEW, ET AL., APPL. PHYS. LETT., 100, 041109 (2012).

Optimizing the active region of interband cascade lasers

G. Sęk[1], K. Ryczko[1], M. Motyka[1], F. Janiak[1], M. Dyksik[1], J. Misiewicz[1], R. Weih[2], M. Dallner[2], S. Höfling[2,3], M. Kamp[2]*

[1]Institute of Physics, Wrocław University of Technology, Wrocław, Poland
[2]Technische Physik, University of Würzburg, Würzburg, Germany
[3]School of Physics and Astronomy, University of St. Andrews, St. Andrews, United Kingdom
*corresponding author: grzegorz.sek@pwr.edu.pl

Applications related to the detection of hazardous and environmentally-relevant gasses drive the growing demands with respect to all the sensor system components, requiring cheap and compact laser sources. This can be well fulfilled by semiconductor lasers, where one of the efficient solutions is interband cascade laser (ICL). Such devices have already been proven to emit at some wavelengths of the mid-infrared (to beyond 10 µm even), i.e. in ranges characteristic for maximal absorption of many gasses, and shown to offer continuous wave single mode operation at room temperature between 3 and 5 µm, and additionally significantly lower power consumption [1] than the more common quantum cascade lasers. However, ICLs still need further developments regarding especially the demanded performances at longer wavelengths, broad bandwidth or widely tuneable devices. We have investigated, both experimentally and theoretically, several modifications in the active region of the ICLs. The considered structures are based on InAs/(Ga,In)(As,Sb) materials forming a broken gap system, i.e. confining electrons and holes in spatially separate layers. The lasers are usually grown on either GaSb or InAs substrates. Our study is aimed at maximizing the optical transition oscillator strength (OS) via tailoring the electronic structure, the related strain and wave function engineering. OS is the most critical parameter of the type II system because it can allow for compensating the intrinsic losses while extending the emission wavelength or the gain bandwidth. We will cover such issues as variation of compositions and thicknesses, importance of the band offsets, the active transition intensity and external factors as temperature or electric field, and finally the predominant carrier loss mechanisms. A combination of two spectroscopic techniques is used, emission-like (photoluminescence) and absorption-like (modulated reflectivity) supported by the energy level calculations employing multiband k·p modelling. We demonstrate that addition of arsenic into the commonly used ternary layer of GaInSb for the holes confinement can significantly enhance the transition oscillator strength, while decreasing the overall strain and keeping still the type II design [2,3]. There is also investigated the use of a triple type II quantum well structure instead of a commonly used double well “W-design”. This allows for simultaneous red shift of the transitions and increase of the oscillator strength. Eventually, further structure optimizations utilizing uncommon material combinations will be discussed.

[1] I. VURGAFTMAN ET AL., NATURE COMMUN. 2, 585 (2011).
[2] F. JANIAK ET AL., APPL. PHYS. LETT. 100, 231908 (2012).
[3] K. RYCZKO, ET AL., J. APPL. PHYS. 114, 223519 (2013).

Gain and Spectral Tuning of Mid-infrared Type II InSb/InAs Quantum Dot Laser Diodes

Q. Lu[1], Q. Zhuang[1] and A. Krier[1]*

[1]Physics Department, Lancaster University, Lancaster, LA1 4YB, UK
*corresponding author: q.lu3@lancaster.ac.uk

The mid-infrared spectral range is technologically important for a variety of applications including gas sensing, optical spectroscopy, bio-medical diagnostics etc. Although type II InSb/InAs QDs have shown electroluminescence up to room temperature and are a promising candidate for diode lasers at wavelengths longer than 3 µm [1], there have been only a few reports of InSb QD lasers [2]. In this work, we demonstrate coherent emission from InSb QDs at wavelengths between 3.02 µm and 3.11 µm at temperature, Tmax up to 120 K using pulsed excitation, with a threshold current density, Jth~1.6 kA cm^{-2} at 4 K. The gain and spectral tuning behaviour were also determined.

We developed a hybrid laser structure containing ten sheets of sub-monolayer InSb QDs in an InAs waveguide sandwiched between a p-$InAs_{0.61}Sb_{0.13}P_{0.26}$ lower cladding layer grown by liquid phase epitaxy and an n+ -InAs plasmonic upper cladding layer grown by MBE. Fig. 1 shows the Jth vs 1/L plot from which the gain of the resulting InSb/InAs QD ridge lasers was estimated based on the relationship between threshold current and cavity length (L). The modal gain of the laser was extracted from the slope of the linear fit, which results in a value of 29 cm^{-1}, (or 2.9 cm^{-1} per InSb QD layer), which is close to that found in type II QW lasers emitting at similar wavelengths. The material gain was estimated to be 19 x10^4 cm^{-1}, which is in the same range as that for type I QDs.

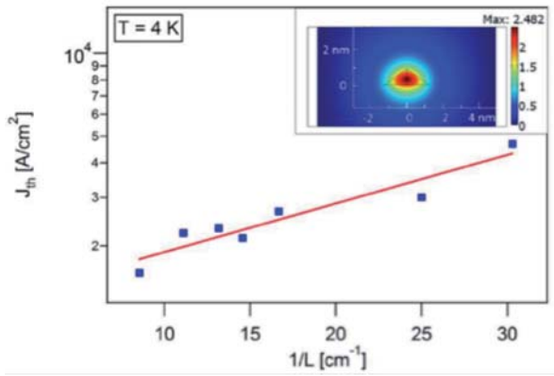

Fig.1. Jth vs 1/L plot of the InSb QD laser diodes at 4 K. The red line shows the linear fit between ln(Jth) and 1/L. The inset shows the central cross section and the ground state heavy hole wave function of a single InSb QD assuming a conical shape.

Previous k.p modeling is in agreement with TEM measurements which confirm that the QDs are approximately 0.9 nm in height and 2.5 nm in diameter, with a density of 10^{12} cm^{-2} [3]. Only holes are confined within the InSb QDs, while electrons exist in the InAs matrix. The heavy hole ground state wave function is shown in the inset of Fig. 1 from which the electron-hole wave function overlap can be estimated to be about 41%. The characteristic temperature (T0) is 101 K in the lower temperature range (T<50 K) but drops to 48 K at higher temperatures, consistent with thermal excitation of the holes out of the QDs. The emission spectrum also changes with temperature at constant current injection. The peak of the laser spectrum shifts to shorter wavelength with increasing temperature when T<50 K. For T>50 K, the peak moves to longer wavelength as temperature increases, as shown in Fig. 2. This phenomenon is caused by the Fermi-Dirac distribution of holes within the InSb QDs ensemble which have a Gaussian size distribution.

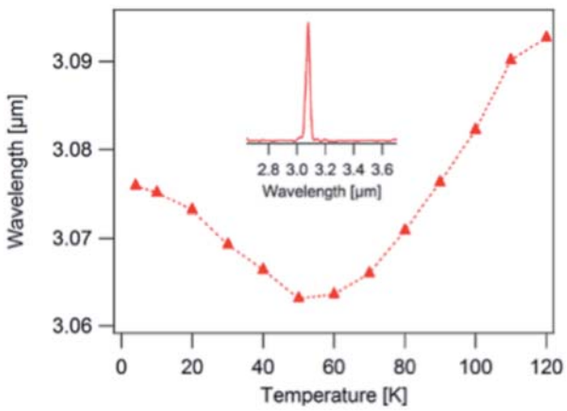

Fig.2. Peak wavelength of the laser emission envelope measured at different temperatures, using 8.0 A 100 ns pulse current injection. The inset shows the emission spectrum at 4 K.

Acknowledgement: This work was supported by the European Marie Curie Initial Training Network PROPHET, (grant No. 264687).

[1] P. J. CARRINGTON, V. A. SOLOV'EV, Q. ZHUANG, A. KRIER, AND S. V. IVANOV, APPL. PHYS. LETT. 93, 091101 (2008).
[2] V.A. SOLOV, I. V SEDOVA, O.G. LYUBLINSKAYA, A.N. SEMENOV, B.Y. MEL, S. V SOROKIN, Y. V TERENT, AND S. V IVANOV, 31, 235 (2005).
[3] G. YEAP, S. RYBCHENKO, I. ITSKEVICH, AND S.K. HAYWOOD, PHYS. REV. B 79, 075305 (2009).

Progress on Simulations and Applications of THz and Mid Infrared (TERA-MIR) Radiation

*M. F. Pereira[1]**

[1]Materials and Engineering Research Institute, Sheffield Hallam University, S1 1WB Sheffield United Kingdom
*corresponding author: m.pereira@shu.ac.uk

In this presentation, I start by briefly outlining the main goals and recent achievements of COST ACTION MP1204 [1],whose main objectives are to advance novel materials, concepts and device designs for generating and detecting THz and Mid Infrared radiation using semiconductor, superconductor, metamaterials and lasers and to beneficially exploit their common aspects within a synergetic approach. We use the unique networking and capacity-building capabilities provided by the COST framework to unify these two spectral domains from their common aspects of sources, detectors, materials and applications. We are creating a platform to investigate interdisciplinary topics in Physics, Electrical Engineering and Technology, Applied Chemistry, Materials Sciences and Biology and Radio Astronomy. The main emphasis is on new fundamental material properties, concepts and device designs that are likely to open the way to new products or to the exploitation of new technologies in the fields of sensing, healthcare, biology, and industrial applications. End users are: research centres, academic, well-established and start-up Companies and hospitals.

Next, I summarize my recent progress in different topics of modeling materials for this range. I start with effective three dimensional anisotropic materials with new expressions for the nonlinear absorption, gain and luminescence of semiconductor superlattices described as anisotropic media. Next the superlattices are fully described in the case of Quantum Cascade Lasers (QCLs) and preliminary results of a cooperation between two teams of COST MP1204, which will lead to the new state of the art QCL simulators are outlined. Solutions for intersubband lasing without inversion using dilute nitride materials are also discussed. The final part of the talk is dedicated to the coupling of light in a microcavity with intersubband excitations considering both intervalence THz transitions [2] and dispersive gain in dilute nitrides.

Research Supported by COST ACTION MP1204: TERA-MIR Radiation: Materials, Generation, Detection and Applications.

[1] M.F. PEREIRA, TERA-MIR RADIATION: MATERIALS, GENERATION, DETECTION AND APPLICATIONS, OPT QUANT ELECTRON, 46, PP. 491–493 (2014).

[2] M. F. PEREIRA JR. AND I.A. FARAGAI, COUPLING OF THZ RADIATION WITH INTERVALENCE BAND TRANSITIONS IN MICROCAVITIES OPTICS EXPRESS, VOL. 22 ISSUE 3, PP.3439-3446 (2014).

Monday, 6 October

Mo-C

QCLs & applications

13:40-15:40

Photonic engineering in terahertz quantum cascade lasers (invited)

Gangyi Xu[1,2,], Yacine Halioua[1], Raffaele Colombelli[1], Lianhe Li[3], Edmund H. Linfield[3], A. Giles Davies[3], Harvey Beere[4], David A. Ritchie[4]*

[1]Institut d'Electronique Fondamentale, Univ. Paris Sud, UMR8622 CNRS, France
[2]Key laboratory of Infrared Imaging Materials and Detectors, Shanghai Institute of Technical Physics, Chinese Academy of Sciences, Shanghai 200083, China
[3]School of Electronic and Electrical Engineering, University of Leeds, Leeds LS2 9JT, UK
[4]Cavendish Laboratory, University of Cambridge, Cambridge, UK
*corresponding author: gangyi.xu@mail.sitp.ac.cn

Significant efforts of photonic engineering have been devoted to terahertz quantum cascade lasers (THz-QCLs) to improve their emission beam quality and power efficiency. To date, coherent single lobed emission with reduced divergence has been obtained in edge- or surface-emitting lasers by using 1D (DFB) or 2D photonic crystals (PhC) as resonators. However, the efficient power extraction of these devices remains a crucial issue.

In surface-emitting THz-QCLs, the fundamental reason of low power efficiency relates to the EM field symmetry of the lasing mode. Lasers naturally operate on the "non-radiative" mode, rather than the "radiative" mode. The former exhibits antisymmetric distribution of the in-plane magnetic field (H//), resulting in low total loss with very low power efficiency. The later shows symmetric H//, which gives rise to relatively high total loss and significantly enhanced power efficiency.

In this paper, we present a novel concept to excite the fundamental radiative mode in second-order distributed-feedback (DFB) surface-emitting THz-QCLs, which leads to high power efficiencies [1]. A 1D graded photonic heterostructure (1D GPH) resonator, in which the grating period decreases regularly from the center to the end of ridge (Fig. 1), is implemented to confine the radiative mode in the center of the resonator and to simultaneously push the non-radiative mode to the lossy boundary. Such architecture reverses the natural mode competition in the second-order DFB lasers, and selectively excites the radiative mode. Judicious design of the 1D GPH resonators allows significantly enhanced power efficiencies without obvious degradation of laser threshold and operation temperature. The GPH lasers feature single-mode emissions with low-divergence single-lobed emission patterns, and exhibit continuous-wave (CW) output power in the tens of milliwatt range [2].

In order to further reduce the beam divergence and improve the output power, we have successfully realized the phase-locked arrays of 1D GPH lasers (Fig. 2), and have realized 2D GPH lasers. The details will be presented in the conference.

[1] G. XU, R. COLOMBELLI, S. P. KHANNA, A. BELAROUCI, X. LETARTRE, L. H. LI, E. H. LINFIELD, A. G. DAVIES, H. E. BEERE, D. A. RITCHIE, NATURE COMMUN. 3, 952 (2012).
[2] G. XU, L. H. LI, N. ISAC, Y. HALIOUA, A. G. DAVIES, E. H. LINFIELD, R. COLOMBELLI, APPL. PHYS. LETT. 104, 091112 (2014).

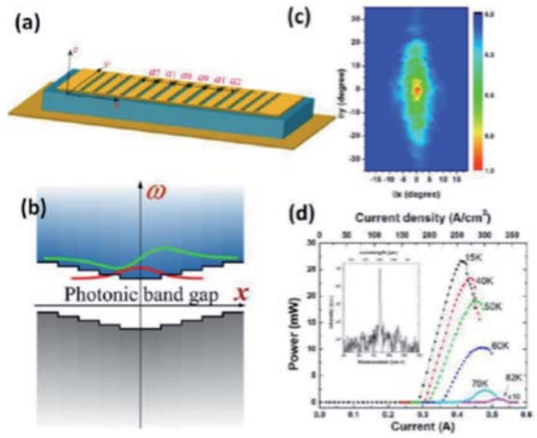

Fig.1. (a) Schematic illustration of a surface-emitting terahertz QCL with a 1D GPH resonator. The lattice spacing (ai) of top metallic grating gradually decreases from the center to each end of the laser ridge. (b) Schematic real-space photonic band diagram of the device. The radiative modes are confined in the center of ridge, whereas the non-radiative modes are delocalized into the lossy boundaries. (c) and (d), Far-field emission pattern, light-current, and spectral characteristics of a typical GPH laser.

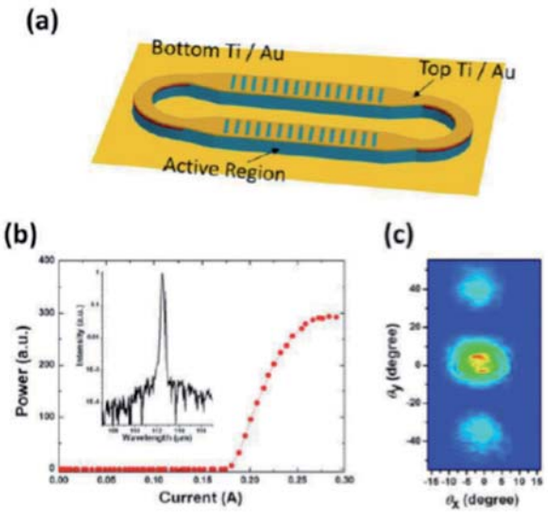

Fig.2. (a) Schematic figure of a phase-locked array containing two identical GPH lasers embedded in a ring resonator. (b) Light-current, and spectral characteristics of an array measured at low temperature. (c) Far-field pattern of the array which indicates that the two GPH lasers are in-phase locked.

Characterization of external cavity quantum cascade laser based NICE-OHMS system

R. Centeno[1], J. Mandon[1], S. M. Cristescu[1], F. J. M. Harren[1]*

[1]Life Science Trace Gas Facility, IMM, Radboud University Nijmegen Heyendaalseweg 135, 6525 AJ Nijmegen, The Netherlands
*corresponding author: r.centeno@science.ru.nl

Abstract: The development of a widely, continuously tunable and mode-hop-free External Cavity Quantum Cascade Laser (EC-QCL) for the detection of medically relevant molecules in combination with Noise-Immune Cavity Enhanced Optical Heterodyne Molecular Spectroscopy (NICE-OHMS) is discussed. Several key issues concerning the development of the laser and its combination with the spectroscopic technique are presented to achieve fast detection and high spectral resolution.

Noise-Immune Cavity Enhanced Optical Heterodyne Molecular Spectroscopy (NICE-OHMS) is an ultrasensitive detection method with sensitivities of 1 x 10^{-14} cm^{-1} in the near infrared (NIR) for sub-Doppler resolution molecular spectroscopy. To advance this technique into the mid infrared, we use EC-QCLs, which are attractive sources for the development of non-invasive and compact gas sensors.

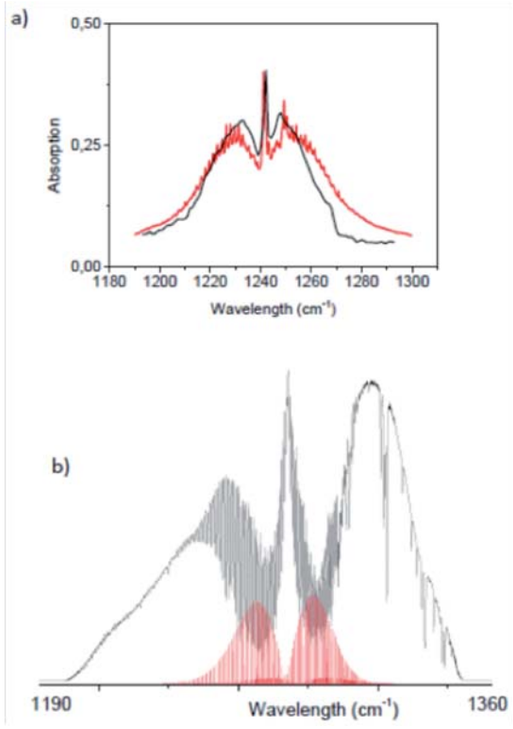

Fig.1: The EC-QCL offers two modes: 1) Fast scanning mode, where it is possible to record broadband spectra of complex molecules and 2) high resolution mode. Panel (a) represents simulated (in red, PNNL) and measured (in black) spectra of 1% ethanol with a recording time of 20 s. Panel (b) shows simulated (red, HITRAN) and measured spectra of 100 ppm nitrous oxide (black) with a recording time of 2 min.

The EC-QCL offers a broadband emission gain between 6.9 and 8.8 µm in the Littrow configuration and achieves a tuning of over 300 cm^{-1} by rotating the grating (138 grooves/mm) to select a single longitudinal mode (<0.001 cm-1) with an average output power of 100 mW. To avoid mode-hops during the scan, a tracking system has been developed to achieve a current maximum of 0.5 cm^{-1} mode-hop free tuning. The laser is suitable for the measurement of molecules with both broadband and small absorption features. Fig. 1a shows the spectrum of ethanol measured at a pressure of 1 atm, with an absorption pathlength of 20 cm and a concentration of 1%. The recording time of the spectrum was 20 s. By increasing the recording time up to a few minutes, the full spectral region can be scanned at high resolution for molecules such as nitrous oxide (N_2O) (Fig. 1b). Here, the concentration was 100 ppm with a resolution of 0.01 cm-1 at otherwise identical conditions.

To achieve high sensitivities, we combined this EC-QCL with the NICE-OHMS technique. The laser frequency is locked to a Fabry–Perot cavity with a finesse of 1500 containing the analyzed gas by direct modulation of the laser current at 20 MHz. An additional modulation at the free spectral range of the cavity (~300 MHz) was applied to achieve noise immunity. We demonstrate this combination for the first time and the first results concerning the performance of the spectrometer, the presence of residual amplitude modulation and the considerations for the EC-QCL are presented. Ongoing research is focused on the detection of hydrogen peroxide (H_2O_2) as an indicator of chronic obstructive pulmonary disease (COPD) in human lungs.

Experimental and theoretical study of the gain saturation in MIR QCL

Virginie Trinite[1], Simon Ferre[1], Louise Jumpertz[1], Gregory Maisons[1], Mathieu Carras[1], Guy-Mael De Naurois[2] Tobias Mansipur[2], Federico Capasso[2]*

[1]III-VGIE 3-5 Lab,91767 Palaiseau cedex
[2]School of Engineering and Applied Sciences Harvard University,Cambridge MA 021138
*corresponding author: virginie.trinite@thalesgoup.com

Introduction

Many domains of applications for Quantum Cascade Laser (QCL) require high performances : high power output and high wall plug efficiency (WPE). For better performances and higher power output, it is important to understand how the gain saturate in presence of photon in the cavity. In fact if we don't take into account photons in the laser cavity, the gain of the medium will vary linearly with current. However, the interaction with the optical wave in the laser cavity changes the distribution of electronic densities on the laser levels and reduce the population's inversion and so the gain. This saturation of the gain can be easily modelized in a 3 level model and gives a rational function:

$$G = G_0 1/(1 + P/P_{sat}) \quad (1)$$

where P is the optical power and 1/Psat is called the saturation of the gain. We will present an experimental determination of Psat and it comparison with theoretical prediction.

Experimental Measurement of the gain and Fabry Perot amplifier model

We have measured the net-gain in a QCL by injecting a DFB laser in a Fabry-perot laser made of the same active region as in [7]. The Fabry-perot laser is driven under pulsed mode. During the time of the pulsed the laser heat up, so that its optical index vary in time. We can then measure the rapid variation in the output power due to Fabry-perot optical mode. The contrast of this fringe give us direct access to the gain of the laser. We can also change the number of photon in the Fabry-perot laser by changing the input optical power coming from the DFB, and so deduce the saturation.

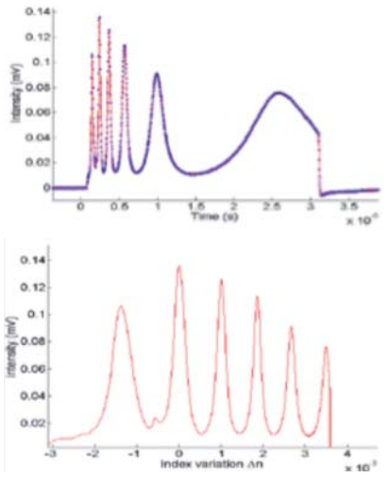

Figure 1: Example of evolution of the output power signal versus time and its conversion in index variation.

Modelisation

We have also analyzed the experimental results with a more sophisticated tools, based on semi-classical Boltzmann-like equation [1-2]. For this model we assume thermalised carrier distribution in each subband, so that only the global population of the subbands enter in balance rate equations. We can take into account various types of scattering mechanisms, including stimulated emission and absorption of photons. We have extended this model to take into account tunneling transport across the injection barrier as in [6]. This type of modeling, without adjustable parameters based on microscopic quantum description of the scattering from state to state, are very a ppealing because it enable predictive calculation of the current-voltage characteristic [6]. With this model we have also a direct access to the gain as the independent sum of contributions of each couple of states:

$$G(\hbar\omega) = \sum_{(i,j)} \frac{\pi e^2 \left|\langle \phi_i | z | \phi_j \rangle\right|^2}{n_{eff}\varepsilon_0 L_p c\hbar} \frac{\gamma}{2\pi} \frac{1}{(e_i - e_j \pm \hbar\omega)^2 + (\gamma/2)^2} (n_i - n_j)$$

(2)

We use an empirical broadening parameter γ, taken to be the same for all transitions, ni and nj are the population of the state ϕi and ϕj with and energy level ei and ej. Lp is the length of the period and neff is the optical index.

External parameters, (as the cavity losses) are needed for the calculation of the power, so it is interesting to be able to directly compare experimental and theoretical gain.

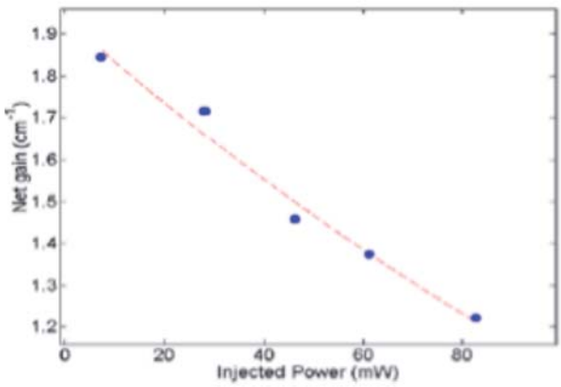

Figure 2: Experimental net gain versus the injected power. Blue point are the experimental point and red line is the fitt curve with the rational form of equation 1

The laser cavity is introduced by solving self-consistently the population of the electrons and the density of photons in the cavity [4]. For each imposed value of the number of photons we recalculate the electron distribution and the gain. After fitting the gain with the rational form of equation 1, we can deduce Psat. We obtain good agreement with the experiment.

[1] R. IOTTI AND F. ROSSI, PHYS. REV. LETT. 87, 146603 (2001)
[2] J.M. TAVISH, D.INDJIN AND P. HARRISON, J. APPL. PHYS. 99, 114505 (2006)
[3] Y. BAI, S. SLIVKEN, S. KUBOYA, S.R. DARVISH AND M. RAZEGHI, NATURE PHOTONICS 4, 99 (2010)
[4] E OUERGHEMMI, V. TRINITÉ AND J. NAGLE, "GAIN COMPRESSION AND POWER SATURATION IN QUANTUM CASCADE LASER", ITQW'09, SEPTEMBER 2009
[5] V.D. JOVANOVIC, P; HARRISON, Z. IKONIC AND D; INDJIN, J. APPL. PHYS. 96, 269 (2004)
[6] R. TERAZZI, J. FAIST, NEW JOURNAL OF PHYSICS 12 (2010)
[7] E. BENVENISTE, S. LAURENT, A. VASANELLI, C. MANQUEST, C. SIRTORI, F. TEULON, M. CARRAS AND X. MARCADET, APPL. PHYS. LETT. 94, 081110 (2009)

High performance room temperature InGaAs/AlGaAs/GaAs quantum cascade lasers

K. Pierściński[1], D. Pierścińska[1], P. Gutowski[1], P. Karbownik[1], A. Trajnerowicz[1], M.Bugajski[1]*

[1]Photonics Dept., Institute of Electron Technology, Al. Lotników 32/46, 02-668 Warsaw, Poland
*corresponding author: kamil.pierscinski@ite.waw.pl

Mid-IR QCLs can be divided into two main categories based on the material system involved, i.e. GaAs- and InP-based devices. The latter offer unquestionable advantages in terms of high temperature, CW operation. The former, however, offer performance in pulsed mode operation at room temperature, which is sufficient in many applications, e.g. absorption spectroscopy, where short pulse operation is required, in order to avoid shift of emission wavelength. Besides that, the cost and complexity of technology and fabrication is much lower for GaAs based devices. The main issue that limits high temperature performance of GaAs-based devices is low conduction band-offset, causing the electrons to escape to 3D continuum of states at elevated temperatures of active region.

There were attempts taken to increase the band offset by e.g. increasing the Al content in the barrier layers. Unfortunately, increased Al content leads to increased inter-valley scattering to X and L minima and consequently to decreased laser performance.

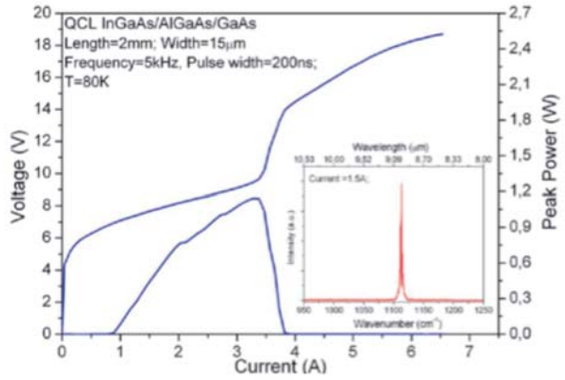

Fig.1. Low temperature (80 K) light-current-voltage characteristic of mid-IR InGaAs/AlGaAs/GaAs QCL. Inset shows emission spectrum registered at 80 K.

In this work we report on the design, realization and characterization of a mid-IR QCLs, based on InGaAs/AlGaAs/GaAs structures grown by molecular beam epitaxy. Devices exhibit performance largely improved over standard AlGaAs/GaAs QCLs. Reduction of threshold current density at 80 K by a factor of 2.4 was observed. Lasing at 9 μm was achieved in the pulse mode up to T = 40°C. Devices showed good thermal performance with characteristic temperature T0 = 120 K.

Various experimental techniques were employed, in order to gain insight into the performance of investigated devices. In order to determine main device parameters (such as WPE, waveguide losses, T0), measurements of temperature dependent Light-Current-Voltage (LIV) characteristics were performed. Additionally, devices were characterized in terms of temperature behavior by means of thermoreflectance spectroscopy, thermal imaging and time resolved spectral measurements. TRS-FTIR spectroscopy provides information about the laser frequency tuning during pulse for different modes of operation.

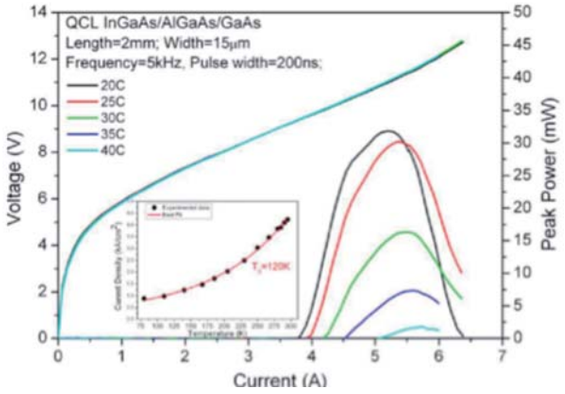

Fig.2. Light-current-voltage characteristics registered at room temperature operation with 200 ns pulses. Maximal peak power at 20C reaches 35 mW per facet. Inset presents threshold current density vs. temperature in the range from 80K to 300K. T0 determined from this data is 120K.

Room temperature operation of far infrared (λ>17 µm) quantum cascade lasers (invited)

*G. Lollia[1,2], M. Bahriz[1,2], A.N. Baranov[1,2], D. Chastanet[3], A. Bousseksou[3], R. Colombelli[3], J. Madéo[4], Y. Todorov[4], C. Sirtori[4], R. Teissier[1,2]**

[1]Université de Montpellier, IES, UMR 5214, F-34000 Montpellier, France
[2]CNRS, IES, UMR 5214, F-34000 Montpellier, France
[3]IEF, Univ. Paris Sud, UMR 8622 CNRS, Orsay, France
[4]MPQ, Univ. Paris Diderot, UMR7162 CNRS, Paris, France
*corresponding author: teissier@univ-montp2.fr

Room temperature far infrared QCLs based on InAs are reported. Different quantum designs and waveguide structures have been studied, leading to a maximum operating temperature of 353 K at λ≈20 µm. Single mode DFB lasers operating up to 333 K have also been fabricated.

In the last decade, InAs/AlSb quantum cascade lasers (QCL) have targeted the short wavelength side (λ=2.6 – 3.5 µm) of the mid-IR spectrum. Yet, they are also promising for the development of far infrared lasers thanks to the small electron effective mass in InAs and to the resulting large inter-subband optical gain. Recently we demonstrated QCLs made of InAs operating at a wavelength of 20 µm [1]. The lasers were grown by molecular beam epitaxy and processed into double metal ridge waveguides. The very low threshold current densities that have been achieved [2], as compared to GaAs and InGaAs based lasers, confirmed the assets of InAs-based devices.

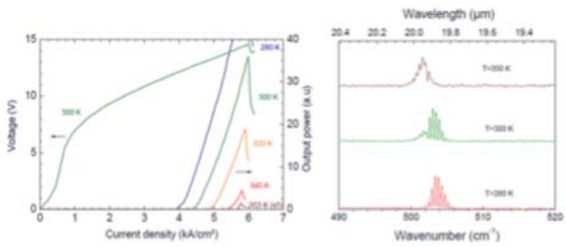

Fig.1 - VI and LI characteristics of a InAs/AlSb QCL based on a dielectric waveguide. The device dimensions are 2.92 mm x 50 µm. The data are recorded in pulse mode (100 ns / 100kHz). Right: emission spectrum at different temperatures.

In this contribution, we will report on the recent progress that we made in this domain. Different active region designs have been explored, by tuning the oscillator strength in the active quantum wells, as well as the dependence of the lasers performances on doping level and injection barrier width. We demonstrated room temperature operation, up to 333 K, at a wavelength of 18 µm with a double metal waveguide [3]. We also fabricated QCLs with a plasmon-enhanced dielectric waveguide. Thanks to the reduced optical losses, we demonstrated above room temperature operation at λ≈20 µm with a record maximum operating temperature of 80°C. Additional characterizations of these devices, such as far field or cavity length dependence measurements, will be presented.

Single mode lasers have also been fabricated, with the use of a periodic patterning of the top metal in double-metal devices. The DFB lasers achieved monomode operation over a large temperature range, from 78 K to 333 K, with a continuous tuning range of 0.38 µm [3].

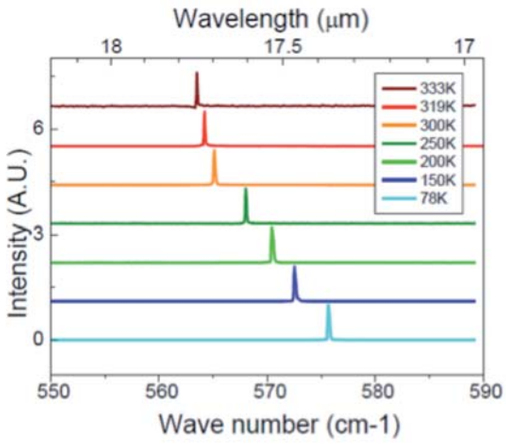

Fig.2. Emission spectra in pulsed regime of a DFB InAs QCL made of a double metal waveguide with top metal patterning. The laser is single mode in a large temperature range from 78 to 333 K.

This work was supported by the French Agence Nationale de la Recherche within the framework of the project DELTA (ANR 2011-NANO-020).

[1] M. BAHRIZ ,G. LOLLIA, A.N. BARANOV, P. LAFFAILLE, R. TEISSIER, ELECTRON. LETT. 49, 19, 1238, (2013)
[2] D. CHASTANET, G. LOLLIA, A. BOUSSEKSOU, M. BAHRIZ, P. LAFFAILLE,, A.N. BARANOV, F. JULIEN, R.COLOMBELLI, R. TEISSIER, APPL. PHYS. LETT. 104, 021116, (2014)
[3] D. CHASTANET, A. BOUSSEKSOU, G. LOLLIA, M. BAHRIZ, F. JULIEN, A.N. BARANOV, R.COLOMBELLI, R. TEISSIER, SUBMITTED TO APPL. PHYS. LETT.

Monday, 6 October

Mo-D

Materials for detectors

16:10-17:20

Diameter Dependent Photocurrent Response in InAsSb wires (invited)

Johannes Svensson[1],, Nicklas Anttu[2], Neimantas Vainorius[2], B. Mattias Borg[1], Lars-Erik Wernersson[1]*

[1]Electrical and Information Technology, Lund University, Box 118, SE-221 00 Lund, Sweden
[2]Solid State Physics, Lund University, Box 118, SE-221 00 Lund, Sweden
*corresponding author: johannes@eit.lth.se

We grow vertical arrays of InAs/InAsSb nanowires from Au particles on InAs or Si/InAs substrates using MOCVD. The composition is varied between InAs and InSb and the diameter is controlled by varying the Au particle density or the V/III. Photoconductors are fabricated using a simple approach with a spin coated organic spacer and evaporated Ti/Au top contacts using a shadow mask. The spectrally resolved photocurrent exhibit peaks, which are shifted towards longer wavelengths with increasing wire diameter. Absorption simulations give good agreement with the experimental data and reveals that the peaks are due to resonant HE11 waveguide modes.

[1] J. SVENSSON ET AL., NANO LETT. 13, 1380 (2013).

High Performance LWIR InAs/GaSb Superlattice Photodiodes with a Single Barrier Structure

Jianxin Chen[1], Zhicheng Xu[1], Jianzhen Pan[1], Yi Zhou[1], Fangfang Wang[1], Jiajia Xu[1], Zhizhong Bai[1], Ruijun Ding[1] and Li He[1]*

[1]Shanghai Institute of Technical Physics, Chinese Academy of Sciences 500 Yutian Road,Shanghai, 200083, China
*corresponding author: jianxinchen@mail.sitp.ac.cn

InAs/GaSb superlattices have attracted significant attentions due to their excellent properties for detection of infrared radiations [1]. An important issue for infrared photodiodes is to reduce their dark currents, especially for long wavelength infrared (LWIR) photodetectors. For that purpose, several approaches have been employed in LWIR superlattice photodetectors, including "M" structure [2], "PBIBN" structure [3] and "CBIRD" structure [4], etc.

In this paper, we will present our recent works on LWIR InAs/GaSb superlattice infrared photodiodes with a single barrier structure. We demonstrated that with optimizing the molecular beam epitaxy (MBE) growth process we can get high performance LWIR superlattice photodiode with a single barrier. The MBE process parameters were optimized at first to improve the crystalline quality. By properly tuning the growth parameters, high quality InAs/GaSb superlattice materials with sharp X-ray diffraction peaks were obtained. The full width at half maximum (FWHM) of the 0th order satellite peak is as narrow as 19". Hall Effect measurements showed that the unintentionally doped LWIR superlattice presented n-type conductivity within the temperature region from 13 K to 300K. The mobility of the superlattice was limited by interface scattering within the most temperature regions. A coherent length and roughness product $\Lambda^*\Delta$=75 Å^2 of the interfaces was extracted.

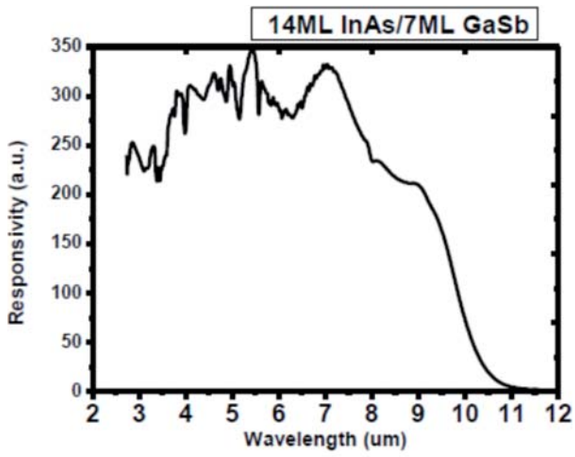

Fig.1. Response spectrum at the 14ML InAs/7ML GaSb superlattice photodiode measured at 77K. The 50% cutoff wavelength was 9.8μm.

The photodiodes have a P-I-N structure with an electron barrier inserted between the P and the I region. The I region consists of 14ML InAs/7ML GaSb, corresponding to a cutoff wavelength of about 10μm and the barrier consists of 7ML InAs/7ML GaSb. Single element photodiodes was fabricated by wet chemical etching. Fig. 1 shows the optical response spectrum of a photodiode at 77K. The 50% cutoff wavelength was measured to be 9.8μm. Fig. 2 shows the current density and differential area product of the photodiode at different biases. A dark current density of 9.1×10^{-5}A/cm^2 at -20mV was measured and the differential resistance area product was 112 Ωcm^2.

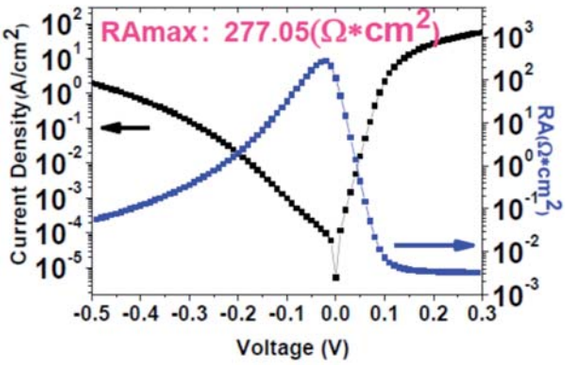

Fig.2. Dark current density and RA curves at different biases measured at 77K

[1] D. L. SMITH AND C. MAILHIOT, J. APPL. PHYS. 62, 2545 (1987).
[2] B-M NGUYEN, D. HOFFMAN, P-Y DELAUNAY, AND M. RAZEGHI, APPL. PHYS. LETT.91, 163511 (2007).
[3] E. A. DECUIR, JR., G. P. MEISSNER, ET AL, OPTICAL ENGINEERING 51, 124001 (2012).
[4] A. KHOSHAKHLAGH, L. HÖGLUND, ET AL, J. VAC. SCI. AND TECHNOL. B, 31, 03C122 (2013).

Multimaterial robust infrared chalcogenide fibers

*G. Tao[1], S. Shabahang[1], and A. F. Abouraddy[1]**

[1]CREOL, The College of Optics & Photonics, University of Central Florida 4000 Central Florida Blvd., Orlando, FL 32765, USA
*corresponding author: raddy@creol.ucf.edu

Chalcogenide fibers offer a potentially wide range of midinfrared (MIR) applications in spectroscopy, sensing, astronomy, and the generation of new coherent laser sources [1]. Chalcogenide glasses are highly transparent throughout the MIR, have high optical nonlinearities, and their physical properties are highly tailorable via compositional engineering. The mechanical brittleness of chalcogenides in general, however, make the use of such fibers challenging. Furthermore, the large chromatic dispersion of these glasses presents obstacles to the full exploitation of their nonlinearities using ultrashort pulses.

We present here several novel approaches to the fabrication of a unique class of multimaterial chalcogenide glass fibers in which a thermoplastic built-in polymer jacket provides mechanical robustness while not participating in the optical functionality, which is dictated by the chalcogenide glass itself. This approach is based on the use of multimaterial coextrusion, where a hybrid glass/polymer billet is extruded under pressure at an elevated temperature to produce a fiber preform [2]. The preform is then continuously drawn into an extended fiber using a traditional thermal fiber drawing process in an ambient environment. This set of techniques enables the fabrication of robust infrared fibers with controllable refractive index and, furthermore, facilitates control over the dimensions of the core and cladding – all in a robust form-factor (Fig. 1).

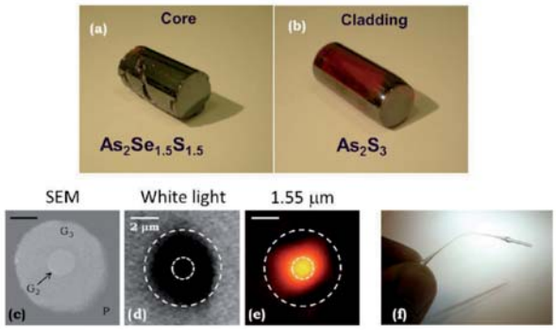

Fig.1. (a), (b) Chalcogenide glass rods used in producing the core and cladding of a high index contrast step-index fiber. (c) SEM of the cross section of the drawn fiber with a 2-micron-diameter core. G2 is the glass in (a) and G3 is the glass in (b). P is a thermoplastic polymer jacket (polyethersulfone). (d) White light transmission to highlight the cladding/jacket interface. (e) Transmitted mode using a 1.55-micron wavelength laser to highlight the core/cladding structure. The scale bars in (c)-(e) are all 2 microns. (f) A robust nano-taper produced by tapering the multimaterial fiber without removing the thermally compatible polymer jacket. The core diameter in this nano-taper is ≈ 500 nm.

Here, we focus on two realizations of multimaterial chalcogenide fibers. In the first, we describe a high refractive index contrast fiber structure for engineering a zero waveguide-dispersion wavelength in the near-infrared optimized for nonlinear applications [2]. In the second realization, we demonstrate a low index contrast tellurium-based chalcogenide fiber that offers a transparency window extending over both midwave and longwave infrared wavelengths – the first robust chalcogenide fiber of its kind [3]. Finally, we present a variation of this approach that enables the fabrication of extended fibers using only ~ 2 g of infrared glass, thereby enabling rapid prototyping of infrared fibers with minimal requirements on glass synthesis and purification, which typically are an obstacle in academic environments.

[1] G. TAO, A. M. STOLYAROV, AND A. F. ABOURADDY, I. J. APPL. GLASS SCIENCE 3, 349 (2012).
[2] G. TAO, S. SHABAHANG, E.-H. BANAEI, J. J. KAUFMAN, AND A. F. ABOURADDY, OPT. LETT. 37, 2751 (2012).
[3] G. TAO, S. SHABAHANG, H. REN, F. KHALILZADEH-REZAIE, R. E. PEALE, Z. YANG, X. WANG, AND A. F. ABOURADDY, OPT. LETT. 39, IN PRESS (2014).

Monday, 6 October

Posters session

17:20-19:30

QEPAS with electrical co-excitation in the NIR and MIR

M. Mordmueller[1], U. Willer[1], W.Schade[1,2].*

[1]Clausthal University of Technology, IEPT and EFZN,Am Stollen 19B, 38640 Goslar, Germany
[2]Fraunhofer Heinrich Hertz Institute, Am Stollen 19B, 38640 Goslar, Germany
*corresponding author: GCDente@gmail.com

A photoacoustic detection scheme based on quartz enhanced photo acoustic spectroscopy (QEPAS) is demonstrated. The tuning fork is excited by a laser induced photoacoustic wave (as usually done) and additionally by an electrically driven oscillation. If both mechanisms act simultaneously, gas absorption is measured as phase dependent sum of the photoacoustically and electrically generated signal amplitudes.
Furthermore, decay times after electrical driving of the tuning fork can be measured. If the photoacoustic excitation is applied subsequent to the electrical one, the decay time can be influenced by photoacoustic excitation, depending on gas concentration and phase between electrical and photoacoustic excitation.

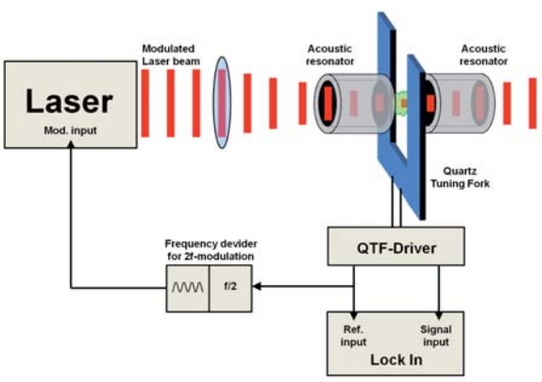

Fig. 1. Scheme of a 2f QEPAS setup with simultaneous electrical co-operation.

Quartz enhanced photo acoustic spectroscopy (QEPAS) found various application in trace gas analysis and industrial sensing since its first demonstration [1]. A typical QEPAS setup comprises a quartz tuning fork (QTF), laser source, lock-in amplifier, and frequency generator. The laser's emission wavelength is set to an absorption line of the trace gas. Since a QTF is used instead of a microphone with broad frequency response, the laser modulation frequency has to match exactly with the QTF's resonant frequency (typ. 32,768 Hz). Amongst others, the resonant frequency is affected by the gas mixture density, which can be a drawback, especially in applications with strongly changing gas compositions, since signal changes can be due to concentration changes of the trace gas to be measured or due to mismatch of modulation and resonant frequency. In this work the QTF is additionally driven by a pierce oscillator circuit, similar to those used in watches. Since this circuit automatically crops up to the applied oscillator the setup always operates at the optimal frequency. All relevant signals can be derived from the driver circuit (Fig. 1). The photoacoustic (PA) signal is obtained by phase sensitive detection or subtracting the electrical offset.
Another way to profit from the ability of electrical and PA signal coupling is applying electrical and PA excitation subsequently (Fig. 2). If the QTF is excited electrically for some time the QTF amplitude decays exponentially after the electrical excitation is switched off.

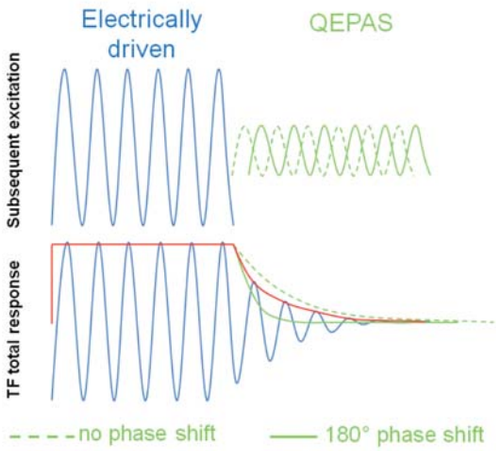

Fig. 2. Illustration of decay times for alternate electrical and photoacoustic tuning fork excitation.

The decay time can either be extended or shortened by applying QEPAS, depending on absorption strength and phase difference between electrical and PA excitation. This enables to use the decay time as measurement instead of the amplitude similar to cavity ring down spectroscopy [2].

[1] A. A. Kosterev, Y. A. Bakhirkin, R. F. Curl, F. K. Tittel, Optics Letters Vol. 27, No. 21 (2002).
[2] Berden, Giel; Engeln, Richard, Cavity ring-down spectroscopy. Techniques and applications. Chichester, U.K: Wiley (2009).

Mid-infrared polarizer with Sb-Ge-Sn-S system chalcogenide glass

Itsunari Yamada[1], Naoto Yamashita[2], Toshihiko Einishi[2], Mitsunori Saito[3], Kouhei Fukumi[4], and Junji Nishii[5]*

[1]Dept. of Electronic Systems Engineering, the University of Shiga Prefecture, Shiga, Japan
[2]Isuzu Glass Co.,ltd. Osaka, Japan
[3]Dept. of Electronics and Informatics, Ryukoku University, Seta, Otsu, Japan
[4]National Institute of Advanced Industrial Science and Technology, Osaka Japan
[5]Research Institute for Electronic Science, Hokkaido University, Sapporo Japan
*corresponding author: yamada.i@e.usp.ac.jp

A mid-infrared wire-grid polarizer with a 500-nm pitch was fabricated on a low toxic chalcogenide glass (Sb-Ge-Sn-S system) by the thermal imprinting of periodic grating followed by the thermal evaporation of Al metal. After imprinting, deposition of Al on the grating at oblique angle produced a wire-grid polarizer. The fabricated polarizer showed polarization with TM transmittance greater than 60% at 5–9 µm wavelengths and an extinction ratio greater than 20 dB.

Mid-infrared wire-grid polarizers consist of metal wires of submicron width. Current commercial infrared wire-grid polarizers become very expensive, since current fabrication process of wire-grid polarizers needs exposure, development and inductively coupled plasma reactive ion etching (RIE) processes. In this paper, we describe formation of submicron-pitch gratings directly on the surface of a Sb-Ge-Sn-S system chalcogenide glass without the toxic elements through a combination of the imprinting process and molding process, and fabricated metal grating with submicron-pitch using Al evaporation [1].

Imprinting process uses the mechanical mold stamping process to deform the resin or glass plates to duplicate the nanostructures from the mold. A silicon carbide (SiC) substrate (Adomap) was used for the mold, since SiC is much harder than Si and SiO2 at high temperature. Figure 1 shows the fabrication process. By using the two-beam interference method and RIE, the SiC mold with the subwavelength grating (500 nm period) was formed.

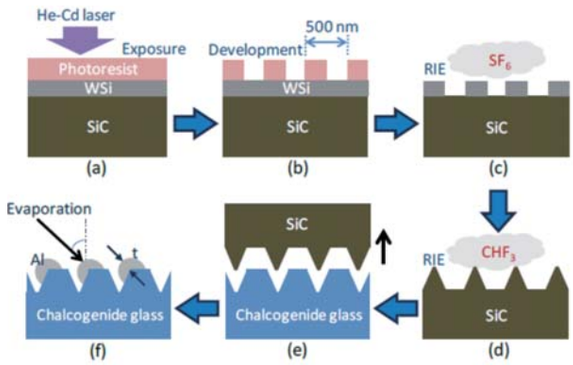

Fig. 1: Schematic illustration of the fabrication process of the wire-grid polarizer. (a) After a WSi layer is deposited on a SiC substrate using the sputtering method, a photoresist is coated onto the WSi layer, and a stripe beam of the He–Cd laser (325 nm wavelength) is irradiated by the two-beam interference method. (b) A photoresist grating is patterned by the development. (c),(d) The WSi layer and SiC are etched using the RIE. (e) One dimensional pattern on the surface of SiC mold is imprinted onto chalcogenide glass. (f) Al was deposited on the grating at an oblique angle by thermal evaporation.

Infrared glass materials have been studied to obtain wide transparency and to remove toxic elements such as As and Se. IIR-SF®1 developed and produced by Isuzu Glass Co., Ltd glass has good transmission in the 0.85–11 µm wavelength range, a refractive index of 2.7 at 10 µm wavelength, low glass transition temperature (230°C), and is a low toxic material. This glass consists mainly of sulfur (Sb-Ge-Sn-S system), and it is less expensive than germanium. The SiC mold coated with carbon and an optically polished chalcogenide glass plate were assembled using a pressing machine [Fig. 1(e)]. The imprinting temperature, pressure, and time were 253°C, 3.8 MPa, and 90 s, respectively. To fabricate the mid-infrared wire-grid polarizers, Al is selected as the wire material because it has a high extinction coefficient. Al was deposited on the grating at oblique angle by thermal evaporation [Fig. 1(f)]. Figure 2 shows the scanning electron microscope (SEM) photograph of the element coated in the Al film. Al grating thickness was 130 nm.

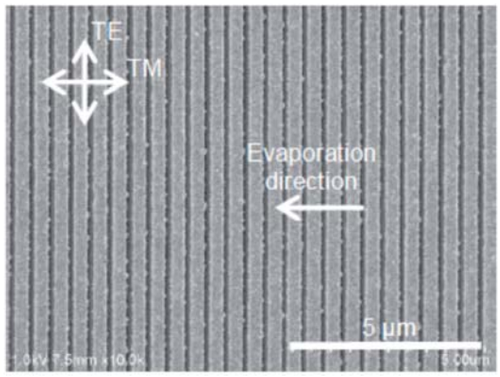

Fig. 2: SEM image of the element deposited Al film (130 nm thickness) by evaporation on the imprinted chalcogenide glass plate. The arrow direction shows evaporation direction.

The transmittance of the fabricated element was measured using a Fourier-transformation infrared spectrometer in the mid-infrared range. Figure 3 portrays transmission spectra of the fabricated element. The transverse magnetic (TM) and the transverse electric (TE) polarizations were measured. The transmittance for TM polarization was greater than 60% in the 5–9 µm wavelength range. The extinction ratio was greater than 20 dB in the 4–11 µm wavelength range. This polarizer can be fabricated at lower costs and simpler fabrication processes compared to conventional infrared polarizers.

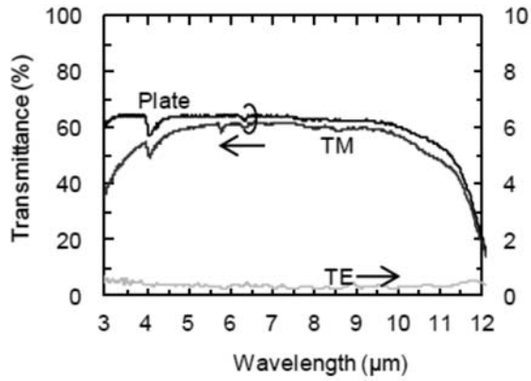

Fig. 3: Transmission spectra of the fabricated element and a chalcogenide glass substrate (2 mm thickness). TE and TM indicate the polarization directions.

[1] I. YAMADA,ET. AL., OPT. LETT., 36, 3882 (2011).

EBIC observation of $In_xGa_{1-x}As$ photodetectors with different indium contents or configurations

Y. G. Zhang[1], K. H. Liu[1], Y. Gu[1], L. Zhou[1], Hsby. Li[1], X. Y. Chen[1], A. Z. Li[1], S. P. Xi[1]*

[1]State Key Laboratory of Functional Materials for Informatics, Shanghai Institute of Mocrosystem and Information Technology, Chinese Academy of Sciences.865 Chang Ning Rd., Shanghai 200050, China
*corresponding author: ygzhang@mail.sim.ac.cn

The demands on InGaAs PDs and FPAs extending into MIR band are increasing, leading to the exploration of GSMBE growth of metamorphic structures on mismatched substrates [1].In those structures the formation defects or dislocations are almost unavoidable, which results in imperfections correlated to the device performance tightly. On the efforts to improve the material quality, an effective and convenient observation method for such imperfections is eagerly expected. Among various methods, imaging scheme with suitable resolution is preferable as the picture of "defect" or its effects might be appraised in a more visual way. Despite the optical microscope, SEM has become a useful tool for its moderate resolution where the secondary electron (SE) is the main mode. Based on SEM, electron beam induced current (EBIC) also has been developed. EBIC in plan-view mode, where the electric junction is normally in the plane of the sample and perpendicular to the beam, has been used to explore the carrier transport and relax features of the materials on the device structure directly, which may reflect the correlation between imperfection and performance of the PD more effectively. To reach this target, the observation of $In_xGa_{1-x}As$ PDs with different indium contents or configurations in both SEandEBICmodes has been done [2].

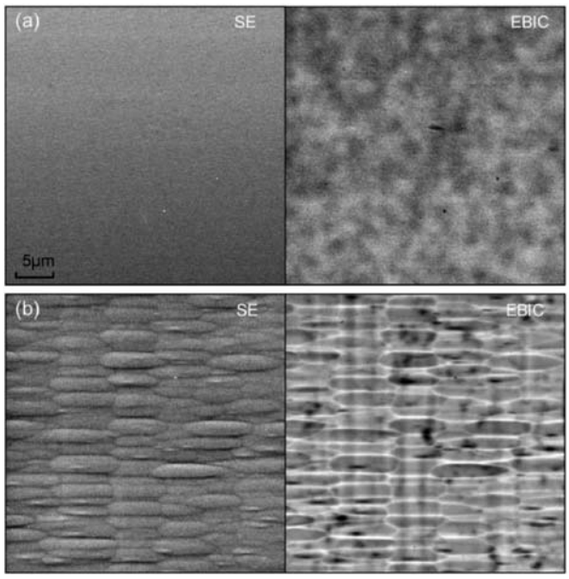

Fig.1. SE (left) and EBIC (right) pictures of $In_xGa_{1-x}As$ PD structures with Indium content x of 0.53 (upper) and 0.83 (bottom) in p-on-n configuration at 10 KV.

Fig.1 shows the SE and EBIC pictures of $In_xGa_{1-x}As$ PD structures with indium content x of 0.53 and 0.83 respectively, both in p-on-n configuration. The electron acceleration voltage is 10 KV. Different types of patterns in both SE and EBIC modes prompting abundant information about those two structures, from detailed differentiation on SE and EBIC pictures the imperfection related to the device performance could be explored based on different contrast mechanisms, especially for the PD with high indium content. Fig.2 shows the SE and EBIC pictures of $In_{0.83}Ga_{0.17}As$ PD structure in n-on-p configuration, where the pn junction is more close to the substrate side, the electron acceleration voltage is also 10 KV.

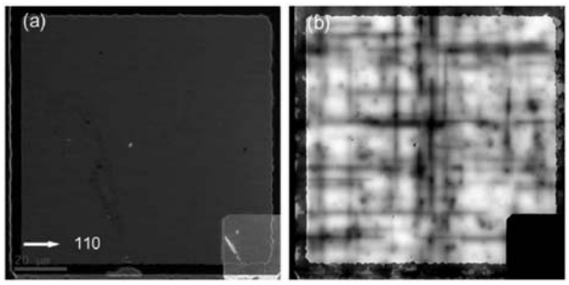

Fig.2. SE (left) and EBIC (right) pictures of $In_{0.83}Ga_{0.17}As$ PD structure in n-on-p configuration at 10 KV.

For this configuration a more diffused imperfection pattern in EBIC picture could be seen compare to these in p-on-n configuration, prompting more information of the formation and propagation of the misfit and threading dislocations. Using a self-developed image processing software the EBIC features of the samples are statistically analyzed, which validated the qualitative correlation between the EBIC data and device dark currents. Fusing of EBIC and SE images has also been attempted to enhance the "defect" visibility. Results indicate that EBIC is feasible to investigate the effects of "defect" on the device performance not only in research work, but also for product quality monitor purpose. More discussion on the details will be presented.

[1] Y. G. ZHANG, Y.GU, CHAP. 17,ADVANCES IN PHOTODIODES (ED G F D BETTA, CROATIA: INTECH), 458 (2011).
[2] Y. G. ZHANG, K. H. LIU, Y. GU ET AL., SEMICON SCI. TECHNOL.29, 035018 (2014).

A trial to move $In_{0.83}Ga_{0.17}As$ PD from InP to GaAs substrate: challenges and opportunities

X. Y. Chen[1], Y. G. Zhang[1], Y.Gu[1], L. Zhou[1], S. P. Xi[1], A. Z. Li[1], Hsby. Li[1]*

[1]State Key Laboratory of Functional Materials for Informatics, Shanghai Institute of Microsystem and Information Technology, Chinese Academy of Sciences, Shanghai 200050, China
*corresponding author: ygzhang@mail.sim.ac.cn

InGaAs photodetectors (PDs) and arrays are attracting particular interests as they can be tailored to cover a wide wavelength range in shortwave infrared band, which is desired to spatial remote sensing applications[1]. The $In_{0.53}Ga_{0.47}As$ PDs grown lattice-matched to In Pare commercially mature with cut-off wavelength at 1.7 µm. For application in longer wavelength region, the indium content should be increased. Currently, the growth of the so-called extended wavelength $In_xGa_{1-x}As$ detector materials with x>0.53 has been explored on InP substrate by using gas source molecular beam epitaxy (GSMBE)[2]. Even if larger lattice mismatch will be introduced, GaAs may still be an attractive substrate for fabrication of InGaAsPDs with large size epitaxial wafers as well as FPAs with more pixels for the advantages of robustness, lower cost and larger size. However, there are few attempts to transfer $In_xGa_{1-x}As$ (x>0.53) PDs from InP to GaAs substrate.

In our recent researches, a series of InP- and GaAs-based $In_{0.83}Ga_{0.17}As$ PDs with $In_{0.83}Al_{0.17}As/In_{0.83}Ga_{0.17}As$ pn heterojunction structures were grown by GSMBE. Their features have been evaluated on both material qualities and device performances. Compared with the InP-based $In_{0.83}Ga_{0.17}As$ PD with lattice mismatch of 2.1%, the GaAs-based PDs with lattice mismatch of 5.9% exhibited an inferior surface morphology and relatively poor structural characteristic [3], which could be ascribed to at least one order in magnitude higher threading dislocation densities in the $In_{0.83}Ga_{0.17}As$ layers, as shown in XTEM images in Fig. 1.

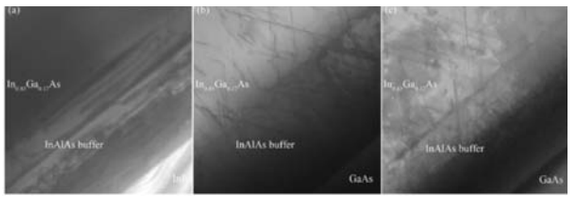

Fig. 1. XTEM images of (a) sample A, (b) sample B and (c) sample C.

Correspondingly for the PDs with the same 50% cut-off wavelengths at about 2.58µm (Fig. 2(a)-2(c)),the dark current at -10 mV of GaAs-based one is about three orders higher than that of InP-based one at 77 K, as shown in Fig.2(e). However, the R_0A of GaAs-based PD is comparable with that of InP-based PD at 300 K [4], as shown in Fig. 2(f). More interestingly, the temperature dependent characteristic of dark current of GaAs-based PDs with such a large lattice mismatch varied with InAlAs buffer strategies due to the different dominant mechanisms. The results indicated that via appropriate structural design, GaAs may be a feasible replacement of InP as substrate for $In_{0.83}Ga_{0.17}As$ PDs in some low-end application area around RT.

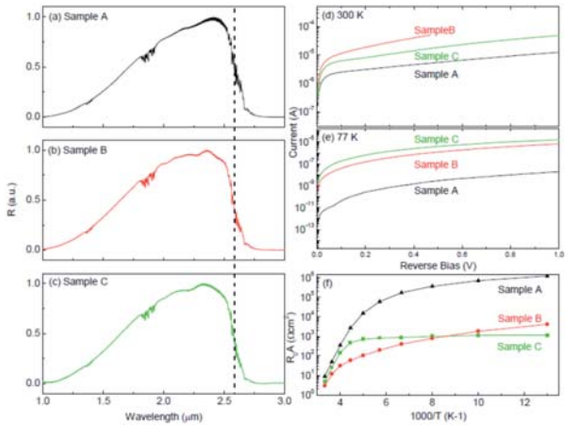

Fig.2. (a)-(c)Normalized responsespectra at RT, (d)-(e)dark currentmeasured at 300 Kand77 K, and (f)temperature dependence of R0A.

Table I Structuralfeaturesand measured results of three samples.

No.	Substrate and buffer scheme	AFM RMS (nm)	FWHM XRD (arcsec)	R_0A (Ωcm^{-2}) 300 K	R_0A (Ωcm^{-2}) 77 K
A	1.9 µm$In_xAl_{1-x}As$(x graded from 0.52 to 0.87)+0.65 µm $In_{0.83}Al_{0.17}As$ on InP	4.8	644	9.07	1.22×10^6
B	1.9µm$In_xAl_{1-x}As$(x graded from 0.10 to 0.87)+0.65 µm $In_{0.83}Al_{0.17}As$ on GaAs	11.3	1638	3.02	4.12×10^3
C	2.5 µm $In_{0.83}Al_{0.17}As$on GaAs	8.6	401	4.93	1.14×10^3

[1] R. W. M. HOOGEVEEN, R. J. VAN DER A, A. P. H. GOEDE, INFRARED PHYS. TECHNOL. 42(1),1-16 (2001).

[2] Y. G. ZHANG, Y.GU, CHAP. 17, ADVANCES IN PHOTODIODES (ED G F D BETTA, CROATIA: INTECH), 458 (2011).

[3] X. Y. CHEN, Y. G. ZHANG, Y. GU, L. ZHOU, Y. Y. CAO, X. FANG, HSBY. LI, J. GRYST. GROWTH 39, 75-80 (2014).

[4] L. ZHOU, Y. G. ZHANG, X. Y. CHEN, Y. GU, HSBY. LI,Y. Y. CAO, S. P. XI,J. PHYS. D: APPL. PHYS. 47, 085107 (2014).

Synchronization modes in WGM-laser with the connected disk resonators

V.V.Sherstnev[1], A.A.Leonidov[1], E.A.Grebenshchikova[1], N.D.Il`inskaya[1], O.Y.Serebrennikova[1], R. Teissier[2,3], A.N.Baranov[2,3], Yu.P.Yakovlev[1].*

[1]Ioffe Physico-Technical Institute, St. Petersburg, 194024, Russia
[2]Univ. Montpellier, IES, UMR 5214, IES, F-34000 Montpellier, France
3CNRS, IES, UMR 5214, F-34000 Montpellier, France
*corresponding author: vic2sherstnev@gmail.com

Creation of a compact radiation sources operating in the mid-IR range (2-5 μm) is one of the most important trends in the development of modern optoelectronics. The relevance of the problem consists in the fact that a large number characteristic lines of absorption of atmospheric pollutants as well as toxic, hazardous gases and liquids is in this region of the spectrum. Single-frequency tunable lasers need to be used as sources of coherent radiation for high-resolution spectrometers.

We reported on WGM-lasers (WGM - whispering-gallery modes), for mid-infrared (2-5 μm) with two optically coupled resonators [1]. Such design provides a single-mode radiation. It should be noted that the post growth technology for creating WGM lasers is close to the technology of LEDs, so it is much cheaper than other types of coherent radiation sources manufacturing (QCW lasers).

We reported on WGM lasers with controlled absorber and with a large range of frequency tuning (~ 400 Å), which is important for the diode-laser spectroscopy [2]. However, this design works in the multimode lasing mode, which complicates its usage in diode laser spectroscopy.

In this work, we report the first results of creating WGM-laser, which would provide a single-mode lasing with frequency tuning. To do this, we have combined the ideas contained in [1-2] and created a laser with two optically-coupled resonators, each of which contained two semi-ring contacts (controlled absorber). Fig.1. photo of the WGM laser.

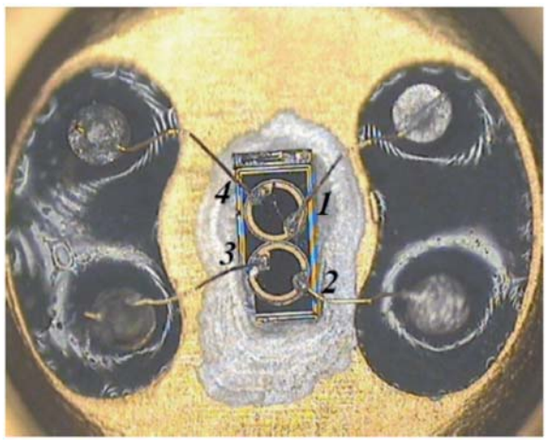

Fig.1. Photo of WGM laser.

Fig.2 shows the spectra of laser with coupled disk resonators when each of the four semi-ring contacts is switched-on separately (Fig.2, a-d), and when all the contacts are switched on simultaneously (Fig.2, e). It is significant that switching-on contacts separately showed multimode lasing in all the current range from 70 to 370 mA. At the same time, the switching-on of all four contacts of disk resonators simultaneously showed single-mode lasing emission, indicating that there is a mode locking in the laser with coupled disk resonators.

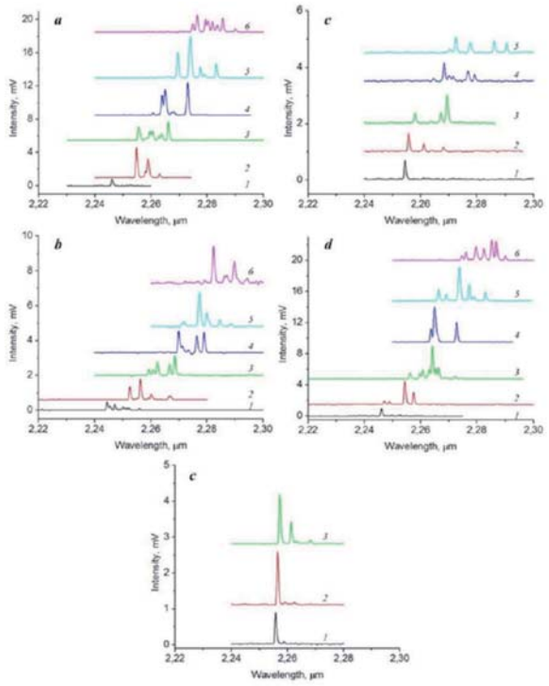

Fig.2. The room temperature electroluminescence emission spectrums of the WGM-lasers (V1079SN #112) dependence on current using QCW at 500 Hz on injection current (1 – 100 mA, 2 – 130 mA, 3 – 160 mA, 4 – 190 mA, 5 – 220 mA, 6 – 250 mA): a – contact №1, b – contact №2, c – contact №3, d – contact №4 and c – at joint switching on all contacts.

WGM-lasers with coupled disk resonators emitting in the mid-IR range (2.2-2.4 μm) were created and studied. It is shown that the separate switching-on of disk resonators of WGM-laser shows only multimode nature of radiation, while the joint switching-on of two disk resonators leads to the single-mode lasing (at current value less than 160 mA).

This work was supported by the project of the Presidium RAS №24, grants 14-02-01118 A, and also state contract No. 11705.004.11.001.

[1] E.A.GREBENSHCHIKOVA, V.V.SHERSTNEV, M.I.LARCHENKOV, O.YU.SEREBRENNIKOVA, N.D.IL`INSKAYA, A.N.BARANOV AND YU.P.YAKOVLEV. PISMA, ZH.TEKH.FIZ (USSR), 38, 7, (2012).
[2] BARANOV A.N., BOISSIER G., TEISSIER R., MONAKHOV A.M., SHERSTNEV V.V., LARCHENKOV M.I., YAKOVLEV YU. P, APPL. PHYS. LETT. 100, 061112 (2012).

Quantum Cascade Detectors in the Very Long Wave Infrared

J. Q. Liu[1], S.Q. Zhai[1], F. Q. Liu[1], Z.G. Wang[1]*

[1]Key Laboratory of Semiconductor Materials Science, Institute of Semiconductors, Chinese Academy of Sciences, Beijing 100083, People's Republic of China
*corresponding author: jqliu@semi.ac.cn

The very long wave infrared (VLWIR, λ > 14μm) is a strategic band for the development of space-based infrared technology, such as atmospheric temperature profiling, pollution monitoring, infrared astronomy and satellite mapping[1-3]. Quantum cascade detectors (QCDs) are photovoltaic devices: they have a built in asymmetric conduction band potential formed by energy band engineering design, which allows for biasless operation. They have clear advantages on the absence of dark current, low background noise, and high operation temperature especially in the VLWIR range [4-6]. In this work, we focus on the VLWIR quantum cascade photodectors involving energy band engineering, material technology, and devices physics. Targeting the common applications, we demonstrate a series of VLWIR QCDs from 14 to 20μm. The dark current density under 1.1×10^{-11} Acm^{-2} and the detectivity above 1×10^{11} $cmHz^{1/2}W^{-1}$ is achieved. Many of them exhibit high performance and give a cheerful prospect for the practical application in the near future.

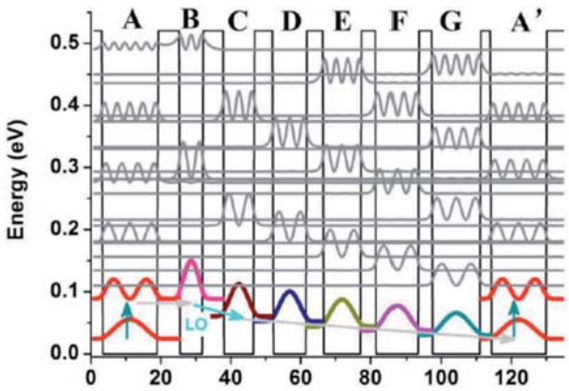

Fig.2. Schematic conduction band structure of sample C. Shown are the squared moduli of the relevant wave functions. The arrows show the transport of the electrons through the structure and the LO represent the LO-phonon resonance for transition between two consecutive levels. This design is based on one LO phonon stair and the sequential energy mini-stairs (7meV for each) formed by several quantum wells and barriers for the extraction of excited electrons.

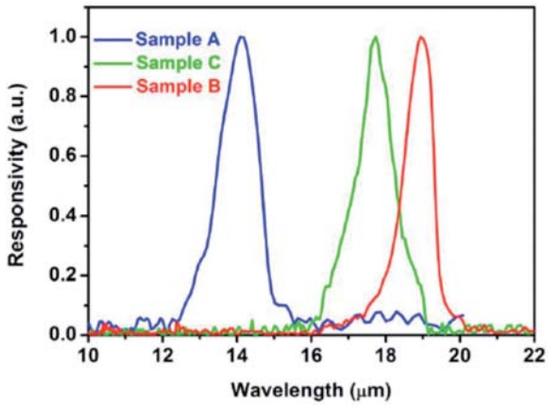

Fig.2. Spectral responsivity of sample A, sample B and sample C. The measurement temperature of sample A, sample B and sample C is 82K, 15K and 15K, respectively.

[1] S. D. GUNAPALA, K. M. S. V. BANDARA, B. F. LEVINE, G. SARUSI, D. L. SIVCO, AND A. Y. CHO, APPL. PHYS. LETT. 64, 2288 (1994).

[2] A. G. U. PERERA, S. G. MATSIK, H. C. LIU, M. GAO, M. BUCHANAN, W. J. SCHAFF, W. YEO, APPL. PHYS. LETT. 77, 741 (2000).

[3] S. HANNA, A. BAUER, H. BITTERLICH, M. BRUDER, L.-D. HAAS, M. HAIML, K. HOFMANN, K.-M. MAHLEIN, H.-P. NOTHAFT, T. SCHALLENBERG, A. WEBER, J. WENDLER, R. WOLLRAB, J. ZIEGLER, PROC. OF SPIE,7826, 78261H-1 (2010).

[4] F. R. GIORGETTA, E. BAUMANN, M. GRAF, L. AJILI, N. HOYLER, M. GIOVANNINI, J. FAIST, AND D. HOFSTETTER, APPL. PHYS. LETT. 90, 231111-1 (2007).

[5] A.BUFFAZ, M.CARRAS, L. DOYENNETTE, A. NEDELCU, X. MARCADET, AND V. BERGER, APPL. PHYS. LETT. 96, 172101-1 (2010).

[6] S.Q. ZHAI, J.Q. LIU, X.J. WANG, N. ZHUO, F.Q. LIU, Z.G. WANG, X.H. LIU, N. LI, AND W. LU, APPL. PHYS. LETT. 102, 191120-1 (2013).

Mid-infrared electroluminescence from inverted HgTe quantum wells

Yu. B. Vasilyev[1], N. N. Mikhailov[2], G. Yu. Vasileva[1,4], Yu. L. Ivanov[1], A.V. Antonov[3], A.V. Ikonnikov[3], and V. I. Gavrilenko[3]*

[1]Ioffe Physical_Technical Institute, RAS, St. Petersburg, 194021 Russia
[2]Rzhanov Institute of Semiconductor Physics, Siberian Branch, RAS, Novosibirsk, 630090 Russia
[3]Institute for Physics of Microstructures, RAS, Nizhny Novgorod, GSP-105, 603950, Russia
[4]St. Petersburg State Polytechnical University, St. Petersburg, 195251 Russia
*corresponding author: yu.vasilyev@mail.ioffe.ru

Narrow-gap HgTe/CdHgTe quantum wells are intensively studied during the last decade. A strong interest to these materials arose due to an unusual energy band structure which is inverted if the HgTe well thickness d exceeds 6.5 nm. In such structures the Γ_8 band of HgTe lies in energy lower than the Γ_6 band and, respectively, subbands Hi in the Γ_8 band have higher energies than Γ_6-based subbands Ei.

Here we report experimental results on mid-infrared (MIR) electroluminescence (EL) emitted from inverted HgTe quantum wells grown on (013) GaAs substrates. The radiation is excited by an external electric field applied along the plane of the quantum wells. We found that the radiation is strongly polarized and emitted only from the sample edges. This means that the MIR radiation is related to intersubband (ISB) transitions in the quantum wells.

The EL spectra were measured with a Fourier transform spectrometer Vertex 80 v Bruker Optics using a step-scan regime. Figure 1 shows radiation spectra for two samples with d =6.5 nm and d =7 nm where distinctive features are related to optical ISB transitions in quantum wells. So the peaks centered at 72 meV in sample 1 and at 69.5 meV in sample 2 can be associated with the H2 – H1 radiative transitions.

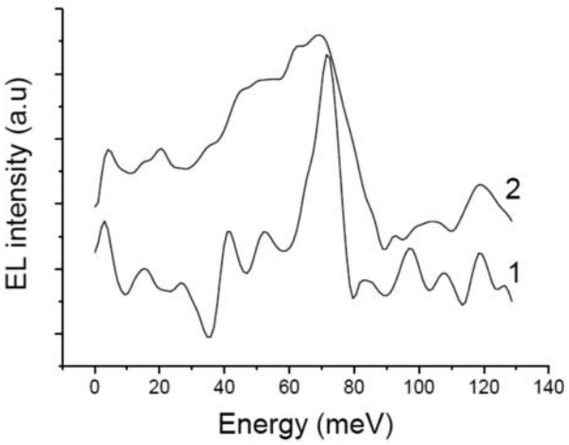

Fig.1. Electroluminescence spectra for two quantum wells with thicknesses d =6.5 nm (1) and d =7 nm (2).

The mechanism of the ISB excitation in such quantum wells is unclear at the moment. As we defined, the quantum wells have n-type conductivity. Usually in this case no optical transitions inside the valence band should be observed. We suppose that in our experiments the optical transitions in the valence band excited either due to a carrier injection from the contacts or due to a Zener tunneling between the conduction and the valence bands as shown in Fig.2, inset. This conclusion is confirmed by the current-voltage characteristics (IVC) plotted in Fig.2. The IVC curves measured in sample 1 at two various temperatures T=77K and T=4.2K show similar behavior and can be described by a power law as $I \sim U^{7/2}$ (T=77 K) and $I \sim U^{5/2}$ (T=4.2 K). Such a behavior is an indication of the injection mechanism of the current.

Fig.2. Current versus voltage characteristics for sample1 measured at two various

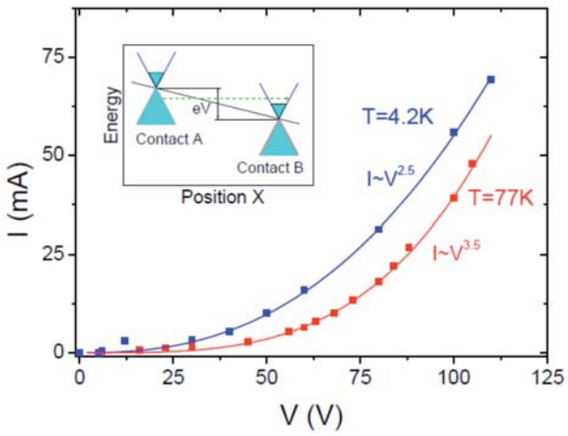

temperatures 4.2 K and 77 K. Inset: schematic diagram of a current flow mechanism at the Zener tunneling.

This work is funded by RFBR (13-02-00326, 14-02-01103) and RF President Grant for Young Scientists (MK-3057.2013.2).

Self-assembled growth of III-V nanowire array on Si for low-cost IR optical sensors

*Jae Cheol Shin[1], Sang Hyuck Kim[2], Won Jun Choi[2],**

[1]Korea Photonics Technology Institute, Gwangju, 500-779, Republic of Korea
[2]Korea Institute of Science and Technology, Seoul, 136-791, Republic of Korea
*corresponding author: wjchoi@kist.re.kr

III-V semiconductor has been successfully utilized in optical devices because of their direct bandgap and high absorption coefficient. Meanwhile, silicon (Si) becomes the most universal platform for the electronics industry; thus integration of these materials provides active optic system with CMOS technology.

In this letter, we report the catalyst-freegrowth of InAsnanowire array on Si substrate.1The InAs nanowires are grown via self-assembled growth method using metal-organic chemical vapor deposition (MOCVD). The nanowire array has been uniformly grown on entire 2 inch Si wafer with the number density of 1 × 10^7/cm^2 without any metal catalyst or pattern assistance (Fig. 1). The structural and optical properties ofInAs nanowire array are examined by using photoluminescence (Fig. 2), X-ray diffraction, and transmission electron microscopy analysis. Cross-sectional TEM image confirms the heterogeneous interface between InAs and Si.

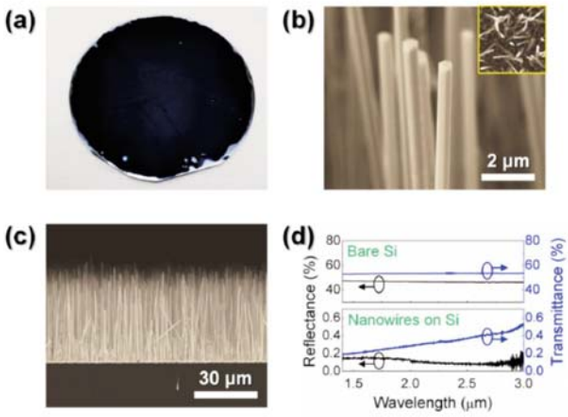

Fig 1. Grwoth of the InAs nanowire array on Si (111) substrate: (a) Optical image of InAs nanowire array on 2 inch Si wafer; (b) 45o tilted SEM image showing that the tip of nanowire is hexagon. Inset is top-view SEM image over a 20 × 20 μm^2 area, indicating the number density of the nanowire array is ~ 1 × 10^7/cm^2; (c) Side-view SEM image presenting that the average height of the InAs nanowire array exceeds 40 μm; and (d) Reflectance and transmittance spectra of the InAs nanowire array on Si along with a bare Si reference sample.

The geometry of the nanowire array, which is a natural stepped-index anti-reflection coating, can significantly enhance light absorption over a large wavelength range. Shown in Fig. 1d are the reflectance and transmittance spectra over the SWIR range (1.4 – 3 μm) measured from the Si sample with the InAs nanowire array along with a bare Si sample as a reference. The nanowire array, which is grown to be more than 50 μm in height, provides ultra-high light absorption over the entire SWIR region.

The wafer-scale, heterogeneous InAs nanowires may enable the low-cost fabrication of nanowire-based optical devices on Si platform with an industrial scale.

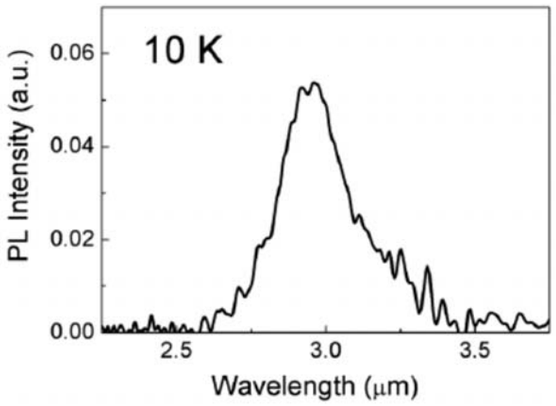

Fig. 2. Photoluminescence spectrum measured from InAs NWs grown on Si (111) substrate.

Acknowledgement: This work was supported by the Agency for Defense Development (ADD) of Republic Korea and the KIST internal program. This research was also supported by the Converging Research Center Program through the Ministry of Education, Science and Technology (2012K001280).

[1] J. C. SHIN, A. LEE, ET AL, ACS NANO, 7, 5463 (2013).

Two-band superlinear electroluminescence in AlSb/InAs(1-x)Sbx/AlSb deep quantum well

*M. P. Mikhailova[1], E. V. Ivanov[1], L. V. Danilov[1], A. A. Petukhov[1], K. V. Kalinina[1], S. I. Slobozhanyuk[1], G. G. Zegrya[1], N. D. Stoyanov[1], Yu. P. Yakovlev[1], A. Hospodková[2], J. Pangrác[2], J. Oswald[2], M. Zíková[2], and E. Hulicius[2]**

[1]Ioffe Physical Technical Institute RAS, 194021, Polytekhnicheskaya 26, St. Petersburg, Russian Federation
[2]Institute of Physics, AS CR, v.v.i., 162 00, Cukrovarnická 10, Prague 6, Czech Republic
*corresponding author: hulicius@fzu.cz

We will report on superlinear electroluminescent (EL) MOVPE structures based on AlSb/InAs1-xSbx/AlSb deep quantum wells grown by MOVPE on n-GaSb:Te substrates. Dependence of the electroluminescence (EL) spectra and optical power on the drive current in nanoheterostructures with a deep AlSb/$InAs_{1-x}Sb_x$/AlSb quantum well at 77 – 300 K temperature range was studied. Intensive two-band superlinear EL in the 0.5 - 0.8 eV photon energy range and optical power enhancement with the drive current at room temperature caused by the contribution of the additional electron-hole pairs, generated at AlSb/InAs interface, due to the impact ionization by the electrons heated at the high energy difference between AlSb and the first electron level Ee1 in the InAsSb QW were found.

Study of the EL temperature dependence at 90 – 300 K range enabled us to define the role of the first and second heavy hole levels in the radiative recombination process. Due to the temperature dependence of valence band offset the EL spectrum revealed radiative transitions from the first electron level Ee1 to the first hole level in the whole temperature range (90 – 300 K) while the emission band related with the transitions to the second hole level occurred only at T > 195 – 200 K.

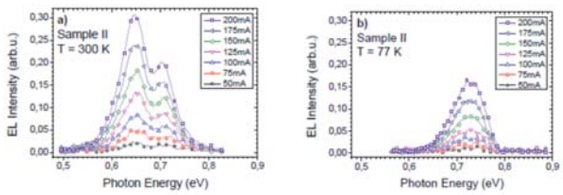

Fig.1. EL spectra of sample B at (x = 12 %) T = 300 K (a) and T = 77 K (b) for currents from 50 mA to 200 mA.

Comparative examination of the nanostructures with high band offsets and different interface types (AlAs-like and InSb-like) reveals more intense EL and optical power enhancement at room temperature in the case of AlAs-like interface that could be explained by the better quality of the heterointerface and more efficient hole localization.

This paper is continuation of our recent paper1 devoted to the superlinear electroluminescent properties of quantum wells (QWs), but the structure was grown with different type of interfaces between AlSb barrier and InAsSb QW. In our previous work the interfaces were grown as AlAs-like while, results presented here are measured on samples with InSb like interfaces between barriers and QW. We have observed intensive two-band superlinear electroluminescence (EL) and we studied the temperature dependence in the range from 77 K to 300 K.

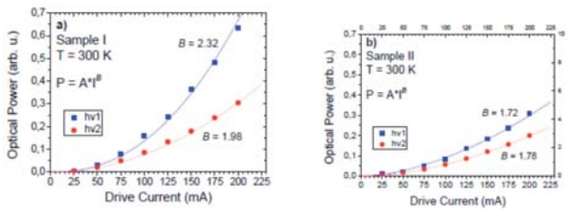

Fig.2. Optical power P vs driving current I for two EL bands of sample A (a) and sample B (b): T = 300 K, dots represent the experimental data, solid lines are approximations by power dependence P = A IB, where B is the exponent value.

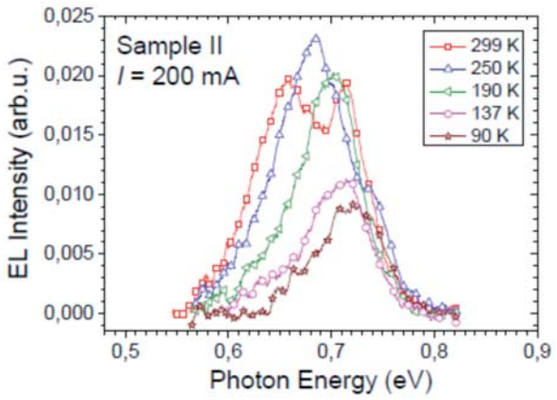

Fig.3. EL spectra of the sample B at 200 mA drive current at different temperatures in the range of 90 – 299 K. The hv2 EL band disappears for temperatures below ~200 K.

[1] M. P. MIKHAILOVA, E. V. IVANOV, L. V. DANILOV, K. V. KALININA, N. D. STOYANOV, G. G. ZEGRYA, YU. P. YAKOVLEV, E. HULICIUS, A. HOSPODKOVÁ, J. PANGRÁC, AND M. ZÍKOVÁ, J. APPL. PHYS. 112, 230108 (2012).

Mid-Infrared Whispering Gallery Mode Emission from InAsSb/InAsPSb Multiple Quantum Wells in a Disk Cavity

Yen-Chih Lin[2], Ming-Hua Mao[1,2,3], Chen-Jun Wu[2], Shao-Huang Li[2], and Hao-Hsiung Lin[1,2,3]*

[1]Department of Electrical Engineering,
[2]Graduate Institute of Electronics Engineering,
[3]Graduate Institute of Photonics and Optoelectronics, National Taiwan University, Taipei 10617, Taiwan
*corresponding author: mhmao@ntu.edu.tw

Mid-infrared disk cavities with InAsSb/InAsPSb multiple quantum wells active medium were fabricated. The photoluminescence spectra were measured at 20 K, and the whispering gallery modes were observed.

Recently, mid-infrared optoelectronic devices are of considerable interest because of their numerous applications such as gas detection, environmental monitoring, and thermal imaging [1, 2]. Because InAsSb has a very narrow bandgap among III-V semiconductors, the InAsSb/InAsPSb heterostructure is a promising candidate for the mid-infrared optoelectronic devices [3]. However, nonradiative Auger recombination drastically affects the performances of the optoelectronic devices in the mid-infrared range. Whispering gallery modes based cavities can have high quality factors due to propagation along the circular periphery by total internal reflection. Thus they are especially important for light sources with low threshold [4].

The sample was grown by molecular beam epitaxy. The active region consists of five multiple InAsSb/InAsPSb quantum wells on GaSb substrate. The process procedures of disk cavities are described in the following. First, a silicon dioxide film was deposited by plasma enhanced chemical vapor deposition. Next, the circular photoresist patterns were defined by photolithography. They were then transferred to the silicon dioxide layer by reactive ion etching. The unprotected region was vertically etched down to the substrate by inductively coupled plasma reactive ion etching.

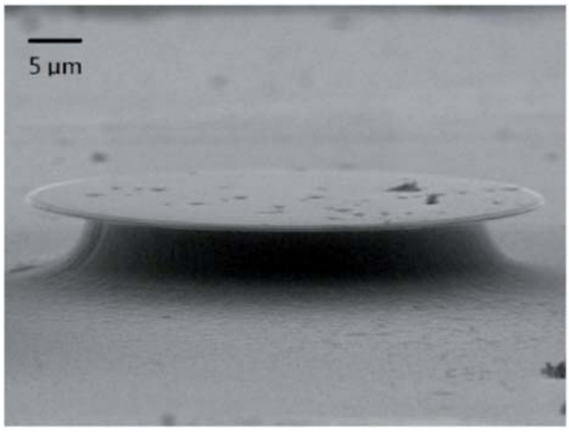

Fig.1. A scanning electron microscope image of the fully processed disk cavity. The diameter of the disk cavity is 50 µm.

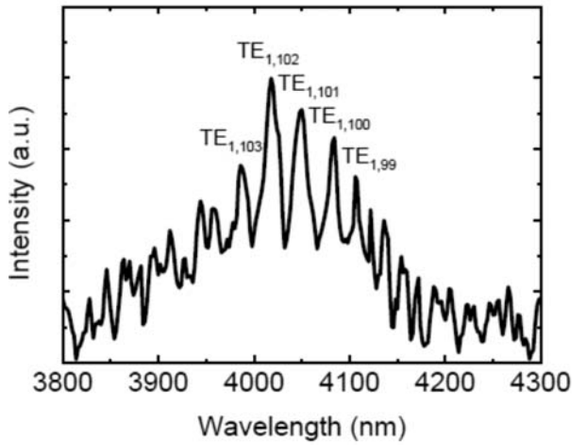

Fig.2. Emission spectrum of a 50-µm-diameter disk cavity at 20 K. The corresponding whispering gallery modes are indicated.

Finally, selective wet etching was applied to form the pedestal of the disk cavities. The scanning electron microscope image of a fully processed 50-µm-diameter disk cavity is shown in Fig. 1. The photoluminescence spectrum at 20 K was measured and whispering gallery modes beyond 4 µm can be clearly observed in Fig. 2. Therefore, the fabricated disk cavity is confirmed to exhibit high optical quality.

This work was supported by the Ministry of Science and Technology, Taiwan, under the Grant No. NSC-101-2221-E-002-166, NSC-102-2221-E-002-196-MY3, and NSC-102-2221- E-002-191-MY3.

[1] J. WAGNER, C. H. MANN, M. RATTUNDE, AND G. WEIMANN, APPL. PHYS. A 78, 505 (2004).
[2] A. BAUER, K. RÖßNER, T. LEHNHARDT, M. KAMP, S. HÖFLING, L. WORSCHECH, AND A. FORCHEL, SEMICOND. SCI. TECHNOL. 26, 1 (2011).
[3] C. J. WU, G. TSAI, AND H. H. LIN, APPL. PHYS. LETT. 94, 211906 (2009).
[4] K. J. VAHALA, NATURE 424, 839 (2003).

Modulation spectroscopy as an optical probe of carrier concentration in laser structures with plasmon-enhanced waveguides

M. Motyka[1], M. Dyksik[1], G. Sęk[1], J. Misiewicz[1] M. Dallner[2], S. Höfling[2], M. Kamp[2]*

[1]Institute of Physics, Wrocław University of Technology, Wrocław, Poland
[2]TechnischePhysik, University of Würzburg,Würzburg, Germany
[3]School of Physics and Astronomy, University of St. Andrews, St. Andrews, United Kingdom
*corresponding author: marcin.motyka@pwr.edu.pl

Interband cascade lasers (ICLs) have been proven to be an interesting alternative to quantum cascade lasers as coherent light sources in the mid-infrared range offering potentially broad range of emission, low thresholds, continuous-wave monomode operation at room temperature and wide tenability [1-3]. All these properties are demanded in many of the gas sensing schemes or in absorption spectroscopy making ICLsapplication-relevant. One of the ways to extend their emission to wavelengths significantly beyond 6 µm is the use of doped bulk-like claddings and employing the plasmonic effect for the waveguiding in structures on InAs substrates [4,5]. This, however, requires optimization of the doping concentration and its control in order to tailor the light confinement and limit the increased losses.We present optical studies of InAs-substrate-based ICLstructures with various doping concentrations in the claddings. In order to precisely control and optimize the doping and to minimize the threshold current a non-destructive optical approach has been used. The plasma characteristic frequency can be determined via the observation of the Berreman effect [6]. This is the so-called plasma-edge effect that occurs when the incident light frequency is varied across the region where the real part of the dielectric function changes sign.Typically, this is necessary to perform reflectance measurements with two orthogonal light polarizations, which allows recognizing the absorption feature related to plasmafrequencies, and hencedetermine the carrier concentration. We have improved the methodfurther by performing modulated reflectivity measurements in a form of fast differential reflectance [7]. This allows detecting a sharp spectral feature at the plasma frequency without the necessity of performing the polarization-resolved experiment.The issue of the modulation mechanism is also discussed.

[1] I. VURGAFTMAN ET AL., NATURE COMMUN. 2, 585(2011).
[2] R. WEIH ET AL., APPL. PHYS. LETT. 102, 231123 (2013).
[3] Y. JIANG,ET AL., J. APPL. PHYS. 115, 113101 (2014).
[4] M. DALLNER ET AL., ELECTRONICS LETT. 49, 286 (2013).
[5] Z. TIAN ET AL., ELECTRONICS LETT.48, (2012).
[6] R.T. HINKEY ET AL., J. APPL. PHYS.110, 043113 (2011).
[7] M. MOTYKA & J. MISIEWICZ, APPL. PHYS. EXP. 3, 112401 (2010).

Highly reflective infrared modulator for the CO_2 laser wavelength range

W. Vandermeiren[1], J. Stiens[1], G. Shkerdin[2], C. De Tandt[1] and R. Vounckx[1]*

[1]Laboratory for Micro- and Photonelectronics, ETRO-FirW VUB, Pleinlaan 2, B-1050 Brussel, Belgium.
[2]Kotelnikov Institute of Radio Engineering and Electronics of the Russian Academy of Science, Vvedenskogo Square 1, 141120 Fryazino (Moscow region), Russia
*corresponding author: wvanderm@etro.vub.ac.be

A quantum well infrared modulator for the CO_2 laser wavelength range is presented here. The working principle is based on intersubband transitions in a single AlGaAs/GaAs quantum well structure. CO_2 laser light at normal incidence is coupled to an evanescent wave by means of a sub-wavelength diffraction grating. Modulation of the zeroth order reflective mode is achieved by applying an electric field across the quantum well. The model for deriving the complex refractive index of the quantum well region is briefly described and used for numerical diffraction efficiency simulations. It is shown that the modulation depth is to a certain degree inversely proportional to the on-state reflectivity of the modulator. Experimental results achieved on different samples with varying grating height and period are presented. This study focuses on grating parameters targeting relatively high on-state reflectivities in the range of 75-95 % and modulation depths in the range of 10-30 %. The experimental results are in good agreement with our model and diffraction efficiency calculations. Absolute modulation depths of the order of 15% were experimentally observed.

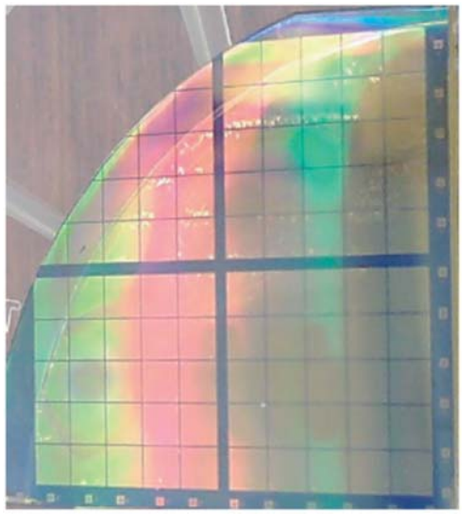

Fig.1. Backside of infrared modulator array.

Quartz-enhanced photoacoustic spectroscopy based carbon disulfide detection using a CW DFB-QCL

*J. P. Waclawek[1], M. Brandstetter[1], H. Moser[1], J. Ofner[1] and B. Lendl[1]**

[1]Institute of Chemical Technologies and Analytics, Vienna University of Technology, Getreidemarkt 9/164 AC, 1060 Vienna
*corresponding author: bernhard.lendl@tuwien.ac.at

A compact gas sensor system based on quartz-enhanced photoacoustic spectroscopy (QEPAS) employing a 4.59 µm continuous wave (CW) distributed feedback quantum cascade laser (DFB-QCL) was developed for detection of carbon disulfide (CS_2) at sub-ppmv concentration levels. The work reports the suitability of the sensor system for process monitoring at rayon industry, where CS_2 is used in big amounts to produce regenerated cellulose fibers.

QEPAS is a sensitive and selective technique that allows measurements of trace gases in an ultra-small acoustic detection module with a total sample volume of a few mm^3 [1]. The technique is based on the use of a 32.768 kHz quartz tuning fork (QTF) as a sharply resonant transducer for acoustic waves, which are induced in an absorbing gas by modulated optical radiation. The QTF is a piezo-electric element which converts its deformation by pressure waves into separation of electrical charges that can be measured either as a voltage or as a current. An enhancement of the QEPAS signal can be achieved when two metallic tubes acting as a micro-resonator (mR) are added to the QTF sensor architecture [2].

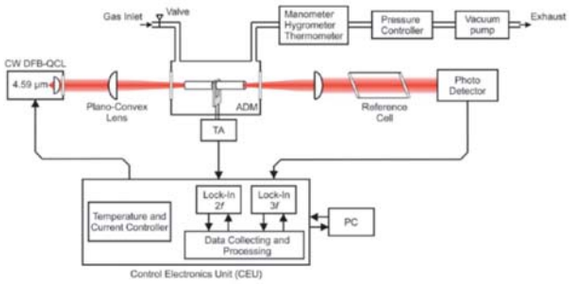

Fig.1. Schematic diagram of the QEPAS based CS2 gas sensor system employing a 4.59 µm CW DFB-QCL.

The sensor system is based on 2f wavelength modulation spectroscopy and QEPAS detection. In order to implement the 2f WMS technique the emission wavelength of the CW DFB-QCL was modulated at half of the QTF resonance frequency $f_{mod} = f_0 / 2$ by embedding a sinusoidal modulation atop of the DC laser current. The detection of the QTF signal was performed at f_0, using an internal lock-in amplifier with a time constant set to 1 sec. To lock the laser frequency to the center of the CS_2 absorption line to avoid any laser drift a reference channel consisting of a reference cell and a photodetector signal demodulated at 3f was employed.

Sensitivity and linear response of the QEPAS sensor was investigated by performing quantitative measurements of CS_2 within the range of 0 to 50 ppmv. Good linearity between signals amplitude and CS_2 concentrations was observed and a sub-ppm detection limit (1σ) was determined for the QEPAS based sensor system.

[1] R. F CURL, F. CAPASSO, C. GMACHL, A. A KOSTEREV, B. MCMANUS, R. LEWICKI, M. PUSHARSKY, G. WYSOCKI, F. K. TITTEL, "QUANTUM CASCADE LASERS IN CHEMICAL PHYSICS." CHEM. PHYS. LETT. 487: 1-18 (2010).

[2] L. DONG, A. A. KOSTEREV, D. THOMAZY, F. K. TITTEL: "QEPAS SPECTROPHONES: DESIGN, OPTIMIZATION, AND PERFORMANCE" APPL PHYS B 100, 627-635 (2010).

P-InAsSbP/no-InAs/n+-InAs photodiodes for operation at moderate cooling (150-220 K)

P.N. Brunkov[1], N.D. Il'inskaya[1], S.A. Karandashev[1], N.M. Latnikova[2], A.A. Lavrov[1], B.A. Matveev[1], A.S. Petrov[3], M.A. Remennyi[1], E.N. Sevostyanov[2], and N.M. Stus'[1]*

[1]Ioffe Physical-Technical Institute RAS, St. Petersburg, Russia
[2]LETI Ul'yanov (Lenin) St. Petersburg Electrotechnical University, St. Petersburg, Russia
[3]Electron National Research Institute, St. Petersburg, Russia
*Corresponding author: bmat@iropt3.ioffe.ru

InAs based photodiodes (PDs) promise considerable advantages over other types of photodetectors in a variety of sensing applications including but not limited to pyrometry and gas analysis. Recently we reported on performance of double heterostructure PDs with InAsSbP claddings and n-InAs active layer sensitive to radiation around 3 μm in a wide temperature range (77-350 K) [1]. Here we study PDs that are less sophisticated than that in [1] because they contain only two epitaxial layers that form P-InAsSbP/no-InAs/n+-InAs single heterostructure operating in a front surface illumination mode at 150-220 K. Lattice matched to InAs epitaxial structures contained a heavily doped n+-InAs (100) substrate (n+ ~10^{18} cm^{-3}), an undoped n-InAs active layer 4–6 μm thick, and wide energy-gap ("window") layer of P-InAsSbP (Zn) (Eg~440 meV) solid solution 2–3 μm thick. The energy gap discontinuities at the type-II heterointerface were ΔEc = 120 meV and ΔEv = –30 meV at 300 K. 330×330 μm square mesa PD chips had a disc anode contact with a diameter of Da = 80 μm in the center of the mesa and broad cathode contact onto n+-InAs substrate. According to Scanning Spreading Resistance Microscopy measurements the displacement of the p-n junction and the interface of InAsSbP and InAs layers was less than 0.3 μm. Peak sensitivity value exhibited weak dependence on temperature variation amounting to 1.1 A/W at 77 K and 1 A/W at 300 K while I-V characteristic strongly depended on temperature (see Fig.1 and Fig.2).

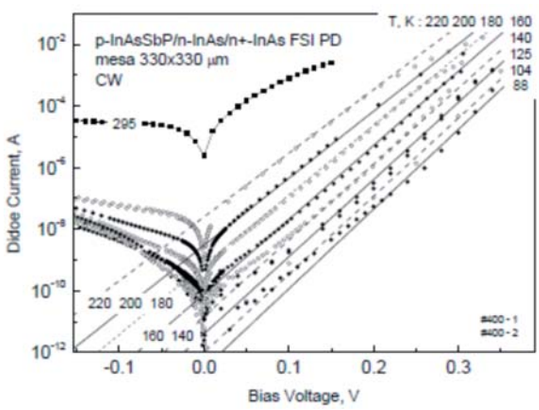

FIG.1 I-V CHARACTERISTICS OF INAS SH PD AT 88, 104, 125, 140, 160, 180, 200, 220 AND 295 K.

In the temperature range of 220 > T > 160 K the forward current had well pronounced tendency to vary as exp(eU/βkT). At low forward bias (3kT/e < U < 0.1 V) and at temperatures below 160 K a leakage current dominated while at high bias (U > 0.1 V) a diffusion in neutral areas and generation-recombination in active layer governed the current.

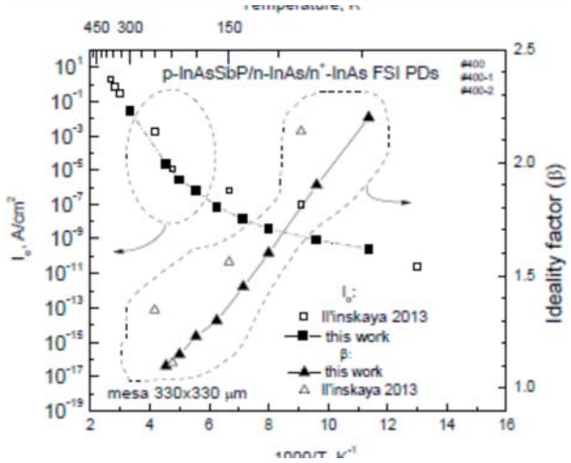

Fig.2 Saturation current Io (squares, left scale) and ideality factor β(triangles, right scale) for InAs SH PD vs reverse temperature. Open symbols present data from [N. D.Il'inskaya et al Technical Physics Letters, 39, 818–821(2013)].

The detectivity value at room temperature (see Fig.3) appeared somewhat smaller than that for the InAs SH and DH backside-illuminated PDs [2], but was higher than for other types of PDs.

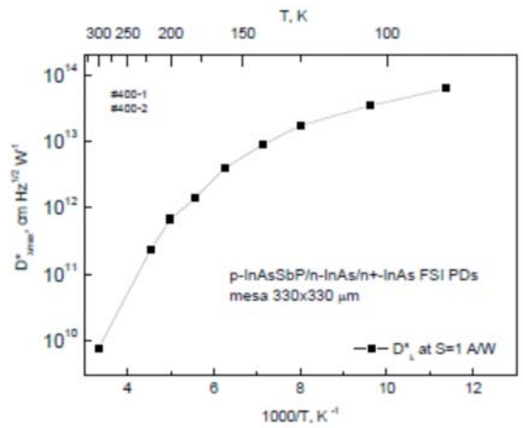

Fig.3 Detectivity at spectra maximum vs reverse temperature in InAs SH PD. Estimations are made at an assumption that SI=1 A/W.

We are aware that the low temperature D* values (T<160 K) in Fig.3 simulated using the above approach were somewhat exaggerated – in fact the leakage current at small bias (see Fig. 1) adds to total noise and reduces the D*. This is not the case for temperatures above 180 K as diffusion current dominates and thus the D* values reflect real PD performance in a photovoltaic mode of operation. The authors are grateful to Regional Center for Material Research and Novel Technology Diagnostic for supporting the study.

[1] P.N. BRUNKOV ET AL, INFRARED PHYSICS & TECHNOLOGY 64, 62–65 (2014).
[2] B.A.MATVEEV ET AL, PROC. SPIE 4650, P.173-178 (2002).

Photodetector based on GaSb with deep quantum well Al(As)Sb/InAsSb/AlAsSb grown by MOVPE for the 0.9-2.0 µm spectral range

I.*Andreev*[1]*, *M.Mikhailova*[1], *G.Konovalov*[1], *E.Ivanov*[1], *Yu.Yakovlev*[1], *E.Kunitsyna*[1], *E.Hulicius*[2], *A.Hospodková*[2], *J.Pangrác*[2], *M.Zíková*[2]

[1]Ioffe Physical-Technical Institute RAS, 194021, Politekhnicheskaya 26, St-Petersburg, Russia
[2]Institute of Physics of the ASCR, v.v.i., 16200, Cukrovarnicka 10, Prague, Czech Republik
*corresponding author: igor@iropt9.ioffe.ru

We report design and study of photodetectors based on n-GaSb/p-GaSb with deep 20 nm AlSb/5 nm $InAs_{0.84}Sb_{0.16}$/20 nm AlSb quantum well and cap p-GaSb layer with 0.5 mm thickness. Heterostructures were grown on n-GaSb:Te (100) substrates by MOVPE in an AIXTRON200 machine. Samples under study had round mesa with 500 mm photosensitive diameter. The luminescent and photoelectrical properties of GaSb-based heterostructures with deep Al(As)Sb/InAsSb/Al(As)Sb quantum well were studied. Intense superlinear luminescence and enhance of the optical power were observed in dependence on drive current in the spectral range of 0.6-0.8 eV at T=77K and T=300K.

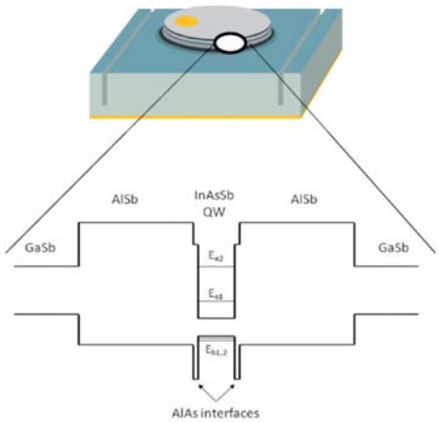

Fig.1. Top: layout of the mesa structure with a 500 µm diameter sensitive area and a 50 µm diameter point contact; bottom: energy band diagram of the original MOVPE grown nanostructure with a deep InAs0.84Sb0.12 QW.

Spectra of photosensitivity and current–voltage characteristics were investigated at 77-300 K. Spectral response of the photodetector was studied at the photovoltaic mode in the range of 0.9-2.0 mm with maximum sensitivity at λ=1.55 mm (T=300K). High quantum efficiency 0.6-0.7 and detectivity D* lmax= (5-7)×10^{10} W^{-1}×cm×$Hz^{1/2}$ were achieved at room temperature.

Zero bias resistance R0=ΔU/ΔI=2-6 kOhm (300K) and R0=10-60 MOhm (77K) were found. Current sensitivity was evaluated as high as 0.75-0.88 A/W for the maximum spectral range at 1.55 mm. The photodetectores demonstrate the capacitance as low as C=2.0-5.0 pF at reverse bias U= −1 V. The speed of response is estimated at $t_{0.1–0.9}$=100–200 ps. The photodetector band width of 2-3 GHz will be reached. A multiplication coefficient of M = 15 has been obtained under reverse bias in low electric fields, which, upon optimization, can be utilized for creating avalanche photodiodes with low noise levels.

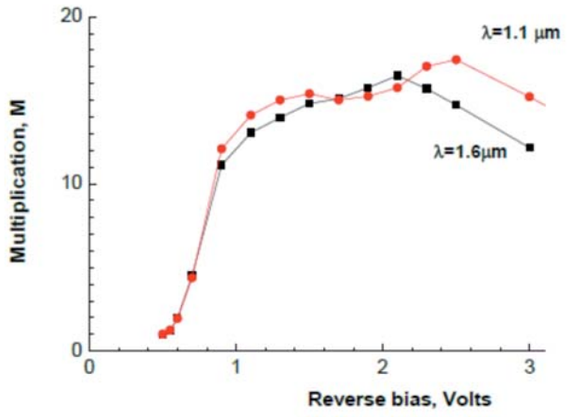

Fig.2. Photocurrent multiplication coefficient in an n-GaSb/Al(As)Sb/$InAs_{0.84}Sb_{0.16}$/Al(As)Sb/p-GaSb heterostructure at T = 300 K as a function of reverse bias.

These quantum well photodetectors are prospective for heterodyne spectroscopy and information technology.

This work is in part supported by Prezidium of Russian Academy of Science Program.

Application of Pd-Oxide-InP Schottky Diodes for Hydrogen Detection

E.A. Grebenshchikova[1], V.V.Sherstnev[1], S.G.Yastrebov[1], Yu.S.Melnikov[2], Yu.P.Yakovlev[1]*

[1]Ioffe Physical-Technical Institute RAS,194021, St.Petersburg, Russia
[2]St.PetersburgState PolytechnicalUniversity, 195251, St.Petersburg, Russia
*corresponding author: lot160g@gmail.com

Hydrogen energy as an alternative branch of power generation is of great scientific interest all over the world, however, its progressis being hampered by difficulties due to hydrogen storage and transportation.

Thesolid state hydrogen sensors used now are mainly based on SnO2films, with the film coating the ceramicsor silicon. The high operating temperature (300-400 C) and low selectivity are the disadvantages of this sensor type [1,2].

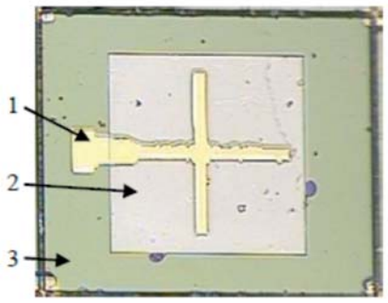

Fig.1. Photo of the Pd-Oxide-InP Schottky DiodeChip (1-Au-contact, 2-Pd layer, 3-InP)

The Schottky diodes with palladium contact have also been previously studied [3.4]. The hydrogen molecules dissociation into positive ions and electron stakes place in the palladium layer. In the present study we developed and investigated the metal-oxide-semiconductor (MOS) InP based structures for the hydrogen sensor. The chip photo is shownin Fig.1. Oxide layer was obtained by electrochemical oxidation of the InP surface. Its thickness in various experiments varied from 300 to 1000 Å. ThePd layer of 250-400 Å was deposited by thermal vacuum deposition.

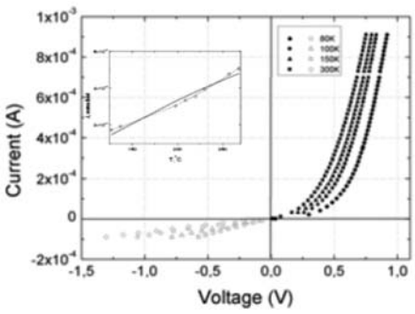

Fig.2. I-Vcharacteristics of the typical «Pd–oxide–n-InP»structure at temperature range 80–300 K (Insert -inclination angle of I-V forward branch linear part vsT)

We investigated electrical and photoelectrical properties of Pd-Oxide-InP Schottky diodes. The studies were conducted both with hydrogen (mixture N2 + 1% H2) and pure air. Current-voltage characteristics (I-V) were investigated in a wide temperature range. The mechanisms of current flow were determined from analysis of variation (I-V) characteristics with temperature as well as the Schottky barrier hight. The photoresponse spectrum of typical Schottky diode sample is shown in Fig.3. The above Schottky diode and LED with a wavelength of 0.9 μm was used in the hydrogen sensor.

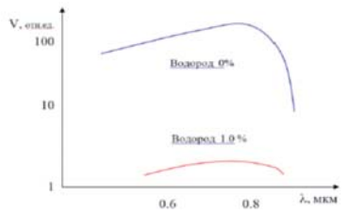

Fig.3.Photoresponsespectrum of the Pd-Oxide-InP schottky diode

Response time of the hydrogen sensorwas 2-5 sec (rise to 0.9 level) while the decay time (down to 0.1) was much longer –60-80 sec. (Fig. 4).

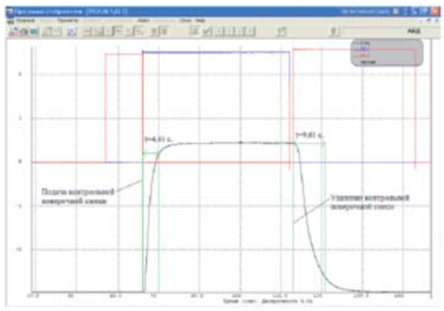

Fig.4.Response time ofhydrogen sensor based on Pd-Oxide-InP (mixture N2 + 1% H2)

In this paper, we demonstrated application of Pd-Oxide-InP Schottky diodes for manufacturing the compact hydrogen sensors with sensitivity threshold as small as 0.01% and speed (2-5 sec) at room temperature as well as low power consumption (Fig. 5).

Fig. 5. Schottky diode based hydrogen sensor

[1] W. GOPEL. PROGR. SURF. SCI., 20, 9 (1985).
[2] SOLID STATE GAS SENSORS, ED. BY P.T. MOSELEY, B.C. TOFIELD (BRISTOL-PHILADELPHIA, HILGER, 1987)P. 51.
[3] S.V. SLOBODCHIKOV, KH.M.SALIKHOV, B.E.SAMORUKOV. FTP. , 37, 5, C.960 (2003).
[4] G.G.KOVALEVSKAYA, M.M.MEREDOV, E.V.RUSSU, KH.M.SALIKHOV ET AL. FTP., 26, 10, C.1750 (1992)

High-Temperature Enhancement of Optical Power in GaSb-based Nanoheterostructures with Deep AlAsSb/InAs1-xSbx/AlAsSb Quantum Wells

M.P. Mikhailova[1], A.A. Petukhov[1], E.V. Ivanov[1], L.V. Danilov[1], K.V. Kalinina[1], N.D. Stoyanov[1], Yu.P. Yakovlev1, A. Hospodková[2], J. Pangrác[2], M. Zíková[2] and E. Hulicius[2]*

[1]Ioffe Physical Technical Institute, 194021, Polytekhnicheskaya 26, St. Petersburg, Russian Federation
[2]Institute of Physics, Academy of Science of the Czech Republic, v.v.i., 16200, Cukrovarnická 10, Prague 6, Czech Republic
*corresponding author: mayamikh@gmail.com

Last years AlSb/InAs(Sb) based structures with quantum wells (QWs) are intensively studied [1]. These materials are promising for mid-infrared spectral range operating on intersubbund transitions between electron states (light-emitting diodes (LEDs), lasers, photodiodes) at T = 77-300 K. But for several applications it is necessary to provide their work up to high temperature (T > 300 K). In [2] it was shown that non-radiative Auger recombination can be suppressed at the type II heterointerface and in nanostructures with deep QWs.

We report firstly on high-temperature enhance of optical power in LEDs based on n-GaSb/AlAsSb/InAs0.84Sb0.16/AlAsSb/p-GaSb QW structure (dQW = 5 nm) grown by MOVPE. Electroluminescence (EL) spectra were measured in 1.8-2.4 μm spectral range under 20-200 mA drive current at temperature from 22 °C up to 180 °C (~300-480 K).

Previously, it was shown that such QW structures exhibit superlinear dependence on drive current at T = 77-300 K. Optical power P can be described as P = A·IB, where I is drive current and exponent value B changes from 2 to 3 at 77 K and 300 K, respectively [3]. This effect was explaned by contribution into radiative recombination of additional electron-hole pairs due to impact ionization (inverse Auger effect) by electrons heated at high conduction band offset between AlAs barrier and first electron level in QW.

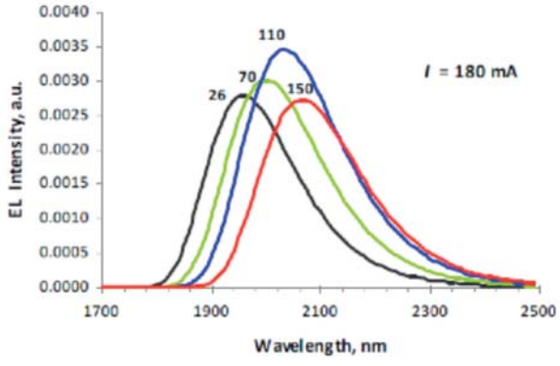

Fig. 1. EL spectra of the type I heterostructure with a deep Al(As)Sb/InAsSb/Al(As)Sb quantum well (d = 5 nm) grown on n-GaSb substrate in the temperature range of 20 – 150 °C at 180 mA drive current. The values of temperature (in °C) are shown next to the curves.

Here, we observed superlinear increase of EL intensity and optical power in 1.5 times at temperature grown from 22 °C up to 110 °C, and then its sublinear decreasing in 110-150 °C temperature range. EL spectra at several temperature values are presented in Fig. 1, and experimental optical power dependence is shown in Fig. 2. Special method for the measuring of EL spectra at high temperature was developed [4].

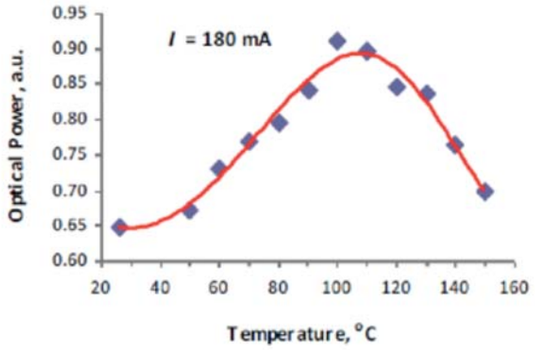

Fig. 2. Experimental temperature dependence of optical power for n-GaSb/Al(As)Sb/InAsSb/Al(As)Sb/p-GaSb QW heterostructure at 180 mA drive current.

Theoretical calculation of recombination rate in the QW LEDs under study was done for the temperature range of 20-200 °C, with taken into account thermoionic emission, Auger recombination and radiative recombination (Fig. 3).

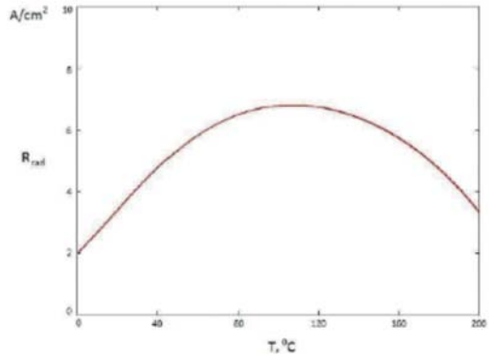

Fig. 3. Theoretical calculation of temperature dependence of radiative recombination rate in n-GaSb/Al(As)Sb/InAsSb/Al(As)Sb/p-GaSb nanoheterostructure at 100 mA drive current

The calculation results agree with experimental curve presented in Fig. 2. Recently, high-temperature enhance of optical power was demonstrated in bulk type II n-GaSb/n-InGaAsSb/p-AlGaAsSb LEDs with high potential barriers those exceeds in several times the band-gap value of narrow-gap active layer [4]. Finally, infrared LEDs based on nanoheterostructures with deep AlAsSb/InAsSb/AlAsSb QWs manifest visible enhancement of optical power at high temperature. The presented devices pave the way for LEDs operation in wide temperature range – from liquid nitrogen up to 200 °C.

This work was supported in part by RFBR grant #12-02-00597.

[1] D. BARATE, R. TEISSIER, Y. WANG, AND A. N. BARANOV, APPL. PHYS. LETT. 87, 051103 (2005).
[2] L. V. DANILOV AND G. G. ZEGRYA, SEMICONDUCTORS 42, 550-556 (2008).
[3] M.P. MIKHAILOVA, E.V. IVANOV, L.V. DANILOV, K.V. KALININA, N.D. STOYANOV, G.G. ZEGRYA, YU.P. YAKOVLEV, E. HULICIUS, A. HOSPODKOVÁ, J. PANGRÁC, AND M. ZÍKOVÁ, J. APPL. PHYS. 112, 230108 (2012).
[4] A.A. PETUKHOV, B.E. ZHURTANOV, K.V. KALININA, KH.M. SALIKHOV, M.P. MIKHAILOVA, YU.P. YAKOVLEV, SEMICONDUCTORS 47 (9), 1270 (2013).

Band discontinuity in InAsPSb alloy system

*Cheng-Ying Tsai[1], Wei-Chieh Chen[1], Po-Han Chang[1], Chih-I Wu1,[3], and Hao-Hsiung Lin[1,2,3]**

[1]Graduate Institute of Photonics and Optoelectronics,
[2]Graduate Institute of Eletronics Engineering
[3]Department of Electrical Engineering, National Taiwan University, 10617 Taipei, Taiwan
*corresponding author: hhlin@ntu.edu.tw

InAsPSb is a promising material for mid-infrared optical devices since its energy gap covers the spectral range varies from 1 to 3 μm when lattice matched to InAs substrate. However, the band discontinuity, an essential parameter for heterostructure, in this alloy is still not clear. In this work, we grew a series of InAsPSb alloys on InAs substrates by gas-source molecular-beam epitaxy (GSMBE) and utilized ultraviolet photoelectron spectroscopy (UPS) to investigate the maximum valence band energy of this alloy system. The detailed GSMBE growth and the alloy composition, determined by electron probe X-ray microanalyzer, have been reported elsewhere [1]. The UPS measurement used a Helium lamp with 21.2 eV photon energy (He I radiation) as the light source and was conducted at a base pressure level of 10-10 torr. The on-set binding energy of the whole UPS spectrum as well as the binding energy of the valence band edge are determined by extrapolating the linear fit of the curve to zero. The difference between He I photon energy and the on-set energy gives the work function of the alloy, while the binding energy of the valence band edge gives the difference between Fermi energy and valence band edge. One this basis, we can find the energy of the valence band edge using vacuum level as the reference of the energy system. The conduction band edge is then calculated by adding the energy gap determined from Varshni equation with the consideration of bowing parameters [2] to the valence band edge. The results are summarized in Table I.

Sample	VB edge (eV)	EF to VB edge (eV)	Work function (eV)	Eg (eV) at 300K	CB edge (eV)
$InAs_{0.09}P_{0.63}Sb_{0.28}$	-5.25	0.35	4.90	1.156	-4.094
$InAs_{0.22}P_{0.52}Sb_{0.26}$	-5.18	0.30	4.88	1.042	-4.138
$InAs_{0.56}P_{0.28}Sb_{0.16}$	-5.15	0.30	4.85	0.742	-4.408
InAs	-5.14	0.35	4.79	0.355	-4.785

Table I. Valence and conduction band edge measured by UPS and energy gap calculated by Varshni equation [2].

As can be seen, the Fermi level is above the valence band edge by 0.3 ~ 0.35 eV despite the composition change. This behavior coincides with the report of Daw and Smith for InGaAs [3]. They suggested that the Fermi level is pinned due to As vacancies at the surface. The valence band maximum shows a strong bowing with the composition. This bowing may result from the strong bond distortion in the alloy [4]. This work was supported by the Ministry of Science and Technology, Republic of China, under the contract, No. NSC 102-2221-E-002-191-MY3.

[1] G. TSAI, D. L. WANG, C. E. WU, C. J. WU, Y. T. LIN, AND H. H. LIN, J. CRYST. GROWTH 301-302, 134-138 (2007).
[2] I. VURGAFTMAN, J. R. MEYER, AND L. R. RAM-MOHAN, J. APPL. PHYS. 89, PP. 5815-5875 (2001).
[3] M. S. DAW AND D. L. SMITH, SOLID STATE COMMUN. 37, PP. 205-208 (1980).
[4] K. C. HASS, R. J. LEMPERT, AND H. EHRENREICH, PHYS. REV. LETT. 52, NO. 1, PP. 77-80 (1984).

Test of mid IR components for space missions

D, Sporea[1], A. Sporea[1], L. Mihai[1], A. Stancălie[1]*

[1]National Institute for Laser, Plasma and Radiation Physics, 409 Atomiştilor St., Măgurele, RO-077125, Romania
*corresponding author: dan.sporea@inflpr.ro

Quantum cascade lasers (QCLs) are seen as a viable alternative to FTIR spectroscopy in space related mission, able [1-3]: to address atmospheric, astrophysical and cometary research; to provide information on gas and dust located into deep space; to assist atmospheric chemistry for detection of specific molecule species in the 3 µm to 12 µm spectral window; to help planetary atmosphere gas tracing and identification. It is planned to use such devices in space missions such as: the Sample Analysis at Mars (SAM) Suite Investigation [4]; the Laser Heterodyne Radiometer (LHR), looking for methane on Mars [5]; the SOFIA experiment (Stratospheric Observatory for Infrared Astronomy) [6]; the ESA In-Orbit Demonstration activity [7].

Three years ago, Romania signed the Agreement for the association to the European Space Agency, and the Romanian Space Agency launched the Program "Space Technology and Advanced Research" to support original research of interest for space applications. Within this frame we are running a project dealing with the evaluation of mid IR components under charge particles and photon irradiation, for possible used in space borne applications. Our conference contribution will present the procedures for the assessment of operating characteristics in the case of QCLs, mid IR detectors (both photovoltaic and photoconductive) and optical materials (transmission and reflection measurements), as well as the irradiation protocols. The project focus is the use of QCLs for methane detection, this application being one of the great interests for spectroscopy in space missions.

The authors acknowledge the financial support of Romanian Space Agency through the contract 67/ 2013. Some of the equipments used in this research were purchased in the frame of the project "CETAL", contract 8PM/2010, financed by UEFISCDI.

[1] M. C. GAIDIS ET AL., FREQUENCY-CONTROLLE SOURCE OF FAR-IR RADIATION FOR SPACE-BORNE APPLICATIONS, IN PROCEEDINGS OF IEEE ULTRASONICS AND FREQUENCY CONTROL CONFERENCE, KANSAS CITY (2000).

[2] J. DEMAISON, K. SARKA, AND E. A. COHEN (EDS.), SPECTROSCOPY FROM SPACE, KLUWER, DORDRECHT, 317 (2001).

[3] C.F. WILSON ET AL., EXPERIMENTAL ASTRONOMY, 33, ISSUE 2-3, 305 (2012).

[4] S. K. ATREYAA ET AL., PLANETARY AND SPACE SCIENCE, 55, ISSUE 3, 358 (2006),

[5] R. L. PASSMORE ET AL., USING IR LASER HETERODYNE RADIOMETRY TO SEARCH FOR METHANE ON MARS, UNIVERSITY OF OXFORD REPORT (2010).

[6] H.-W. HÜBERS ET AL., LIQUID-CRYOGEN FREE FRONT-END FOR A 2.5-THZ HETERODYNE RECEIVER, PROCEEDINGS OF 22ND INTERNATIONAL SYMPOSIUM ON SPACE TERAHERTZ TECHNOLOGY, TUCSON, 12 (2011).

[7] D. WEIDMANN, R. ROSE AND M. JENKINS, A FULLY INTEGRATED, MINIATURIZED QUANTUM CASCADE LASER HETERODYNE RADIOMETER FOR EO, PRESENTED AT NCEO/CEOI CONFERENCE, NOTTINGHAM (2012).

The Application of Desorption Mass Spectrometry Technique to the Growth of >3µm diode lasers in MBE

R. Kaspi[1], A. Lu, C. Yang[1], T. Newell[1], S. Luong[1]*

[1]Air Force Research Laboratory, Directed Energy Directorate Albuquerque, New Mexico, 87117 USA
*corresponding author: ron.kaspi@us.af.mil

GaSb-based type-I quantum well diode lasers emitting at >3µm are in demand for a variety of spectroscopic applications, yet are a challenge to produce due to the diminishing hole confinement barrier. The use of AlInGaAsSbquinary barriers and InGaAsSb quantum wellsprovides some relief to this [1], however the molecular beam epitaxy (MBE) growth of such mixed As/Sb heterostructuresremains challenging and necessitates extensive ex-situ composition calibration.

We use the desorption mass spectrometry (DMS) technique to analyze the desorbed Sb species in real-time during MBE [2]. We demonstrate that the DMS technique may be used to calibrate the V/III ratio, the group-III ratio, as well as the As/Sb ratio (Fig. 1) in alloys prior to the growth of a heterostructure. We also further develop the DMS technique for use during the growth of digitally grown mixed As/Sb quaternary or quinary alloys.

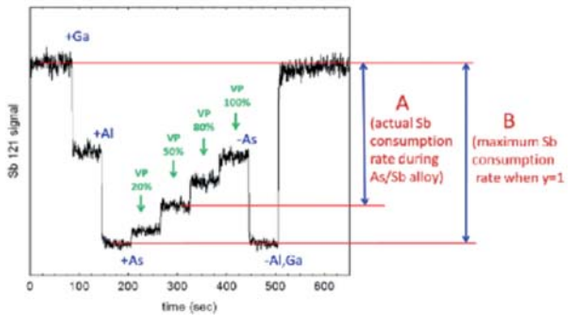

Fig.1. In-situ DMS calibration of As/Sb content in AlGaAs1-ySby alloy with As valve position (VP). Sb-content y is given by A/B.

For demonstration purposes, we start with an un-calibrated MBE system, use the DMS technique to calibrate all of the previously undetermined MBE parameters and grow a ~3.3µm diode laser heterostructure in only one attempt. The design nominally contains $Al_{0.9}Ga_{0.1}As_{0.07}Sb_{0.93}$ clad layers, a 600-nm thick $Al_{0.2}In_{0.25}Ga_{0.55}As_{0.25}Sb_{0.75}$waveguidewith three 10-nm thick $In_{0.52}Ga_{0.48}As_{0.24}Sb_{0.76}$QWs.

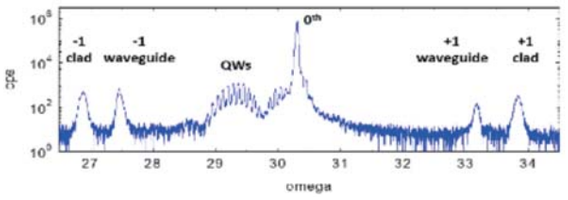

Fig.2. (004) omega/2θx-ray diffraction spectrum of laser heterostructure, indicates excellent lattice-match of digital alloy clad and waveguide layers using DMS technique.

The x-ray diffraction (004 Ω/2θ)spectrum shown in Fig.2 indicates excellent lattice match of the clad and waveguide layers that are digitally grown. The QWs are compressively strained approximately 1.5%.

Near room temperature pulsed LI results for the 1mm x 100µm uncoated gain-guided device are shown in Fig.3. At 20 C, and λ~3.28µm, a total output power of ~42mW is obtained at an injection current of 4.5 A. At 4 C, ~140mW of total output is obtained. These results compare well with the best results published at ~3.3µm to date [3].

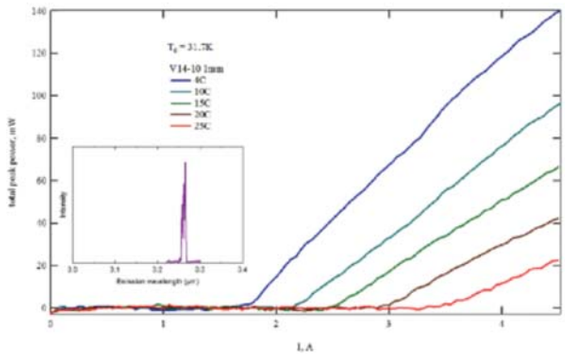

Fig.3. LI characterization of 1mmx100µm uncoated gain-guided devices using 500ns pulses at 10 kHz.

Given that the laser described here was grown without any ex-situ calibration growths, this study demonstrates the value of the DMS technique to quickly converge toward acceptable growth recipes for complicated mixed As/Sb heterostructures without the need for time consuming and costly additional growths for calibration.

[1] M. GRAU, C. LIN, O. DIER, C. LAUER, AND M.-C.AMANN, APPL. PHYS. LETT. 87, 241104 (2005).
[2] R. KASPI, W.T. COOLEY, K.R. EVANS, J. CRYSTAL GROWTH 173, 5 (1997).
[3] G. BELENKY, L. SHTERENGAS, G. KIPSHIDZE, AND T. HOSODA, IEEE J. SEL. TOPICS IN QUANTUM ELECTRONICS 17, 1426 (2011).

Short-wave Infrared PbS Colloidal Quantum Dot Photodetectors with AlOx Atomic Layer Deposition Passivation

*Chen Hu[1,2,3], Alban Gassenq[1,2], Yolanda Justo[2,3], Kilian Devloo-Casier[4], Hongtao Chen[1,2,5], Haolan Zhao[1,2], Christophe Detavernier[4], Zeger Hens[2,3] and Günther Roelkens[1,2]**

[1]Photonics Research Group-INTEC, Ghent University-imec, Sint-Pietersnieuwstraat 41, 9000 Ghent, Belgium
[2]Center for Nano- and Biophotonics, Ghent University, Belgium
[3]Physics and Chemistry of Nanostructures Group, Ghent University, Krijgslaan 281-S3, B-9000 Gent, Belgium
[4]Department of Solid State Sciences, CoCooN, Ghent University, Krijgslaan 281-S1, 9000 Gent, Belgium
[5]IMEC, Kapeldreef 75, 3001 Leuven, Belgium
*corresponding author: gunther.roelkens@intec.UGent.be

Short-wave infrared (SWIR) detectors are typically based on III-V epitaxial materials, resulting in expensive devices, especially when used in a linear on two-dimensional focal plane array. Colloidal quantum dots (QDs) as a new optoelectronic material, provides an alternative way to achieve SWIR photodetectors, either as discrete components or being integrated on photonic integrated circuits. The colloidal QDs are prepared by simple hot injection chemical synthesis, which provides a significant cost reduction. Due to the quantum size effect, the electrical and chemical properties of QDs can be easily modified. Moreover, the fact that the suspension of QDs is in solution allows straightforward integration on large area substrates.

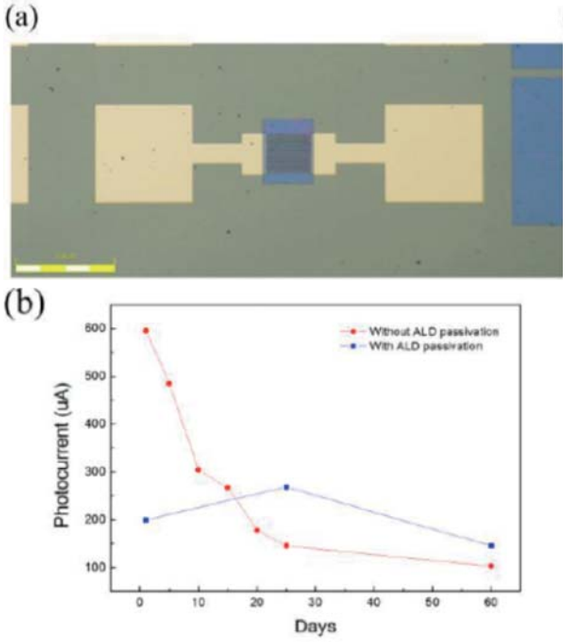

Fig.1. a) Top view of PbS QD photodetector; b) Photocurrent of S^{2-} terminated PbS photodetectors with 1 mW incident power at different time intervals. The bias voltage is 2V.

In this study, PbS colloidal QDs were investigated for SWIR photodetector applications. Starting from colloidal QDs with their as-synthesized organic ligands, a layer-by-layer approach is used to fabricate uniform, ultra smooth and crack-free QD films. Each cycle involves a deposition of a QD layer by dip coating, the replacement of native organic ligands by inorganic moieties (S^{2-} and OH^-), followed by a thorough cleaning of the film afterwards. Here the short inorganic ligands are used to facilitate the charge carrier transport. The PbS QD films are fabricated on a pair of interdigitated gold electrodes. Afterwards a selective wet-etching approach is used to achieve micropatterned QD film and the resulting films are then passivated with aluminum oxide film through atomic layer deposition (ALD) to realize air stable devices.

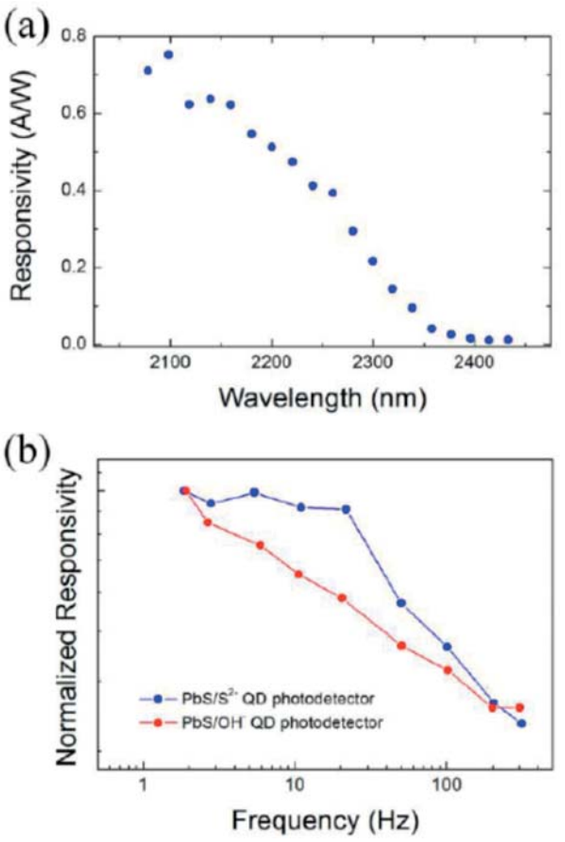

Fig.2. a) Detector responsivity as a function of wavelength for S^{2-} capped PbS QD photodetector with 276 μW incident power; b) Responsivity versus modulation frequency measured at a wavelength of 2250 nm with 5 mW incident power.

After passivation, the QD photodetectors exhibit improved stability and performance in air. A 2.4μm cut-off wavelength is obtained. The detector time response is suitable for imaging applications.

[1] G. KONSTANTATOS, I. HOWARD, A. FISCHER AT AL., NATURE 442, 180-183 (2006).
[2] I. MOREELS, K. LAMBERT, D. SMEETS AT AL., ACS NANO 3(10), 3023–3030 (2009). [3] C. HU, T.AUBERT, Y. JUSTO AT AL., NANOTECHNOLOGY 25, 175302 (2014).

Long-wave ZGP optical parametric oscillator pumped by a Ho:YLF laser

Yuan Ligang[1], Zhao Hong[1], Han Long[1], Chen Guo[1], Zhou Shouhuan[1]*

[1]Scicence and Technology on Solid-state Laser Laboratory, Beijing 100015, China
*corresponding author: greenlaser@sina.com

A high power long-wave infrared laser based on $ZnGeP_2$ optical parametric oscillator pumped by a 2.05 μm Ho:YLF laser at 5KHz pulse repetition rate is reported. When the idler wavelength is tuned at 8.05μm, the maximum output power from the OPO resonator up to 5.1W was obtained at the total pumping power of 55.8W, and the pump to idler conversion efficiency is about 9.1%. At the maximum output power conditions, the measured laser beam quality M2 factor is Mx2 = 4.5, My2 = 4.4 respectively. The wavelength tuning range from 7.5–8.5μm is also achieved by rotating the ZGP crystal. Spectral measurements of OPO output confirm good agreement with theoretical calculations.

Anodic Oxide Grown on the InP Substrate for Gas-Sensing Devices

E.A. Grebenshchikova[1], S.G.Yastrebov[1], V.V.Sherstnev[1], Yu.S. Melnikov[2], Yu.P.Yakovlev[1]*

[1]Ioffe Physical-Technical Institute RAS, 194021, St. Petersburg, Russia
[2]St. Petersburg State Polytechnical University , 195251, St. Petersburg, Russia
*corresponding author: lot160g@gmail.com

Oxide films were grown onto (100) InP substrate (n-type $5x10^{16}cm^{-3}$). Method of anodic oxidation taking place in a solution of phosphoric acid was exploited for this purpose. The current densities in the oxidation cell were varied within the range (1.25-43.2 mA/cm^2) for the whole sets of experiments. The anodizing process was interrupted just after a time interval suitable for formation of the oxide layer, i.e. just after the moment when the current through the oxidation cell dropped dramatically. The oxide films thicknesses and their surface morphology were investigated with scanning electron microscopy and ellipsometry. The Pd layer was deposited onto the top of the oxide films and Au contact was maintained onto the back side of InP substrate, that allowed us to measure the current-voltage characteristics (CVC) of metal (Pd) – oxide (assuming In_2O_3) – semiconductor (InP) structure (MOS-structure). Analysis of CVC shows the favor of Poole –Frenkel emission (PFE) mechanism taking place in the course of electrons transportation through the oxide layer [1]. The model of PFE was exploited for analysis of temperature dependences of CVC measured in a range (90-306) K. It was shown that contribution of two types of PFE centers contributing to CVC is enough to fit the experimental data. These centers resemble potential well with a depth characterizing barrier that an electron must cross to move from one center to another. Heights of two barriers were estimated by a numerical fit of the PFE model equations to the temperature dependence of the selected CVC experimental points taken for a certain voltage, 0.6 V, and occurred to be 0.11±0.05 eV and 0.14±0.06 eV. A sensitivity of the MOS-structure to hydrogen was discovered, that might be promising for practical applications.

[1] S.SZE, PHYSICS OF SEMICONDUCTOR DEVICES , 2ND EDITION, SECTION 7.3.4.

Quantum cascade laser quartz-enhanced photoacoustic absorption spectroscopy for simultaneous monitoring of atmospheric multi-species (CH_4, N_2O and H_2O vapor)

Hongming Yi[1,2], Olivier Laurent[3], Weidong Chen[1], Michel Ramonet[3], Rabih Maamary[1], Eric Fertein[1], Xiaoming Gao[2]

[1]Laboratoire de Physicochimie de l'Atmosphère, Université du Littoral Côte d'Opale, Dunkerque, France
[2]Laboratory of Atmospheric Physico-Chemistry, Anhui Institute of Optics and Fine Mechanics, CAS, Hefei, China
[3]Laboratoire des Sciences du Climat et de l'Environnement, 91191 Gif sur Yvette
*corresponding author: chen@univ-littoral.fr

In the present work, a sensor based on QEPAS incorporating a mid-IR external cavity quantum cascade lasers (EC-QCL, Daylight Solutions Inc.) was developed for simultaneously monitoring atmospheric CH_4, N_2O and water (H_2O) vapor around 8 µm. the developed QEPAS sensor platform, time series measurements of atmospheric CH_4 (~2 ppm) and N_2O (300 ppb) have been performed over several days at the LSCE. Real-time Kalman filtering has been implemented to significantly improve the measurement precision. Under the optimal condition, minimum detection limits of 50 ppb for CH_4, 30 ppb for N_2O, and 500 ppm for H_2O were achieved.

Methane (CH_4) and nitrous oxide (N_2O) are the important greenhouse gases. Reliable real-time monitoring of CH_4 and N_2O concentration change in the atmosphere is of great interest in atmospheric science, environmental and agricultural monitoring, and industrial process analysis [1]. Quartz-enhanced photoacoustic spectroscopy (QEPAS) [2] is one of the most robust and sensitive spectroscopic techniques allowing sensitive detection of trace gas in a very small air-sample volume (few mm^3). It is very suitable for applications requiring a compact, lightweight, and low cost sensor architecture.

In the present work, a sensor based on QEPAS incorporating a mid-IR external cavity quantum cascade lasers (EC-QCL, Daylight Solutions Inc.) was developed for simultaneously monitoring atmospheric CH_4, N_2O and water (H_2O) vapor around 8 µm. This EC-QCL can be coarsely mode-hop free tunable over 40 cm^{-1} from 1223 to 1263 cm^{-1}, with output powers in excess of 35 mW over the whole spectral coverage and a maximum output power of 80 mW. The QEPAS setup involved off-beam spectrophone configuration using a 5.8 mm long micro-resonator with an inner diameter of 0.80 mm [3].

In order to test and validate the developed QEPAS sensor platform, time series measurements of atmospheric CH_4 (~2 ppm) and N_2O (300 ppb) have been performed over several days at the LSCE. Real-time Kalman filtering has been implemented to significantly improve the measurement precision. Due to the photoacoustic (PA) relaxation effect [4-6], PA signal from CH_4–dry zero air mixtures are smaller than that measured in CH_4–N_2 mixtures because of a slow relaxation rate of oxygen decreasing the PA signal amplitude. H2O vapor present in the atmosphere provides a positive effect by speeding-up the relaxation rate to increase PA signal of CH_4. As a result, the presence of atmospheric water vapor might enhance QEPAS detection sensitivity for CH_4. This is a very important issue for sensor calibration and stability in particular for photoacoustic-based CH_4 sensor. In the present work, the impact of atmospheric water vapor on PA signal of CH_4 and N_2O has been investigated, for the first time, in the mid-IR. The results show that water vapor has a positive enhancement effect on the PA signal of CH_4 that increases with H_2O concentration up to a H_2O concentration of 2.22% (after that, the water vapor effect becomes negligible). This water vapor concentration value is higher than that observed in the near-IR DFB laser based PA sensor [4-7], which reveals a serious issue to be addressed: real-time stabilization and measurement of RH for calibration? Whereas, H_2O effect on PA signal of N_2O is not observable. Under the optimal condition, minimum detection limits of 50 ppb for CH_4, 30 ppb for N_2O, and 500 ppm for H_2O were achieved (using a lock-in time constant of 1 s, with measurement precisions (peak-peak value) of 100 ppb for CH_4 and 30 ppb for N_2O, respectively.

Recent researches [8] show that N_2O emission currently is the single most important ozone-depleting emission and is expected to remain the largest throughout the 21st century. This further emphasizes the importance of long-term measurements of N_2O. The developed cost-effective QEPAS sensor fulfills this need and it is well adapted for simultaneous monitoring of CH_4 and N_2O emission fluxes from soil, farm, combustion of fossil fuels, peat, biofuels, and other emission source.

Experimental detail and preliminary results will be presented. The problems encountered by the QEPAS technique applied to trace gas monitoring and the further improvements will be discussed.

Acknowledgments. The financial supports from the NexCILAS (ANR-11-NS09-0002) and the CaPPA (ANR-10-LABX-005) contracts, as well as the IRENI program are acknowledged.

[1] IPCC, "FOURTH ASSESSMENT REPORT OF THE INTERGOVERNMENTAL PANEL ON CLIMATE CHANGE" (2007)
[2] A.A. KOSTEREV, F.K. TITTEL, D.V. SEREBRYAKOV, A.L. MALINOVSKY, I.V. MOROZOV, REV. SCI. INSTRUM. 76 (2005) 043105
[3] H. YI, K. LIU, W. CHEN, T. TAN, L. WANG, X. GAO, OPT. LETT. 36 (2011) 481-483
[4] S. SCHILT, J.-P. BESSON, L. THÉVENAZ, APPL. PHYS. B 82 (2006) 319-329
[5] N. BARREIRO, A. PEURIOT, G. SANTIAGO, V. SLEZAK, APPL. PHYS. B 108 (2012) 369–375
[6] H. YI, W. CHEN, A. VICET, Z. CAO, X. GAO ET AL., APPL. PHYS. B (2013), DOI: 10.1007/S00340-013-5713-X
[7] A. LINK, R. SAUTER, U. HAAS, J. PHYS. IV FRANCE 125 (2005) 841-844
[8] A.R. RAVISHANKARA, JOHN S. DANIET, ROBERT W. PORTMANN, SCIENCE 326 (2009) 123-125

Supercontinuum generation in robust multimaterial chalcogenide nano-tapers

*S. Shabahang[1], G. Tao[1], and A. F. Abouraddy[1]**

[1]CREOL, The College of Optics & Photonics, University of Central Florida 4000 Central Florida Blvd., Orlando, FL 32765, USA
*corresponding author: raddy@creol.ucf.edu

To harness the large optical nonlinearities offered by chalcogenide glass fibers in the infrared, two perennial challenges must be addressed. First, the robustness of chalcogenide fibers must be overcome to allow for convenient usage of such fibers in optical apparatus. Second, the high chromatic dispersion of chalcogenides must be countered by opposing waveguide dispersion, which requires dispersion engineering in large index contrast structures offering strong field confinement.

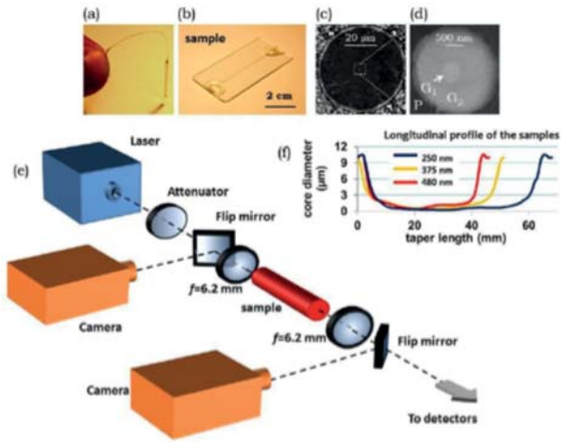

Fig.1. (a) A robust nano-taper. (b) Sample mounted on a glass slide. (c)-(d) SEM of the cross section at the midpoint of the nano-taper. P: polyethersulfone; G1: As2S1.5Se1.5; G2: As2S3. (e) Setup for supercontinuum generation. (f) Measured diameter profile along the nano-tapers used in the experiments.

We present here the results of linear and nonlinear experiments carried out on a new generation of robust multimaterial chalcogenide fibers that address these challenges. Exploiting a novel multimaterial coextrusion technique, we produce step-index fiber preforms comprising a built-in thermally mechanical polymer jacket [1].

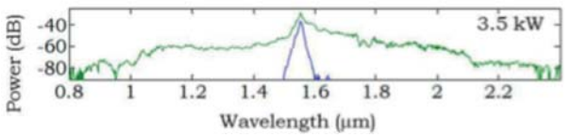

Fig.2. Example of a supercontinuum spectrum generated by a 1-ps pulse at 1.5 μm using the sample in Fig.1.

The preform is thermally drawn continuously into a fiber which may then be tapered to produce robust nano-tapers without removing the polymer jacket. By utilizing a sulfide chalcogenide glass for the cladding and a selenide chalcogenide glass for the core, we ensure large index contrast and thus strong field confinement even at submicron-diameter core sizes. We have characterized the chromatic dispersion of the bulk glass using spectral interferometry and used these results to extract the waveguide dispersion achieved in the nanotapers [2]. Next, we built a theoretical model to predict the nonlinear behavior of these tapers, specifically the potential for infrared supercontinuum generation [3]. Finally, we have carried out experiments using commercially available low-power laser sources, having both picosecond and femtosecond pulse-widths, to produce more than one octave of supercontinuum infrared spectrum [3,4].

[1] G. TAO, S. SHABAHANG, E.-H. BANAEI, J. J. KAUFMAN, AND A. F. ABOURADDY, OPT. LETT. 37, 2751 (2012).

[2] S. SHABAHANG, G. TAO, M. P. MARQUEZ, H. HU, T. R. ENSLEY, P. J. DELFYETT, AND A. F. ABOURADDY, J. OPT. SOC. AM. B 31, 450 (2014).

[3] S. SHABAHANG, G. TAO, J. J. KAUFMAN, AND A. F. ABOURADDY, J. OPT. SOC. AM. B 30, 2498 (2013).

[4] S. SHABAHANG, M. P. MARQUEZ, G. TAO, J. J. KAUFMAN, M. U. PIRACHA, D. NGUYEN, P. J. DELFYETT, AND A. F. ABOURADDY, OPT. LETT. 37, 4639 (2012).

Heterodyne receivers with HEB mixers and compact LO sources for sensitive THz detections

Y. Delorme[1], F. Defrance[1], A. Feret[1], R. Lefevre[1], T. Vacelet[1], F. Dauplay[1], M. Wiedner[1], R. Colombelli[2], and Y. Jin[3]*

[1]Observatoire de Paris – LERMA, CNRS/Université Paris 6, Paris, France
[2]Institut d'Electronique Fondamentale, Université Paris-Sud, Orsay, France
[3]Laboratoire de Photonique et de Nanostructures, CNRS, Marcoussis, France
*corresponding author: yan.delorme@obspm.fr

We are developing superconducting Hot Electron Bolometer (HEB) mixers operating at THz frequencies and have obtained excellent noise temperature at 2.5 THz [1] with as local oscillator (LO) an optically pumped FIR gas laser which is suitable in a laboratory environment but too massive and power hungry for embedded experiments. We have experimented two solid state sources: a frequency amplifier-multiplier chain based on recent Schottky technology and a new type of THz source based on quantum cascade laser (QCL). Measurements performed around 2.7 THz have demonstrated very promising results for future observation missions.

The mixer consists of a phonon-cooled NbN HEB connected to a planar antenna integrated to an extended hemi-spherical silicon lens. The quasi-optical structure is calculated with a full wave electromagnetic solvera and a hybrid approach combining geometrical and physical optics. Heterodyne measurements have been performed by using the Y factor method. The first experiment has been performed with a source from Virginia Diodes Inc. [2]. It works around 2.6 THz and is based on microwave oscillators followed by amplifier-multiplier chains. The peak power measured at room temperature and in an open laboratory environment is below 2 µW. To be able to pump a HEB mixer for heterodyne measurement, we have developed a test setup using a Martin-Puplett Interferometer (MPI) to overlay the beams of the blackbodies and the LO. The measured mixer's noise temperature is about 1500 K after the correction of the quasi-optical losses in the MPI including atmospheric losses. In our second experiment, the local oscillator is a distributed feedback surface-emitting quantum cascade laser using a GPH resonator [3]. The laser operates in continuous wave mode at 2.7 THz and provides enough power to fully pump the HEB. So the Y factor measurement can be performed with a film of mylar as beam splitter to couple the QCL and the RF signals to the HEB and the noise temperature of about 1400 K has been obtained.

This work has been mainly funded by the CNES - Centre National d'Etudes Spatiales.

[1] Y. DELORME, R. LEFEVRE, W. MIAO ET AL. "A QUASI-OPTICAL NBN HEB MIXER WITH 800K DSB NOISE TEMPERATURE AT 2.5 THZ," PROCEEDINGS OF THE 22ND ISSTT, TUCSON, APRIL 2011.

[2] WWW.VADIODES.COM

[3] G-Y. XU, R. COLOMBELLI, S.P. KHANNA ET AL. "EFFICIENT POWER EXTRACTION IN SURFACE-EMITTING SEMICONDUCTOR LASERS USING GRADED PHOTONIC HETEROSTRUCTURES," NATURE COMMUNICATIONS 3, 952, 2012.

Terahertz spectroscopy of strained layer InAs/GaInSb superlattices

M. Patrashin[1], N. Sekine[1], K. Akahane[1], I. Hosako[1]*

[1]National Institute of Information and Communications Technology, 4-2-1 Nukuikitamachi, Koganei, Tokyo 184-8795, Japan
*corresponding author: mikhail@nict.go.jp

This presentation describes investigation of optical properties of strained layer InAs/GaInSb superlattices (SL) that were developed for long-wavelength, terahertz detectors. The SL samples with a designed energy gap of 10-50 meV at T=50K were measured by means of Terahertz Time Domain Spectroscopy and Fourier Transform Infrared Spectroscopy at temperatures 10-300K. Energy band structures of the SLs and their temperature dependence were calculated by using the eight-band k.p method. Measured transmittance and reflectance spectra were used to evaluate the SL energy gap, the carrier concentration and mobility. The characteristics are compared with the theoretical values and with those obtained from the variable magnetic field Hall effect measurements.

[1] M. PATRASHIN, I. HOSAKO, K. AKAHANE, "TYPE-II INAS/GAINSB SUPERLATTICES FOR TERAHERTZ RANGE PHOTODETECTORS", PROC. SPIE VOL. 8188, 81880G (2011).

[2] H. KALA, G. UMANA-MEMBRENO, M. PATRASHIN, I. HOSAKO, K. AKAHANE, J. ANTOSZEWSKI, L. FARAONE, "IN-PLANE CARRIER TRANSPORT IN INAS/INGASB SUPERLATTICES FOR VLWIR DETECTORS", PROC. SPIE VOL. 9100, (2014).

Brewster "mode" to monitor optically the doping concentration in highly doped semiconductor layers

Thierry Taliercio,[1,2,] Vilianne Ntsame Guilengui,[1,2] Laurent Cerutti,[1,2] Eric Tournié,[1,2] and Jean-Jacques Greffet[3]*

[1]Univ. Montpellier, IES, UMR 5214, F-34000, Montpellier, France
[2]CNRS, IES, UMR 5214, F-34000, Montpellier, France
[3]Laboratoire Charles Fabry, Institut d'Optique, Univ. Paris Sud, UMR CNRS 8501, 2 av. Fresnel, 91127 PALAISEAU, France.
*corresponding author: thierry.taliercio@univ-montp2.fr

We investigate highly-doped InAsSb layers lattice matched onto GaSb substrates by angular-dependent reflectance. A resonant dip is evidenced near the plasma frequency of thin layers. Based on Fresnel coefficient in the case of transverse electromagnetic wave, we propose that this resonance is due to the excitation of a leaky electromagnetic mode, the Brewster "mode", propagating in the metallic layer deposited on a dielectric material. Potential interest of this mode for in-situ monitoring during device fabrication is also discussed.

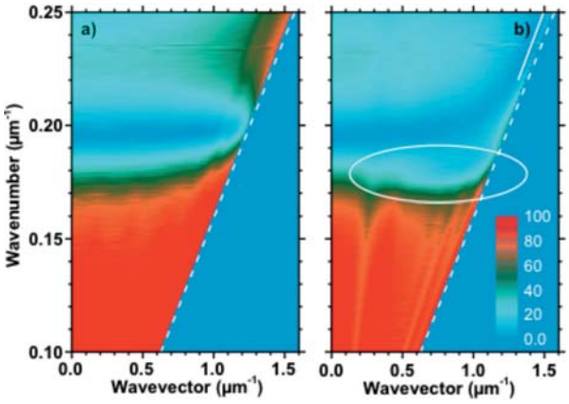

Fig. 1 shows reflectance dispersion of a 1 µm thick layer of InAsSb layer Si-doped at 6 x10^{19} cm^{-3} (Sample A). Fig. 1-a corresponds to the s-polarized (TE) reflectance dispersion whereas Fig. 1-b corresponds to the p-polarized (TM) reflectance dispersion.

Fig. 1: Reflectance dispersion of sample A obtained by angular resolved reflectance a) under s-polarization (TE) or b) under p-polarization (TM) experiment. The white dashed line is the light line in air. The white ellipse selects the resonant dip near the plasma frequency.

The plasma wavenumber, v_p, of the sample is near 0.17 μm^{-1}. Below vp (red part) the InAsSb layer behaves like a metal whereas beyond v_p the InAsSb layer behaves like a dielectric. In the latter we can see interferences due to the multilayered structure of the sample (InAsSb/GaSb). We can identify the resonance under p-polarized light that we can attribute to the Brewster mode (white ellipse). We have developed simulation based on Fresnel coefficient in the case of transverse electromagnetic wave. Using matrix transfer model or solving the dispersion relation of the structure [1] allowed demonstrating that this resonance is due to the excitation of a leaky electromagnetic mode, the Brewster "mode", propagating in the metallic layer deposited on a dielectric material. The Fig. 2 show reflectance dispersion by simulation (Fig. 2-a), and by experiment (Fig. 2-b), in the case of a 1 µm thick layer of InAsSb layer Si-doped at 2 x10^{19} cm^{-3} (Sample B).

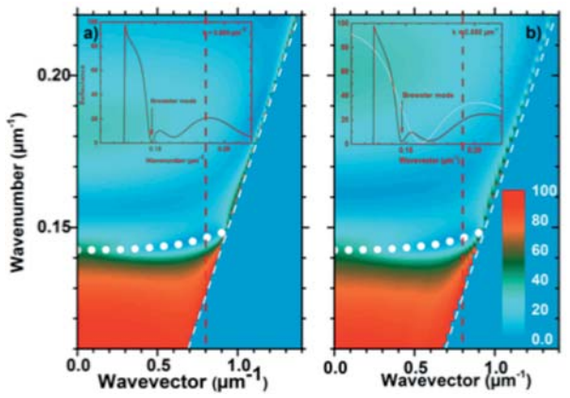

Fig. 2: Reflectance dispersion under TM or p polarization of sample B obtained by angular resolved reflectance a) simulation or b) experiment. The white dashed line is the light line in air. The white circles correspond to wavenumbers associated to the dispersion relation calculated with eq. (3) of ref. 1 with sample B parameters. Insets correspond to the spectra for k = 0 (white) or 0.800 µm-1 (red) corresponding to the red dashed line of the 2D image.

The white circles correspond to wavenumbers associated to the dispersion relation calculated with eq. (3) of ref. 1 with sample B parameters. We can observe a good agreement between experiment and simulation.

This mode can be used for in-situ monitoring during epitaxy of device heterostructures. Fig. 3 shows an example of plasma frequency versus carrier density in the case of Si doped InAs. The black squares correspond to data extracted from ref. 2. The red dashed line is a power law fitting the InAs data.

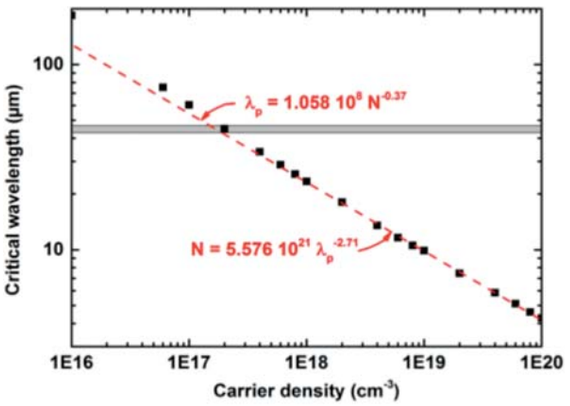

Fig. 3: Critical wavelength, λp, versus the carrier density in the case of InAs. The red dashed line corresponds to the power law extracted from Fig. 3. The grey part of the figure corresponds to the Reststrahlen band due to optical phonon.

[1] T. TALIERCIO, V. NTSAME GUILENGUI, L. CERUTTI, E. TOURNIÉ, AND J.-J. GREFFET SUBMITTED TO OPTICS EXPRESS.
[2] M.P. MIKHAILOVA, IN HANDBOOK SERIES ON SEMICONDUCTOR PARAMETERS, M. LEVINSHTEIN, S. RUMYANTSEV AND M. SHUR, ED., (WORLD SCIENTIFIC, LONDON, 1996) VOL. I, PP. 147-168.

Three mirror Off Axis Integrated Cavity Output Spectroscopy using a Quantum Cascade Laser for the detection of ethylene

R. Centeno[1], J. Mandon[1], S. M. Cristescu[1], F. J. M. Harren[1]*

[1]Life Science Trace Gas Facility, IMM, Radboud University Nijmegen Heyendaalseweg 135, 6525 AJ Nijmegen, the Netherlands
*corresponding author: r.centeno@science.ru.nl

We demonstrate the performance of a compact and robust gas sensor based on a pulsed quantum cascade laser in combination with off-axis integrated cavity output spectroscopy (OA-ICOS) in an improved three mirror configuration. For regular OA-ICOS a detection limit of 10 ppbv (part-per-billion volume) is demonstrated for ethylene in 2 min averaging time. An improved three mirror configuration OA-ICOS scheme showed a 4 times increase in sensitivity as compared to standard OA-ICOS. The sensor was used for ethylene detection from apples, stored under controlled atmosphere conditions.

For the development of a compact and easy to operate ethylene detector to monitor and control its emission in growth chambers, greenhouses and fruit storage facilities, we combined a quantum cascade laser with OA-ICOS (Fig. 1). The room temperature laser (wavelength 915 cm^{-1}, laser pulses 30 ns, repetition rate 1 MHz) was wavelength tuned over ~0.25 cm^{-1} with a 4 kHz repetition frequency. We optimized the off-axis diameter of the cavity and the scanning frequency of the laser and achieved a signal-to-noise ratio of 140. The system is a stand-alone unit independent of additional cooling liquids requiring only external power. Furthermore, our OA-ICOS system provides real-time measurements of ethylene with a high finesse cavity yielding 10 ppbv in 128 s averaging time, which is equal to a noise equivalent absorption sensitivity of ~$1 \cdot 10^{-8}$ cm^{-1} $Hz^{-1/2}$. The effect of controlled atmosphere conditions on the ethylene production of apples was successfully measured, showing its applicability to fruit storage.

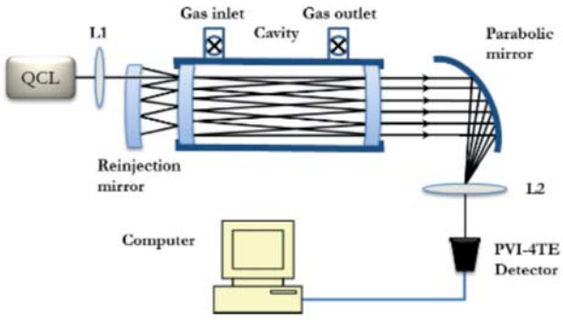

Fig.1: Schematic of the experimental setup. QCL: pulsed quantum cascade laser; L1, L2: focusing and collimating lens, respectively; PVI-4TE detector: four stages thermoelectrically cooled detector.

The sensitivity of the OA-ICOS system can be enhanced by a factor 4 by using a re-injecting mirror to reflect the light into the cavity (Fig. 1). Simulations indicate that carefully choosing the parameters of the cavity and re-injection mirror yield enhancements of up to one order of magnitude. The practicality of this system and future improvements will be discussed.

The study of the injector doping on lasing properties of 4.3µm InAlAs-InGaAs-InP quantum cascade lasers

Y. Y. Li[1], A. Z. Li[1], Y Gu[1], K Wang[1], C. F. Cao[1], H S B Y Li[1], Shumin Wang[1]*

[1]State Key Laboratory of Functional Materials for Informatics, Shanghai Institute of Microsystem and Information Technology, Chinese Academy of Sciences, Shanghai 200050, People's Republic of China
*corresponding author: azli@mail.sim.ac.cn

Currently, significant progresses of mid-infrared quantum cascade lasers (QCLs) that emit more light than heat in continuous-wave operation at room temperature with power up to watts[1, 2] have been achieved. In order to accelerate and to carry forward QCLs applications in emerging strategic areas, efforts to fulfill this target are to improve QCLs materials and devices with stabilized performance.

The research of the QCL was initially focused on optimizing active region in order to obtain continuous-wave operation at room temperature with low threshold currents density. The injector doping density is an important factor that influences the lasing properties of laser at continuous-wave operation. It is demonstrated that the effect of the injector doping densities on lasing properties of InAlAs-InGaAs-InP QCLs at 4.3µm.

For the experimental investigations of the injector doping effects, three wafers with different average injector doping concentrations of1.68, 1.94 and 2.07E^{17}cm^{-3} have been grown. The "double-phonon-resonance" active region was used in our lasers. The material system of QCL was InGaAs/InAlAs/InP lattice matched to InP substrate and was grown by gas source molecular beam epitaxy. Figure 1 shows a typical x-ray diffraction pattern and simulation for the 30 stages QCL whole structure employed in this study. The wafers were then processed into ridge waveguide lasers, details of device processing and measurement setup were described in ref. [3].

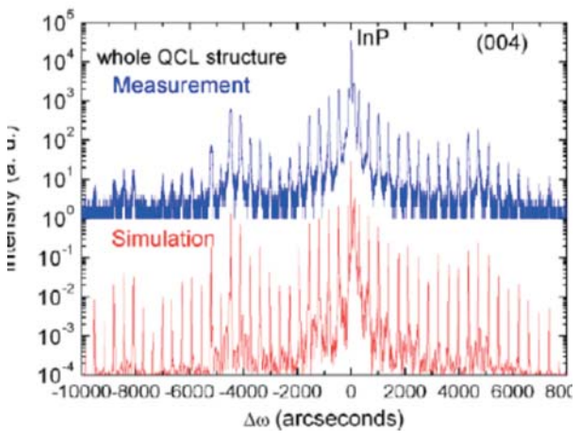

Fig.1. A typical x-ray diffraction pattern and simulation for the 60 stages QCL whole structure employed in this study.

In the QCLs, the injector doping density should be large enough to achieve population inversion and make the gain to become larger than the losses. The increased doping density initially increases the population inversion and allows for higher injected currents in the same voltage, as shown in Figure 2 (a). But an increasing doping of injector increases the scattering rate of electrons from the injector back into the active region and the optical losses due to free-carrier absorption, both effects will reduce the gain. Figure 2 (b) shows the light output power versus current curves of three different doped lasers, the QCL with 6.5E^{17}/cm^{3} exhibited the lowest threshold current of 0.82A at 77K.

Fig.2. a) The voltage versus current curves of three different doped lasers. b) The

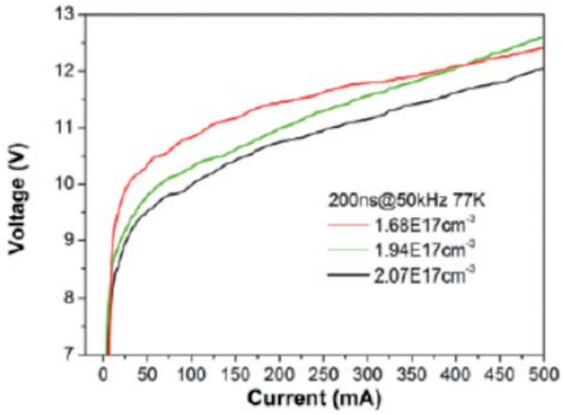

(a)

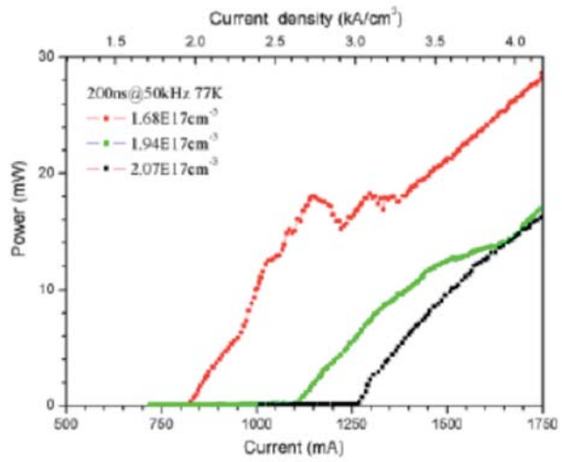

(b)

light output power versus current curves of three different doped lasers.

In conclusion, the lasing properties of 4.3µm different doped QCLs have been studied, laser with high doped injectors had higher injected currents, high characteristic temperature but higher threshold current and lower power.

This work is financially supported by the National Natural Science Foundation of China projects under contract No. 60906047.

[1] M.RAZEGHI, IEEE J .SEL. TOP. QUANT., 15, 941 (2009)
[2] Y.BAI, S.SLIVKEN, ET AL, NATURE PHOTONICS, 4, 99 (2010)
[3] LI A Z, XU G Y, ET AL, J. CRYSTAL GROWTH, 278, 770 (2005)

GaAs-$Al_xGa_{1-x}As$ superlattices with mixed disordered and its effect on the wavelengths infrared laser

R Djelti[1], S Bentata[1], Z Aziz[1] and A Besbes[1]*

[1]Département Sciences et technique, Faculté des sciences et de la technologie Université Abdelhamid Ibn Badis - Mostaganem Laboratoire de technologie et propriétés du solide BP 227 Mostaganem 27000, Algérie.
*jdocfst@yahoo.fr

Laser infrared radiation, having a wavelength between ultraviolet and visible, has a number of highly interesting applications in biological imaging, surface chemistry, and high-field condensed matter studies. Many materials have been the subject of investigation in the infrared. Interest has focused on wavelengths between (4 µm and 20 µm) length required by the IR photodetectors and IR cameras but in recent years, the focus is increasingly on longer wavelengths required on space applications telecommunications, rapid detection and new opto-electronic devices. The interesting aspect of this work is the systematic study of the influence of correlated structural disorder on the transmission property and wavelenght of Dimer and Trimer Height Barrier Superlattices (DHBSL/THBSL). Ours system consists of a stack ultra fine layer of semiconductor which are alternated periodically, where the small gap material (GaAs) plays the well potential role, and the large gap material (AlGaAs) plays the barrier potential role.

For the dimer structure, the electron will emit on 11.02 µm wavelength corresponding to jump 182 meV, while the trimer structure electron will emit on three wavelengths (38.19 µm, and 66.21 µm 104.52 µm) respectively corresponding to jump (50 meV, 30 meV and 20 meV). We notice that this wavelength range matches to the range required by the infrared photodetectors (4 to 20 µm), infrared cameras (8 to 12 µm), fluid detectors and biological molecules detectors (60 to 200 µm).

We have observed from measurements of wavelength, that the introduction of correlated structural disorder by (Doublet, Triplet, Quadruplets, Quintuplets…) provides more wavelengths located above visible domain (far-infrared, microwave).

Keywords: superlattices (SLs), correlated structural disorder, transmission coefficient, Laser infrared wavelength (IR)

Spectroscopic , Surface texture, and Optical Properties study of $Si_{1-x}Ge_x$/p-Si<100> MQWs at room Temperature

*Kifah Q. salih Esmail[1]**

[1]Ministry of higher education & scientific Research h/p:00964-07711973084, Iraq-Baghdad
*Corresponding author: mekqs10@yahoo.com

In the recent years, study of $Si_{1-x}Ge_x$/p-Si<100> MQWs at room temperature have attracted considerable attention and display several attractive electron and optical properties for optoelectronic applications. The spectroscopic studies such as FTIR spectra, surface texture (AFM) and optical properties (refractive index) are interested for device applications. The aim of this work to give new results of $Si_{1-x}Ge_x$/p-Si<100> MQWs at room temperature. We applied new simple thermal method for that. This study used 10-period multiple quantum wells of $Si_{0.8}Ge_{0.2}$/p-Si<100>,with 5 nm well width and were grown using LPCVD technique. Spectroscopic, surface texture and optical properties were performed using FTIR homemade system, AFM and Ellipsometry respectively . All measurements have done at room temperature. We have reported change in the refractive index, FTIR spectra and surface texture after treatment. In this paper, we demonstrate the optimum results.

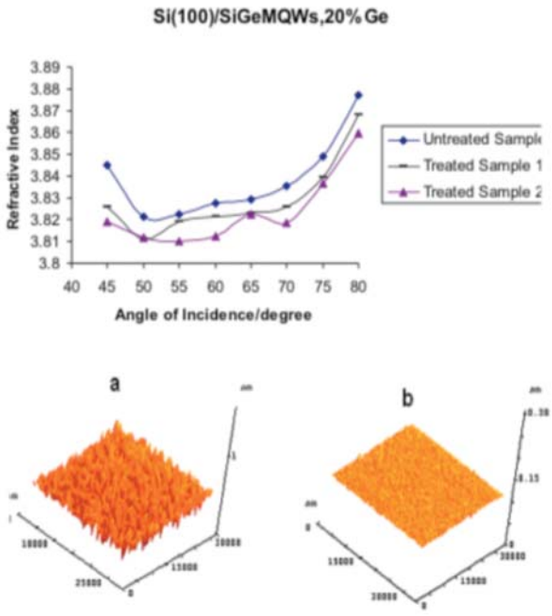

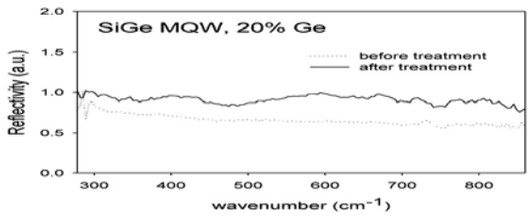

[1] V.A. EGOROV, G.E. CIRLIN, A.A. TONKIKH, V.G. TALALAEV, A.G. MAKAROV, N.N. LEDENTSOV, V.M. USTINOV, AND P. WERNER, PHYSICS OF THE SOLID STATE, VOL.46, NO.1, 49-55(2004).

[2] P. MURZYN, C.R. PIDGEON, J.P.R. WELLS, I.V. BRADLEY, Z. IKONIC, R.W. KELSALL, P. HARRISON, S.A. LYNCH, D.J. PAUL, D.D, ARNONE, D.J. ROBBINS, D.NORRIS AND A.G. CULLIS, APPL. PHYS. LETTERS, 1-3(2002).

[3] M.R. HASHIM, KIFAH. Q. SALIH, D. BAGNELL AND P. IAMRAKSA, ELECTROCHEMICAL SOCIETY PROCEEDINGS VOLUME, 299-303, (2004-07) HAWAI.

Tuesday, 7 October

Tu-A

Mid-IR Sources: Lasers II

8:00-10:20

20 Years of Interband Cascade Lasers and Related Devices (invited)

*Rui Q. Yang[1]**

[1]School of Electrical and Computer Engineering, University of Oklahoma, Norman, OK, USA
*corresponding author: Rui.Q.Yang@ou.edu

Interband cascade (IC) lasers [1-5] are quantum-engineered mid-infrared (IR) lasers that combine the advantages of conventional interband diode lasers and quantum cascade (QC) lasers [6]. It has been 20 years since the proposal of the IC laser concept in a poster presentation [1] at the *7th International Conference on Superlattices, Microstructures and Microdevices,* held in August of 1994. The presentation mainly discussed some approaches to achieve intersubband lasing; while the idea of utilizing interband transitions for a cascade laser with the use of type-II InAs/GaSb quantum well structures was discussed only briefly. Hence, the title of the presentation (and the corresponding paper [2] published in 1995) focused on infrared lasers based on intersubband transitions. Another factor was that this title had been given for the submitted abstract to the conference in early of March 1994 before the demonstration of QC lasers was reported in the April issue of Science [6]. At that time, the author was very interested in the first realization of an intersubband laser, a topic he had worked on for several years [7-9]. After seeing the report of QC lasers in Science, the author's activities largely shifted to the development and implementation of IC lasers.

This talk will discuss, from a retrospective view, how IC lasers have been developed from an initial concept to practical devices, and how the concept has been expanded to other related optoelectronic devices such as IC IR photodetectors (ICIPs) and photovoltaic cells [10-12]. Personal opinions and comments on some subjects will be given along with the discussion.

[1] R. Q. YANG, "INFRARED LASER BASED ON INTERSUBBAND TRANSITIONS IN QUANTUM WELLS", 7TH INTER. CONF. ON SUPERLATTICES, MICROSTRUCTURES AND MICRODEVICES, PAPER P3.80, BANFF, CANADA, AUG. 22-26, 1994.

[2] R. Q. YANG, "INFRARED LASER BASED ON INTERSUBBAND TRANSITIONS IN QUANTUM WELLS," SUPERLATTICES AND MICROSTRUCTURES 17, 77 (1995).

[3] J. R. MEYER, I. VURGAFTMAN, R. Q. YANG, AND L. R. RAM-MOHAN, "TYPE-II AND TYPE-I INTERBAND CASCADE LASERS", ELECTRON. LETT., 32, 45 (1996).

[4] R. Q. YANG, "NOVEL CONCEPTS AND STRUCTURES FOR INFRARED LASERS", CHAPTER 2 IN LONG WAVELENGTH INFRARED EMITTERS BASED ON QUANTUM WELLS AND SUPERLATTICES, ED. M. HELM, SINGAPORE: GORDON AND BREACH SCIENCE PUBLISHERS, 2000.

[5] I. VURGAFTMAN, ET AL., "INTERBAND CASCADE LASERS WITH LOW THRESHOLD POWERS AND HIGH OUTPUT POWERS", IEEE J. SELECT. TOP. QUANTUM ELCTRON., 19, 1200210 (2013); AND REFERENCES THEREIN.

[6] J. FAIST, F. CAPASSO, D. L. SIVCO, C. SIRTORI, A. L. HUTCHINSON, AND A. Y. CHO, "QUANTUM CASCADE LASERS", SCIENCE 264, 553 (1994).

[7] R. Q. YANG AND J. M. XU, "POPULATION INVERSION THROUGH RESONANT INTERBAND TUNNELING", APPL. PHYS. LETT., 59, 181 (1991).

[8] R. Q. YANG AND J. M. XU, "LEAKY QUANTUM WELLS: A BASIC THEORY AND APPLICATION", CAN. J. PHYS., 70, 1153 (1992).

[9] R. Q. YANG, "PHASE TIME DELAY FOR INTERBAND TUNNELING IN LEAKY QUANTUM WELLS", PHYS. LETT. A, 186, 339 (1994).

[10] R. Q. YANG, Z. TIAN, Z. CAI, J. F. KLEM, M. B. JOHNSON, AND H. C. LIU, "INTERBAND-CASCADE INFRARED PHOTODETECTORS WITH SUPERLATTICE ABSORBERS", J. APPL. PHYS., 107, 054514 (2010).

[11] R. Q. YANG, Z. TIAN, J. F. KLEM, T. D. MISHIMA, M. B. SANTOS, AND M. B. JOHNSON, "INTERBAND CASCADE PHOTOVOLTAIC DEVICES", APPL. PHYS. LETT., 96, 063504 (2010).

[12] R. Q. YANG, H. LOTFI, L. LI, R. T. HINKEY, H. YE, J. F. KLEM, L. LEI, T. D. MISHIMA, J. C. KEAY, M. B. SANTOS, AND M. B. JOHNSON, "QUANTUM-ENGINEERED INTERBAND CASCADE PHOTOVOLTAIC DEVICES", PROC. OF SPIE, 8993, 899310 (2014); AND REFERENCES THEREIN.

Pseudomorphic and metamorphic schemes for InP-based 2-3 µm quantum well lasers

Y. Gu[1], Y. G. Zhang[1], Y. Y. Cao[1], X. Y. Chen[1], L. Zhou[1], S. P. Xi[1], A. Z. Li[1], Hsby. Li[1]*

[1]State Key Laboratory of Functional Materials for Informatics, Shanghai Institute of Mocrosystem and Information Technology, Chinese Academy of Sciences,200050 Shanghai, China
*corresponding author: ygzhang@mail.sim.ac.cn

Mid-infrared semiconductor lasers in the wavelength range of 2-3 µm have aroused increasing interests as their applications on medical diagnostics, environmental sensing, etc. are expected. Besides the main approach of antimony-containing type-I quantum well (QW) lasers on GaSb substrates, InP-based $In_xGa_{1-x}As$ (x>0.53) QW structure is an attractive alternative to accessing to this wavelength range, both from the view points of the superior quality of InP substrate and mature growth and processing technology of InP-based antimony-free structures. In this approach, the indium composition in InGaAs QW should be increased, therefore the strain in QW becomes the main challenge and restrains the wavelength increase. By using pure InAs [1] or triangular InAs-containing QW [2],RT-CW lasers around 2.3 µm have been reached.

In this presentation, we will review our recent works on InP-based QW lasers in 2-3 µm wavelength range by using pseudomorphic and metamorphic schemes, respectively [3-5]. The energy-band diagrams are shown in Fig. 1 schematically. In the pseudomorphic scheme, triangular shape QW was applied to increase the lasing wavelength while restricting the strain.

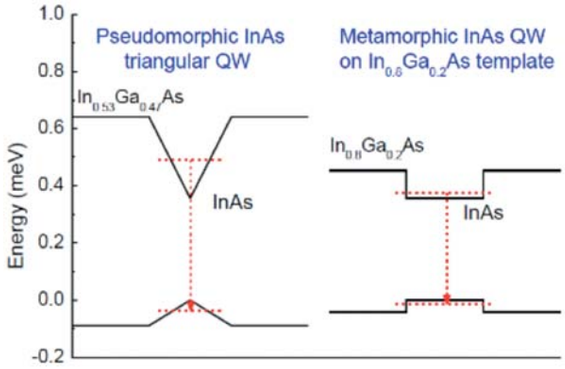

Fig.1. Schematic energy-band diagrams of pseudomorphic triangular and metamorphic InP-based type-I QW.

Digital alloy technology was used to construct the triangular QW during the MBE growth, where the compositional graded well profile was approximated by short period supperlattice of InAs and $In_{0.53}Ga_{0.47}As$ at digitally setting thicknesses. The effects of various structural and processing parameters on the laser performances were investigated and optimized in detail. The lasers with CW lasing from 2.2 to 2.4 µm at RT have been achieved by adjusting the triangular QW width from 10 nm to 19 nm, whose typical lasing spectra are shown in Fig. 2. To extend the emission wavelength longer, metamorphic scheme was employed. A metamorphic $In_{0.8}Al_{0.2}As$ template was grown on InP substrate to produce a virtual substrate with larger lattice constant than InP, and InAs QWs were then grown on the $In_{0.8}Al_{0.2}As$ template.

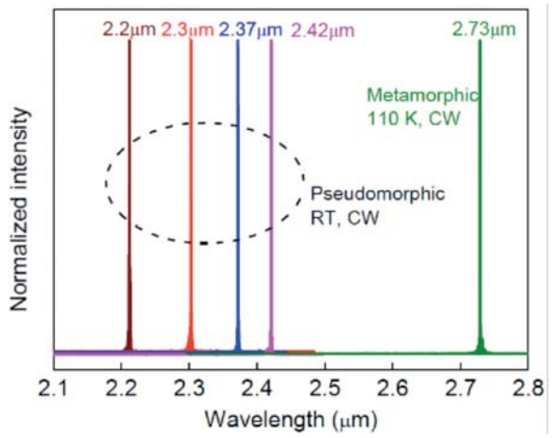

Fig.2. Normalized lasing spectra of demonstrated InP-based antimony-free type-I QW lasers.

Therefore, the InAs well layer can be much wider to increase the lasing wavelength. Considering the limited material choices, the barrier and waveguide layers were optimized carefully. By using this metamorphic scheme, lasers with lasing wavelength up to 2.73µm under CW operation have been demonstrated by applying 15 nm InAs QWs. At present the highest working temperature is at 110 K mainly due to the limitations of material quality and carrier confinements.

[1] T. SATO, M. MITSUHARA, N. NUNOYA, ET AL., IEEE PHOTONICS TECHNOL. LETT. 20, 1045 (2008).
[2] G. BOEHM, M. GRAU, O. DIER, ET AL., J. CRYST. GROWTH 301-302,941 (2007).
[3] Y. GU, Y. G. ZHANG, Y. Y. CAO, ET AL., APPL. PHYS. EXPRESS 7, 032701 (2014).
[4] Y.Y. CAO, Y. G. ZHANG, Y. GU, ET AL., IEEE PHOTONICS TECHNOL. LETT. 26, 571 (2014).
[5] Y.Y. CAO, Y. G. ZHANG, Y. GU, ET AL., APPL. PHYS. LETT.102, 201111 (2013).

Index-coupled distributed-feedback GaSb-based lasers diodes in the 2.3 to 3µm wavelength range

Q. Gaimard[1,2], A. Larrue[3], L. Cerutti[1,2], Y. Rouillard[1,2], O. Gauthier-Lafaye[3], R. Teissier[1,2], A. Vicet[1,2].*

[1]Univ. Montpellier, IES, UMR 5214, F-34000, Montpellier, France
[2]CNRS, IES, UMR 5214, F-34000, Montpellier, France
[3]CNRS ; LAAS ; 7 avenue du colonel Roche, F-31077 Toulouse Cedex 4, France
*corresponding author: gaimard@ies.univ-montp2.fr

Tunable single-frequency lasers in the 2.3 to 3µm wavelength range, working in continuous wave regime, at room temperature, are needed to develop trace gas sensors, to identify and quantify several gases such as methane and ethylene for environmental purposes. We report on the design and development of 2nd order distributed-feedback (DFB) antimonide-lasers diodes working in this wavelength range.

The structures were grown by molecular beam epitaxy on GaSb substrate. We have chosen an index-coupled approach of the Bragg filter, in order to not degrade the lasers performances. We performed simulation analysis to adjust the Bragg grating period and the global geometry of the structure, to optimize both modal discrimination and optical power of the lasing mode. The grating is realized by holographic lithography. Two technological processes were investigated:

- Side-wall corrugation of the laser ridge, based on an Inductively Coupled Plasma Cl-based deep etching. The quality of the etching can be observed on figure 1.

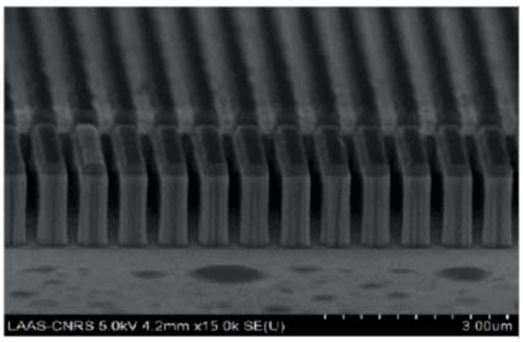

Fig.1. SEM picture of the side-wall corrugation after etching process

- Buried grating, based on an epitaxial regrowth procedure. Regrown interface is shown on figure 2.

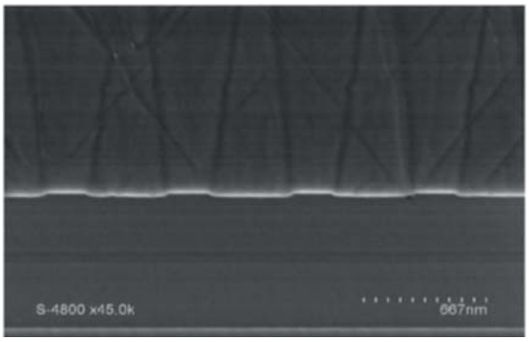

Fig.2. SEM picture of the buried grating after regrowth

We will present the performances of the components working around 2.3µm, realized from both technological developments. They exhibit side mode suppression ratio (SMSR) up to 30dB (figure 3) and the optical power reaches 20mW on a few nanometer large tuning range. Potential utilization will also be illustrated by methane measurements. Upper wavelengths (2.7µm and 3µm) components will also be presented.

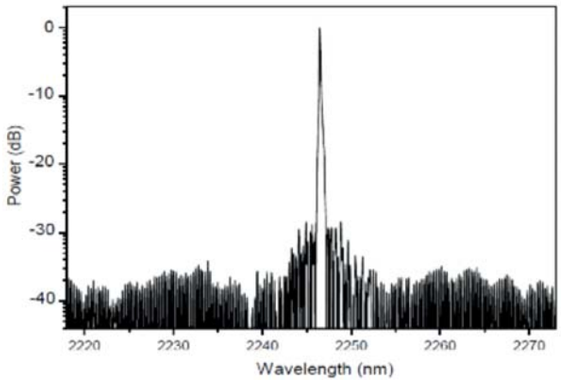

Fig.3. DFB spectrum, SMSR = 30dB

This work is supported by the ANR NexCILAS international project, ANR MIDAS project, by NUMEV labex and RENATECH technological support.

Mid-IR Quantum Well Lasers with a Temperature Insensitive Threshold Current

A. R. Adams[1], I. P. Marko[1], J. Mukherjee[1], S. J. Sweeney[1]*

[1]Advanced Technology Institute and Department of Physics, University of Surrey, Guildford GU2 7XH, UK
*corresponding author: alf.adams@surrey.ac.uk

Despite the success of quantum well lasers in the mid-IR wavelength range, their threshold current is often very sensitive to temperature which has led to the need for active cooling and associated control electronics to stabilize the system. However, such coolers often consume more energy than the laser they are controlling. They also tend to have far less long-term reliability than the laser diode itself. There are consequently many circumstances where it would be advantageous and cheaper to simply compensate for temperature variations by mechanisms built into the epitaxial structure of the laser chip itself. There are several mechanisms that may cause the threshold current (Ith) of mid-infrared semiconductor lasers to increase rapidly with increasing temperature, T. These include thermal broadening of the gain spectrum, thermally activated carrier escape, Auger recombination and inter-valence band absorption. Normally all of these processes act together to cause Ith to increase as T increases. However, here we present a novel design of quantum well active region [1] in which carriers released from some of the wells are fed to the other wells in such a way that these mechanisms compensate rather than augment one another. This idea is, in principle, applicable to a range of materials systems, structures, cavity geometries and operating wavelengths so we first demonstrated the effect in well-established standard 1.55µm GaInAsP/InP edge emitting lasers. The devices were first designed using computer simulation and then grown by MOVPE with seven 6nm wide InGaAsP quantum wells. The results [2] are shown in Fig 1.

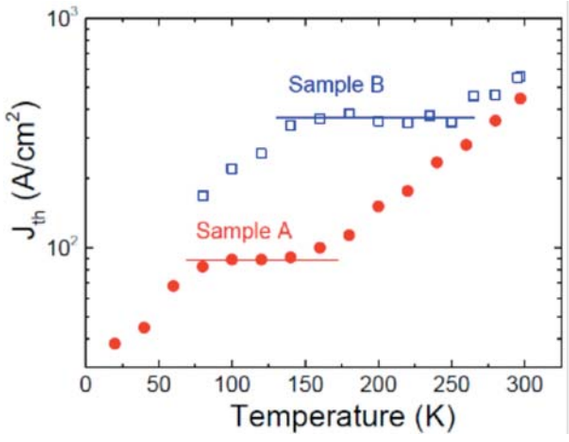

Fig. 1. Temperature dependence of threshold current density in two InGaAsP/InP 1.5 µm laser structures grown according to a simulated design with predicted temperature insensitive behaviour.

In sample "A" a constant threshold current between 80K~ 150K was achieved and this was successfully moved to approximately 140K to 270K in the second sample "B". Extending this work into the mid-infrared, we have undertaken simulations of an InGaAsSb/GaSb device using a similar approach and the first preliminary results are shown in Fig 2.

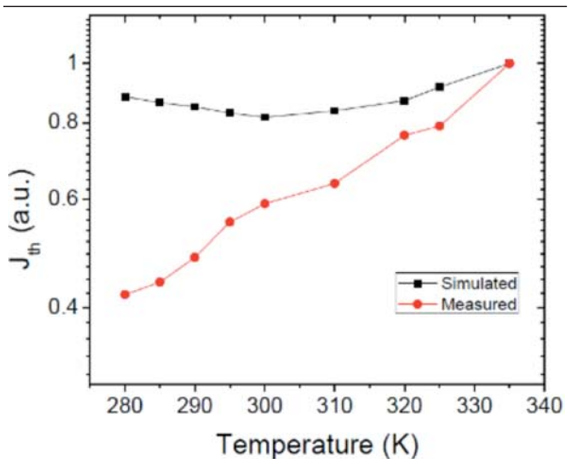

Fig. 2. Simulated temperature dependence of threshold current density in a GaInAsSb/GaSb laser (emitting at 2.28 µm) normalized to the measured Jth (at 335 K) for similar structure emitting at 2.37µm shown for comparison.

The design of the edge emitting device was based on an experimental laser structure and operated at 2.28µm. Experimental results for a standard 2.37µm InGaAsSb/GaSb laser are shown for comparison in Fig 2 and indicate clearly the improved temperature stability that could be obtained with the new design, as shall be discussed further at the conference.

[1] A. R. ADAMS, INTERNATIONAL PATENT APPLICATION WO2012/153136 (2012).
[2] A. R. ADAMS, I. P. MARKO, J. MUKHERJEE, S. J. SWEENEY, A. GOCALINSKA, E. PELUCCHI AND B. CORBETT IEEE ISLC (2014).

Fiber Combining of Mid-IR Lasers

L.B. Shaw[1], R.R. Gattass[1], L.E. Busse[1], F.H. Kung[2], D.J. Gibson[1], V.Q. Nguyen[1], G. D. Chin[2], I.D. Aggarwal[3] and J.S. Sanghera[1]*

[1]Naval Research Laboratory, Code 5620, Washington, DC, USA 20375,
[2]University Research Foundation, Greenbelt, MD, 20770
[3]Sotera Defense Solutions, Crofton, MD 21114
*corresponding author: brandon.shaw@nrl.navy.mil

Multimode fiber combiners provide a compact, robust method for incoherent power and spectral combination of multiple light sources. In the near-IR, silica fiber fused fiber power combiners are often used for combining the output of several diode lasers to pump fiber lasers. In the mid and long-wave IR, fiber combiners fabricated from IR transmitting chalcogenide fiber allow power scaling and spectral beam combining of the output of several quantum cascade lasers and interband cascade lasers without the use of bulk optical elements and in a small form factor package with reduced sensitivity to thermal and vibrational instabilities.

In a N x 1 fiber combiner, N fibers are collected into a bundle inserted in an outer glass tube and tapered by heating and pulling to laterally fuse the bundle into a single output fiber structure. The number of fibers, N, chosen is often based upon the natural hexagonal packing order of cylindrical fiber shapes, i.e., N=7, 19, 61... The optical fields launched into the N input fiber ports of the combiner are guided and modally overlap in the taper region as shown in Figure 1(a). For maximum light transmission and combiner efficiency, the multimode fiber coupler must satisfy the brightness conservation condition

$$\sum_{i=1}^{N} d_{in}^2 NA_{in}^2 = d_{out}^2 NA_{out}^2 \quad (1)$$

where *NAin* and *NAout* are the numerical aperture of the input and output fiber, din and dout are the dimension of the input cladding and output core, respectively; and N is the number of ports in the combiner.

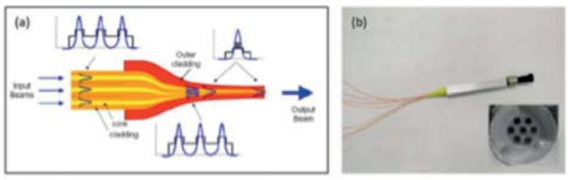

Fig.1. (a) Schematic of fiber combiner concept. (b) Picture of packaged fiber combiner and with close-up of output face

We have demonstrated a 7 x 1 IR fiber combiner using IR transmitting As_2S_3 fiber [1]. A picture of the packaged combiner is shown in Figure 1(b) below. The combiner showed a flat spectral response within the transmission range of the As_2S_3 fiber from ~ 1 to 6 µm. Input port transmission efficiency varied from 76.3% to 90.9%, with an average transmission of 84% as shown in Table 1 below.

Port #	P1	P2	P3	P4	P5	P6	P7	Average
Transmission	89.6	85.5	76.3	76.7	86	83.1	90.9	84.0%

Table 1. Representative port transmission for 7x1 multimode combiner measured at 1.98 µm wavelength

Spectral combining was demonstrated by combining the output of two quantum cascade lasers operating at 4.65 µm and 4.67 µm with a diode laser at 1.93 µm as shown in Figure 3 below. We will report on our progress on increasing the efficiency of the combiner, packaging the combiners and fiber coupling to quantum cascade lasers, and extending the transmission region of the combiners to cover the 2-12 µm wavelength range.

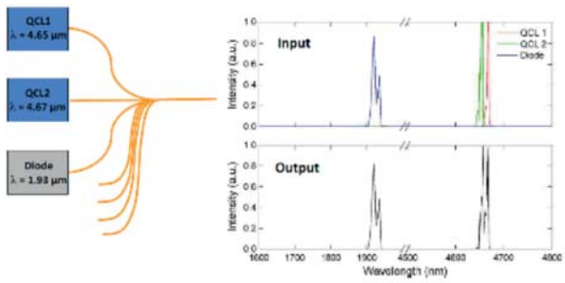

Fig.2. Spectrally combined output of a 4.65 µm quantum cascade laser, a 4.67 µm quantum cascade laser and a 1.93 µm diode laser.

[1] R.R. GATTASS, L.B. SHAW, L.E. BUSSE, J. S. SANGHERA, ET. AL., IEEE PHOTONICS JOURNAL, 5, DOI: 0.1109/JPHOT.2013.2281611 (2013)

InP-based dilute nitride semiconductors as mid-infrared materials for optical applications (invited)

*Y. Kawamura[1]**

[1]Graduate school of enginnering, Osaka Prefecture University, Gakuen-cho 1-2 Naka-ku Sakai 599-8570 Osaka, Japan
*corresponding author: kwmr@riast.osakafu-u.ac.jp

Dilute nitride semiconductors were first developed for GaAs-based 1.3~1.5 μm wavelength lasers for optical fiber communication systems [1]. InP-based dilute nitride semiconductors are also very promising materials for mid-infrared light emitting devices, which are desirable for many applications, such as pollution monitoring, chemical gas analysis and medical diagnostics. The large merit of InP-based dilute nitride semiconductor devices is that the high level technology for InP-based optical devices developed through the research on 1.3~1.5 μm lasers for optical communication systems can be used. In this paper, we report experimental results for InAsSbN single quantum well (SQW) lasers and InGaAsN/GaAsSb type II multiple quantum well (MQW) light emitting diodes grown by plasma-assisted molecular beam epitaxy (MBE) on InP substrates[2,3].

The InAsSbN SQW laser diodes were grown at 450 ˚C on n-type (100) InP substrates. N and Sb compositions are 1% and 2%, respectively. The diodes had a broad-stripe structure of 80 μm width having 400 μm cavity length. Figure 1 shows the temperature dependence of the electroluminescence (EL) spectra of the SQW laser with a 3 nm-InAsSbN SQW active layer. The injection current is 30 mA. The EL peak wavelength is as long as 2.54 μm at 300K. Laser operation was obtained up to 220K. Figure 2 shows the lasing spectrum of the InAsSbN SQW laser diode at 220K. The samples were annealed at 600˚C for 30 sec. It is known that the lasing wavelength is 2.36 μm at 220K. The characteristic temperature T0 is 66K.

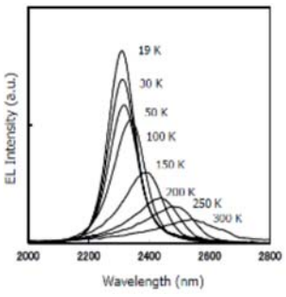

Fig.1 Temperature dependence of EL spectrum of the InAsSbN SQW laser.

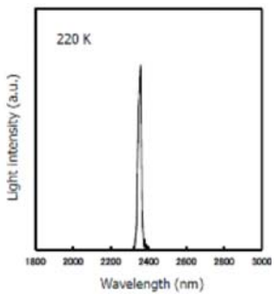

Fig.2 Lasing spectrum of the InAsSbN SQW laser at 220K.

The InGaAsN(7 nm)/GaAsSb(3 nm) type II MQW light emitting diodes (LEDs) were also grown at 480°C on n-type (100) InP substrates. N composition is 1%. The temperature dependence of the EL spectrum of the InGaAsN/GaAsSb type II MQW LED was shown in Fig.3, in which the injection current is 50 mA. The EL peak wavelength is 2.86 μm at 300K. Figure 4 shows the temperature dependences of the EL peak energy for the InGaAsN/GaAsSb type II MQW LED (N=1%) and InGaAs/GaAsSb type II MQW LED (N=0%). It is clear that the peak energy difference between these two diodes is 100 meV at all temperature regions, which is consistent with our previous results for InGaAsN layers on InP.

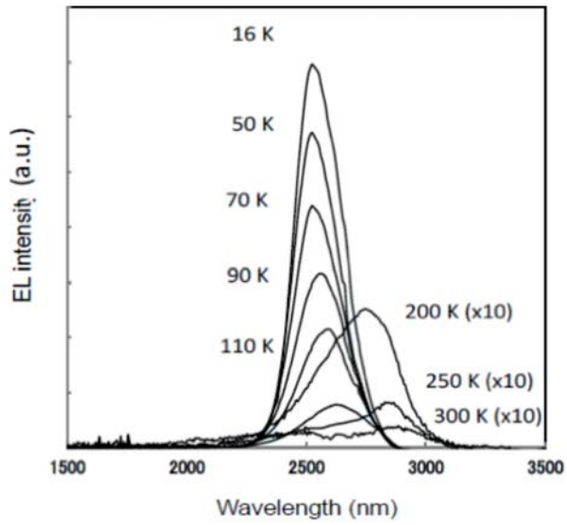

Fig.3 Temperature dependence of EL spectrum of the InGaAsN/GaAsSb MQW LED.

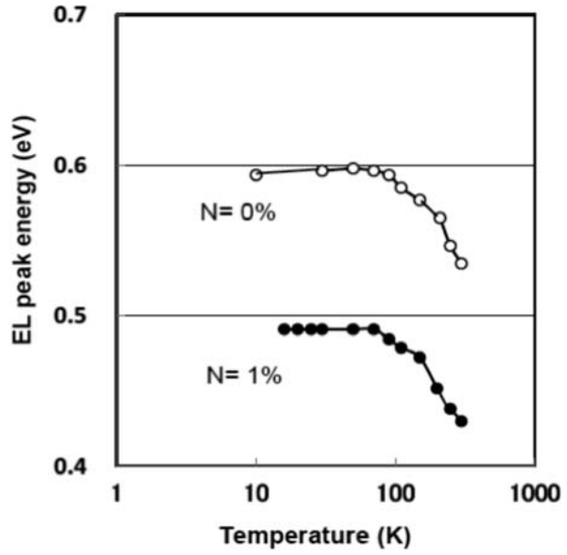

Fig.4 Temperature dependence of EL peak energy of the InGaAsN/GaAsSb MQW and InGaAs/GaAsSb MQW LEDs.

[1] M. KONDOW, K. UOMI, A. NIWA, T. KITATANI, S. WATAHIKI AND Y. YAZAWA, JPN. J. APPL. PHYS. 35, 1273 (1996)
[2] T. SHONO, S. MIZUTA AND Y. KAWAMURA, J. CRYSTAL GROWTH 378, 69 (2013)
[3] Y. KAWAMURA AND T. SAHASHI, JPN. J. APPL. PHYS. 53, 028004 (2014)

Tuesday, 7 October

Tu-B

Photonic integration for sensors

10:50-12:20

Heterogeneous silicon photonics for SWIR/MWIR applications (invited)

*G. Roelkens[1]**

[1]Photonics Research Group, Ghent University / imec Sint-Pietersnieuwstraat 41, B-9000 Ghent, Belgium
*corresponding author: gunther.roelkens@intec.ugent.be

In this paper I review our work on silicon photonic integrated circuits for spectroscopic sensing applications. Silicon photonics is an emerging technology for the realization of high-speed transceivers. However, the application range is not limited to optical communication. The wide transparence range of group IV materials such as silicon and germanium enable photonic integrated circuits operating in the mid-infrared. Passive waveguide circuits containing spectrometers have been realized both in the short-wave infrared (on silicon-on-insulator) and in the mid-infrared (on silicon-on-insulator and germanium-on-silicon). In order to realize chip-size spectroscopic sensors the integration of light sources (lasers, LEDs) and photodetectors are required as well. For this purpose GaSb-based layer stacks are bonded on the silicon waveguide circuits, which are then processed into opto-electronic components. This way, a InGaAsSb on silicon spectrometer with 46 channels was demonstrated, operating in the 1.5-2.5 µm wavelength range. Laser integration has been demonstrated as well in this wavelength range. An alternative approach for photodetection in this wavelength range is the integration of PbS and HgTe colloidal nano-crystal films on silicon waveguide circuits. Short-wave infrared photoconductors integrated on silicon were demonstrated. An alternative approach to mid-infrared light generation is the use of the large Kerr nonlinearity of silicon together with the broad dispersion engineering feasible in high index contrast silicon photonic waveguide circuits. This way, the efficient generation of mid-infrared radiation is possible using 'standard' optical pump sources. We demonstrated the generation of 3.6 µm radiation using a pump around 2 µm wavelength and a signal in the telecommunication wavelength band. Also, an octave spanning frequency comb in the 1.5-3µm wavelength range using spectral broadening in a silicon photonic wire was demonstrated. Using silicon photonic technology we demonstrate the on-chip spectroscopic detection of glucose at physiologically relevant concentrations.

Combining EC-QCL and MOEMS technology: an approach for miniaturization and fast wavelength scanning

R. Ostendorf[1],, D. Bleh[1], A. Merten[2], J. Grahmann[2], R Schmidt[1], M. Kunzer[1], S. Hugger[1], J. Wagner[1]*

[1]Fraunhofer Institute for Applied Solid State Physics, Tullastrasse 72,79108 Freiburg, Germany
[2]Fraunhofer Institute for Photonic Microsystem, Maria-Reiche-Strasse 2, 01109 Dresden
*corresponding author: ralf.ostendorf@iaf.fraunhofer.de

Broad band tunable external cavity quantum cascade lasers (EC-QCL) are promising and versatile mid-infrared (MIR) light sources combining high brightness and wide spectral coverage of more than 300 cm^{-1}. Therefore, EC-QCLs are well-suited for the integration in optical spectroscopy systems for the identification of chemical compounds, making use of the strong absorption lines in the so-called fingerprint region from 3µm to 10 µm. Since many applications in the chemical, pharmaceutical and the food industry require not only in situ process information but also short analysis times in the range of seconds or even below to perform quasi real-time monitoring, the wavelength scan rate of the EC-QCL has to be in the range of sveral Hz up to even kHz.

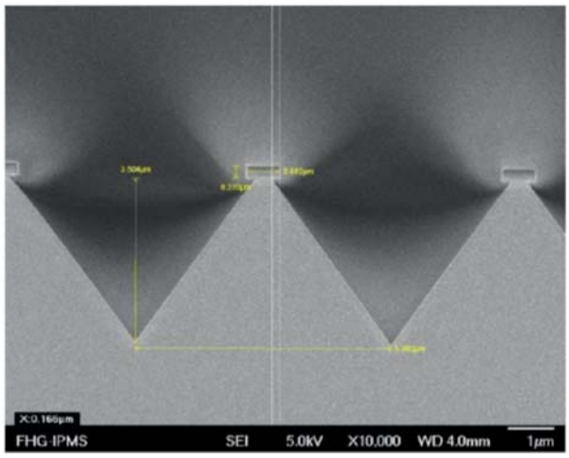

Fig.1. Scanning electron microscope picture of a tapered grating optimized for application in a miniaturized EC QCL (parallel polarization, period: 5.38 µm, 186 l/mm).

The integration of Micro-Opto-Electro-Mechanical Systems (MOEMS) as wavelength selective element in the external cavity allows for the development of a very compact and fast tunable laser source, providing high power spectral density in the MIR range for spectral analysis. The challenge for the implementation of the MOEMS scanning grating is to provide high diffraction efficiency over a wide spectral range as well as a large grating diameter in order to achieve a sufficiently high spectral resolution. Thus, various grating geometries such as rectangular and trapezoidal diffraction gratings have been simulated and manufactured either by photolithographic processes or rapid prototyping using a picosecond laser based micro-machining. The diffraction efficiency of the gratings has been optimized with regard to polarization of the QCL as well as the orientation of the grating in the external cavity.

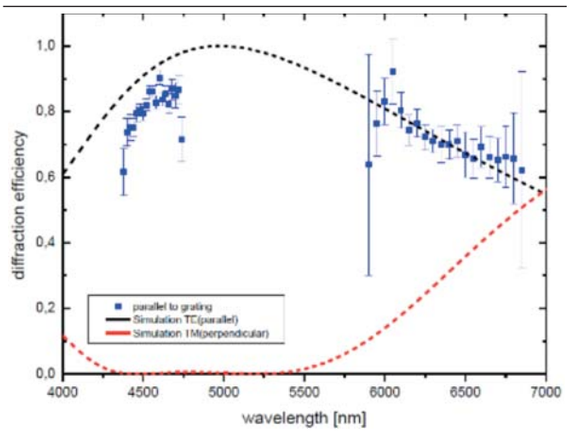

Fig.2. Dashed lines: Simulated diffraction efficiency for different orientations of the tapered grating in the external resonator (black: parallel polarization, red: perpendicular polarization). Blue dots: Measurement of the diffraction efficiency performed with a tunable EC QCL.

Based on these results the optimized grating structure was integrated in a MOEMS scanner with a scan rate of 1 kHz, a grating diameter of 5 mm and large mechanical deflection angles. First results on a compact and fast scanning MIR light source combining an EC QCL with a MOEMS scanning grating as wavelength selective element will be presented.

MIR Photonic Integrated Circuits for Laser Spectroscopy

L. J. Orbe[1], G. Carpintero[1], G. Maisons[2], C. Gilles[2], F. Boulila[2], M. Carras[2]*

[1]Universidad Carlos III de Madrid, Av. de la Universidad 30, 28911 Leganés, Spain
[2]III-V Lab, Campus de Polytechnique 1, Av. Augustin Fresnel, 91767 Palaiseau, France
*corresponding autor: lorbe@ing.uc3m.es

In laser-based optical stand-off spectroscopy, laser radiation interacts with gas chemical substances which have absorption lines over the Mid-Infrared (MIR) spectrum. Low-cost, small-footprint and widely tunable laser sources in this range can potentially have a huge impact on the development of Tunable Diode Laser Spectroscopy instruments.

Quantum Cascade Lasers (QCL) are coherent light sources in the MIR range, attracting great interest in covering the MIR for sensing applications[1],[2]. Currently, Distributed Feedback (DFB) QCLs provide a narrow-linewidth single-mode emission spectrum which is perfectly suited for trace gas detection, requiring wavelength tuning of a few tens of wavenumbers to detect multiple gas species. DFB QCLs have demonstrated wide wavelength range operation from the MIR to the Terahertz and achieve high output powers in continuous-wave operation at room temperature. The only drawback is that a single DFB QCL has a limited tuning range. In order to overcome this issue, arrays of DFB QCL, composed of tenths of emitters have been developed as a solution for broad tunability [3]. The main objective of is to develop a MIR Photonic Integrated Circuit (PIC) through the monolithic integration of the QCL array and a multiplexer scheme achieving a widely tunable source in the MIR range suitable for laser spectroscopy. In order to pursue that objective, we present our recent advances in passive multiplexer schemes in order to achieve monolithic integration with the DFB QCL array, which include a comparison between numerical simulations and experimental results for all of the components of the PIC toolbox, a waveguiding analysis and multiplexer schemes, such as Y-junction and Echelle grating based multiplexers. Experimental results show propagation losses as low as 2dB/cm at 7.4µm for straight waveguides. Experimental results over Y-junction and Echelle multiplexers were also obtained and compared to the expected values.

We will highlight the use of Echelle gratings as the optimum multiplexer solution, as they present advantages such as size reduction and minimized diffraction aberrations as well as size advantage in comparison to other multiplexer schemes; which make them ideal for compact low cost applications [4] .

[1] FAIST, J., HUGI, A., RIEDI, S., BISMUTO, A., HINKOV, B., GINI, E., BLASER, S., BECK, M., ISLC 2, 3, 7-10 (2012)

[2] LEE, BENJAMIN G., BELKIN, M.A., PFLUGL, C., DIEHL, L., ZHANG, H.A., AUDET, R.M., MACART HUR, J., BOUR, D.P., CORZINE, S.W., HUFLER, G.E., CAPASSO, F., JQE 45, 5, 554-565 (2009)

[3] DIEHL, L., LEE, B.G., ZHANG, H.A., PFLUGL, C., BELKIN, M., FISHER, M., WITTMAN, A., FAIST, J., CAPASSO, F., CLEO: QELS (2009).

[4] WU, MINGCHO, YUNG-JUI CHEN, JLT 12, 11, 1939-1942 (1994)

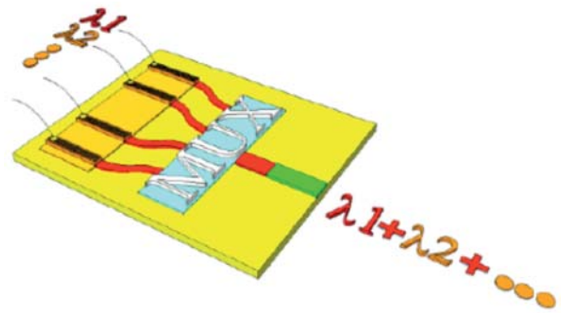

Fig. 1. Scheme of the monolithic tuneable sources based on an array of DFB QCL and a multiplexer.

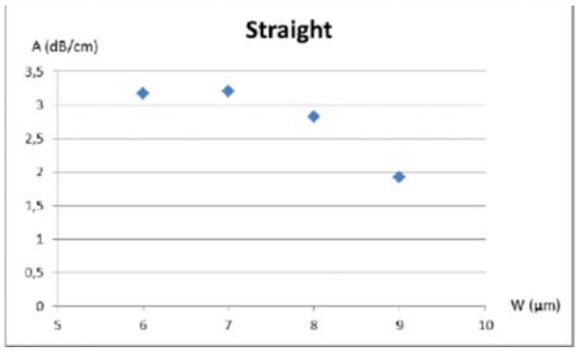

Fig. 2. Experimental measurements of losses over straight waveguides at 7.4 µm.

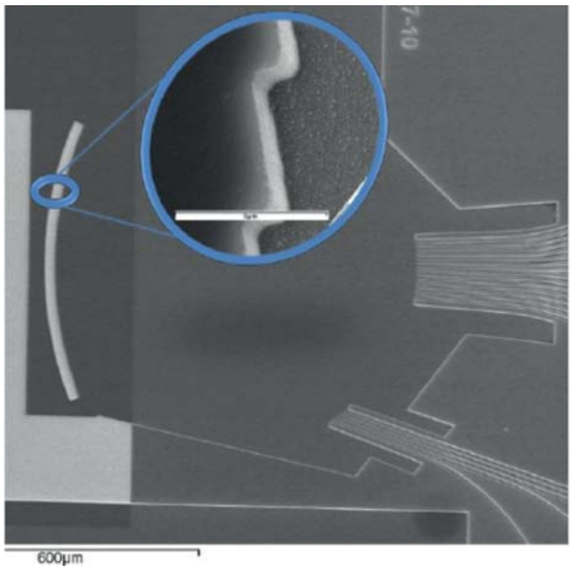

Fig. 3. SEM picture of the Echelle multiplexer. Inset : SEM picture, zoom on the diffraction grating tooth

Widely tunable QCL source based on multiplexed QCL arrays

M. Brun[1], F. Boulila[2], P. Labeye[1], P. Barritault[1], G. Maison[2], S. Boutami[1], S. Nicoletti[1], M. Carras[2]*

[1]CEA-LETI Minatec Campus, 17 rue des Martyrs 38054 Grenoble cedex 9, France
[2]3-5 lab, Campus Polytechnique, 1 Avenue Augustin Fresnel, 91767 Palaiseau, France
*corresponding author: brun.mickael@cea.fr

The need for broadly tunable sources for Mid-Infrared spectroscopy has been identified for years. This is particularly true for chemical spectroscopy where detecting complex molecules or a set of simple molecules require sources with narrow line width and tunable over a few tens of wave numbers. To achieve the realization of such a monolithic broadly tunable source, III-V Lab together with LETI has developed a new approach base on multiplexed distributed feedback quantum cascade laser arrays. Recently developed Si based multiplexers operating in the mid IR open the possibility to combine beams from different DFB lasers to a single output.

We present the first prototype of a hybrid tunable source around 4.5 µm covering 2180 cm^{-1} to 2280 cm^{-1} with TM00 beam quality. We will show the realization of laser arrays at various wavelengths (from the 4.5µm region to the 9.5µm region) and compare the different technologies using, or not, iron doped InP for thermal management. The design and realization of the multiplexing device based on low loss SiGe/Si waveguides1 will be detailed. Then we will show how all these building blocks have been assembled towards the fabrication of the monolithic source largely tunable source. The performance and characteristics of the source will be described.

[1] M. BRUN, P. LABEYE, G. GRAND, J.-M. HARTMANN, F. BOULILA, M. CARRAS, S. NICOLETTI, OPT EXPRESS. 22(1), 508 (2014).

Tuesday, 7 October

Tu-C

Special session: IR Sensing systems

13:20-15:40

Mid-IR spectroscopy in medical diagnostics using tunable quantum cascade lasers (invited)

W. Mäntele[1], M. Pleitez[1], O. Hertzberg[1], T. Lieblein[1], A. Bauer[1], H. v. Lilienfeld-Toal[2]

[1]Institut für Biophysik, Goethe-Universität Frankfurt am Main Max-von-Laue-Strasse 1, D-60438 Frankfurt am Main, Germany
[2]Elté Sensoric GmbH, Wilhelm-Schoeffer-Strasse 33, Gelnhausen, Germany
*corresponding author: maentele@biophysik.uni-frankfurt.de

Mid-Infrared spectroscopy has proven to be highly specific for the spectroscopic analysis of body fluids, cells and tissues. With the advent of the quantum cascade laser (QCL) in the late nineties, powerful narrow-band single wavelength IR emitters, multi-wavelength sources, or, with an external cavity (EC), tunable EC-QCLs are now available. Their power reaches to hundreds of mW and their tunability can extend over several 100 cm^{-1}, sufficiently broad to scan the entire IR fingerprint region within some tens of msec. Probably their most pronounced advantage is their use in a pulsed mode, which makes them an ideal IR light source for photometric measurement of IR radiation absorbed in skin or tissues in combination with photoacoustic or photothermal detection.

The lecture presents our most recent developments in QCL applications for the measurement of skin parameters and body fluids in vitro and in vivo in comparison with FT-IR experiments. Photoacoustic detection methods with ultrasound resonance cells and novel photothermal detection methods are described that are optimized for pulse frequencies and pulse energies of QCLs and that open the possibility for the analysis skin layers [1].

Probably the most attractive application is the use of QCLs and photoacoustic/photothermal detection for the non-invasive measurement of glucose in skin for diabetes patients [2]. Glucose exhibits a highly specific molecular fingerprint in the MIR around 8-11 µm which can be easily used for the reagent-free quantitative analysis of glucose (and other substances) in blood or other body fluids [3]. The lecture will describe the physiochemical background, the technical realization, and the validation of this method on diabetes patients. Further biomedical applications of MIR technology will be discussed [4].

[1] Pleitez M., Lieblein T., Bauer A., Hertzberg O., v. Lilienfeld-Toal H., Mäntele W. (2013) Ultrasound photoacoustic cell for in vivo mid-IR spectroscopy of human epidermis: Low interference by changes of air pressure, temperature, and humidity caused by skin contact opens the possibility for a non-invasive monitoring of glucose in the interstitial fluid. Review of Scientific Instruments 84, 84901-84908

[2] Pleitez M., Lieblein T., Bauer A., Hertzberg O., v. Lilienfeld-Toal H., Mäntele W. (2012) In Vivo Noninvasive Monitoring of Glucose Concentration in Human Epidermis by Mid-Infrared Pulsed Photoacoustic Spectroscopy. Anal. Chem. 85,1013-1020

[3] Hoşafçı G., Klein O., Oremek G., Mäntele W. (2006). Clinical chemistry without reagents? An infrared spectroscopic technique for determination of clinically relevant constituents of body fluids. Anal. Bioanal. Chem, 387,1815-1822

[4] Roth A., Dornuf F., Klein O., Schneditz D., Hafner-Gießauf H., Mäntele W. (2012) Infrared spectroscopy in hemodialysis: reagent-free monitoring of patient detoxification by infrared spectroscopy. Anal. Bioanal. Chem., 403, 391-399

Recent advances in mid-infrared quantum and interband cascade laser-based trace gas detection (invited)

F.K.Tittel[1], W. Ren[2], W. Jiang[1], Y. Cao[1], N.P. Sanchez[2], L. Lu[1], D. Jiang[1], J.J. Allred[1], P. Paticimo[3], V. Spagnolo[3], R.J. Griffin[2]

[1]Department of Electrical & Computer Engineering, MS 366
[2]Department of Civil and Environmental Engineering. MS 318 Rice University, 6100 Main Street, Houston, TX 77005-1827, USA
[3]Dipartimento Interateneo di Fisica, Università e Politecnico di Bari Via Amendola 173, I-70126, Bari, Italy

This talk will focus on recent advances in the development of sensors based on infrared semiconductor lasers for the detection, quantification and monitoring of trace gas species and their application in atmospheric chemistry, medical diagnostics, life sciences, industrial process control and national security. Specifically, the development of compact trace gas sensors, in particular based on quantum cascade (QC) and interband cascade (IC) lasers that permit the targeting of strong fundamental rotational-vibrational transitions in the mid-infrared and that are one to two orders of magnitude more intense than overtone transitions in the near infrared, will be considered.

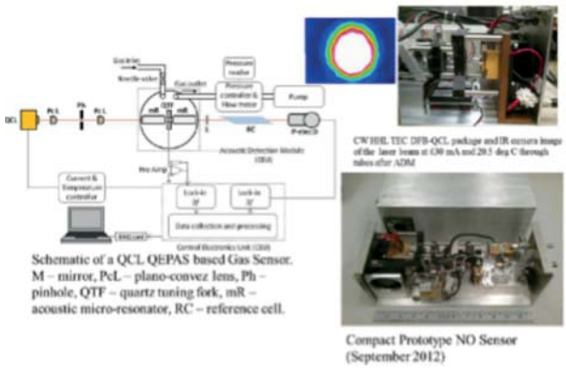

Fig.1. CW TEC DFB QCL based QEPAS NO Gas Sensor

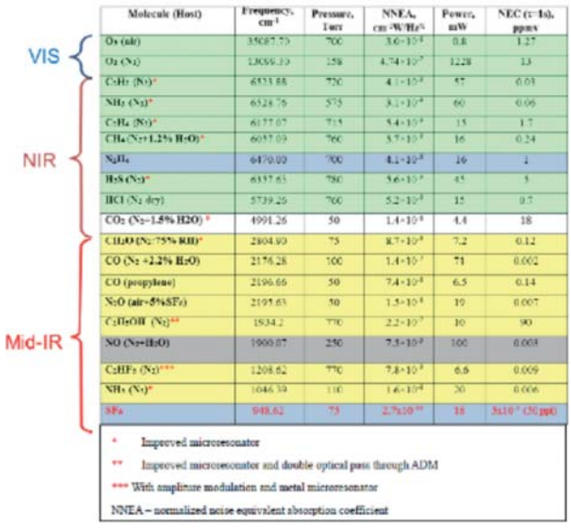

Fig 2. QEPAS Performance for Trace Gas Species (October 2014)

The spectroscopic detection and monitoring of seven molecular species (ammonia (NH_3), nitric oxide (NO) (see Fig. 1), carbon monoxide (CO), sulfur dioxide (SO_2), methane (CH_4), nitrous oxide (N_2O) and hydrogen peroxide (H_2O_2)) will be described explicitly. These molecules were detected using QCL and ICL based conventional photoacoustic (CPAS) and quartz-enhanced photoacoustic spectroscopy (QEPAS). CPAS and QEPAS can achieve minimum detectable absorption losses in the range from 10^{-8} to 10-11 $cm^{-1}/\sqrt{Hz}$ (see Fig. 2). Several recent examples of real-world applications of field deployable gas sensors will be described [1-4]. Future work will include the development of intracavity QEPAS (I-QEPAS) in order to obtain significantly lower minimum detectable gas concentration levels of < 10 pptv. Furthermore we envision a continuous THz QEPAS sensor using a THz source operating at room temperature based on intracavity difference frequency generation from mid-IR QCLs [5].

[1] R. LEWICKI, M. JAHAJAH, Y. MA, P. STEFANSKI, J. TARKA, M. RAZEGHI, F.K. TITTEL, SPIE PRESS, CH. 23, 597-632 (2013)
[2] F.K.TITTEL, R. LEWICKI, WOODHEAD PUBLISHING LIMITED , CH. 15, 579-629 (2013)
[3] M. JAHJAH, W. JIANG, N. P. SANCHEZ, W. REN, P. PATIMISCO, V. SPAGNOLO, S.C. HERNDON, R.J. GRIFFIN, F. K. TITTEL, OPT. LETT., 39, 957-960 (2014).
[4] W. REN, W. JIANG, N.P. SANCHEZ, P. PATIMISCO, V. SPAGNOLO, C. ZAH, F. XIE, L. C. HUGHES, R. J. GRIFFIN, F. K. TITTEL, APPL. PHYS. LETT., 104, 041117 (2014).
[5] Q.Y. LU, N. BANDYOPADHAY, S. SLIVKEN, Y. BAI, M. RAZEGHI , APPL. PHYS. LETT. 104, 221105 (2014)

Mid-infrared laser-based trace gas detection for sensitive chemical sensing within Life Science (invited)

Frans J.M. Harren[1]

[1]Trace gas research Group, Institute of Molecules and Materials, Radboud University, Heyendaalseweg 135, 6525 AJ, Nijmegen, the Netherlands
*corresponding author: F.Harren@science.ru.nl

There is an increasing interest to develop monochromatic sources (interband lasers, quantum cascade lasers, optical parametric oscillators) in the mid-infrared wavelength region to detect trace gas emissions from biological tissue and from breath of human subjects. Nowadays, such lasers deliver relatively high power and narrow linewidth, and can be designed for any desired wavelength within the infrared wavelength region, between 2.5 to 12 µm. Sensitive detection of specific gases becomes into reach thanks to the strong fingerprint absorption spectra of molecular gases and the exact tuning capabilities of lasers. When lasers are combined with sensitive spectroscopic techniques, such as photoacoustic spectroscopy or optical cavity enhanced spectroscopy, gases can be determined extremely sensitive, under atmospheric conditions [1,2].

To deliver on-site analysis and to reduce costs, within medicine there is an increasing interest in the development of sensitive and selective methods for breath analysis, to monitor diseases reliably and non-invasively. Investigations have been made in the relation between nitric oxide and asthma [3], carbon monoxide from breath and between hydrogen cyanide and Pseudomonas Aeruginosa bacteria, infesting Cystic Fibrosis patients [4].

Also, recent developments will be discussed of dual mid infrared Frequency Comb Fourier Transform Spectroscopy for infrared spectroscopic sensing [5].

[1] D.D. ARSLANOV, M. SPUNEI, J. MANDON, S.M. CRISTESCU, S.T. PERSIJN, F.J.M. HARREN, LASER AND PHOTONICS REVIEW 7, 188 (2013).
[2] S.M. CRISTESCU, S.T. PERSIJN, S. TE LINTEL HEKKERT, F.J.M. HARREN, APPL. PHYS. B 92, 343 (2008).
[3] D. MARCHENKO, J. MANDON, S.M. CRISTESCU, P.MERKUS, F.J.M. HARREN, APPL. PHYS. B, 111, 359 (2013).
[4] D.D. ARSLANOV, M.P.P. CASTRO, N.A. CREEMERS, M. SPUNEI, J. MANDON, S.M. CRISTESCU, P. MERKUS, F.J.M. HARREN, J. OF BIOMED. OPT. 18, 107002 (2013).
[5] Y. JIN, S.M. CRISTESCU, F.J.M. HARREN, J. MANDON, OPT. LETT. 39, 3270 (2014).

Compact sensor for trace gas monitoring based on Quartz Enhanced Photoacoustic Spectroscopy

*T. Nguyen Ba[1,2], M. Triki[1,2] and A. Vicet[1,2]**

[1]Univ. Montpellier, IES, UMR 5214, F-34000, Montpellier, France
[2]CNRS, IES, UMR 5214, F-34000, Montpellier, France
*corresponding author: a.vicet@univ-montp2.fr

The development of compact optical sensor for trace gas species is more and more important for many fields of applications such as environmental monitoring, industrial process control and medical diagnostics. Quartz Enhanced Photoacoustics Spectroscopy (QEPAS) [1] has been proven to be an attractive tool for the selective and sensitive detection and quantification of molecular trace gas since its invention in 2002. This technique has shown a large range of applications with compact and cheap setups, based on the use of a commercial quartz tuning fork (QTF) as an efficient acoustic transducer. The optical energy absorbed by the gas results in a periodic thermal expansion which gives rise to a weak acoustic pressure wave. This pressure excites a resonant vibration of the QTF thereby generating an electrical signal via the piezoelectric effect.

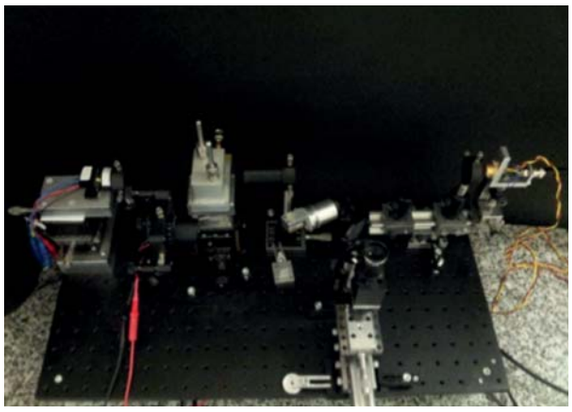

Fig.1. Laboratory QEPAS bench for ethylene detection.

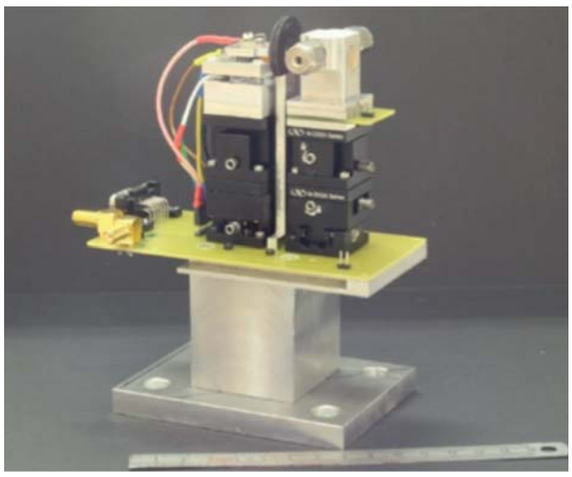

Fig.2. Compact QEPAS-based sensor for methane detection.

In this paper, we report on the development of two QEPAS-based sensors using quantum wells antimonide distributed feedback (DFB) lasers emitting at 2.3 µm and 3.3 µm [2]. These devices were developed for environmental measurements, such as methane and ethylene detection. Our recent results obtained on a laboratory bench (Fig. 1) and a brand new compact setup (Fig.2) will be reported. They show very good sensitivity and open the way to agronomic and industrial applications.

This work is supported by the international ANR NexCILAS project and NUMEV labex.

[1] A. A. KOSTEREV, Y. A. BAKHIRKIN, R. F. CURL, AND F. K. TITTEL, "QUARTZ-ENHANCED PHOTOACOUSTIC SPECTROSCOPY.," OPT. LETT. 27(21), 1902–1904 (2002).

[2] T. NGUYEN BA, M. TRIKI, Q. GAIMARD, Y. ROUILLARD, AND A. VICET, "QUARTZ ENHANCED PHOTOACOUSTIC SPECTROSCOPY (QEPAS) WITH ANTIMONIDE COMPOUNDS IN VERY COMPACT SYSTEMS," F. BERGHMANS, A. G. MIGNANI, AND P. DE MOOR, EDS., 91410H (2014) [DOI:10.1117/12.2051663].

Highly reactive nitrous acid (HONO) detection by Quartz-enhanced photoacoustic spectroscopy (QEPAS)

Hongming Yi[1,2], Rabih Maamary[1], Xiaoming Gao[2], Markus W. Sigrist[3], Weidong Chen[1,]*

[1]Laboratoire de Physicochimie de l'Atmosphère, Université du Littoral Côte d'Opale, Dunkerque, France
[2]Laboratory of Atmospheric Physico-Chemistry, Anhui Institute of Optics and Fine Mechanics, CAS, Hefei, China
[3]Laser Spectroscopy and Sensing Laboratory, Institute of Quantum Electronics, ETH Zurich, Switzerland
*corresponding author: chen@univ-littoral.fr

We report on high sensitivity and high selectivity detection of gaseous HONO with ultrashort residence time using quantum cascade laser quartz-enhanced photoacoustic spectroscopy (QEPAS). The HONO absorption line located at 1254.85 cm^{-1} with a line intensity of ~10^{-20} cm^{-1}/(molecule.cm^{-2}) was used for interference-free spectroscopic monitoring. A power normalized minimum detection limit of 5 ppbv.W HONO was achieved at 70 mbar using a laser output power of 50 mW and a lock-in time constant of 1 s.

It is well known that nitrous acid (HONO) acts as an important source of hydroxyl free radical (OH). However, despite its importance and several decades of research, the sources and sinks of HONO as well as their formation mechanism in the atmosphere are still not completely defined and understood. Field observations show that the modeled HONO concentrations are often significantly below observed values, suggesting a large missing source of HONO [1-3]. This is due to the difficulty in measuring this highly reactive short-lived species. Assessment of HONO concentration is very challenging, because its reactivity and solubility combined with its fast photolysis process makes it subject to sampling-induced artifacts and losses. It is highly required: (1) ultrahigh sensitivity and measurement precision (typical HONO concentrations vary from 30 pptv to several ppbv in the early morning), (2) fast time response and high spatial resolution (its atmospheric lifetime is only a few minutes), (3) the residence time within the sampling system as short as possible to minimize the losses due to its reaction with other species and/or wall surfaces and hence to ensure high measurement accuracy. A number of analytical techniques have been developed for HONO monitoring in the atmosphere. They can be classified into two categories: 1) analysis of HONO in the aqueous phase after chemical conversion by wet chemical methods or 2) analysis of HONO in the gas phase using spectroscopic techniques. However, each of these techniques suffers from various limitations in terms of detection limit, sampling approach, and potential interference effects.

In the present work, we report our first attempt to realize high sensitivity and high selectivity detection of gaseous HONO with ultrashort residence time using modern quartz-enhanced photoacoustic spectroscopy (QEPAS). A spectrophone involving off-beam coupled QEPAS [4] excited with an external cavity quantum cascade lasers (EC-QCL) was developed which allowed us to probe the strong absorption lines in the ν_3 H-O-N bending mode of the trans-HONO near 1255 cm^{-1}. With the photodetector-free QEPAS sensing platform we monitored HONO within a very small gas-sample volume (of few mm^3) with high sensitivity. This permits a significant reduction of air sampling residence time. The developed QEPAS sensor was evaluated using HONO concentrations varying from 70 ppmv down to 1 ppmv. As no standard gas reference is commercially available, the QEPAS sensor calibration was performed by means of lab-generated HONO samples calibrated by direct absorption spectroscopy using the spectral data reported in Ref. [5]. The absorption line located at 1254.85 cm^{-1} with a line intensity of ~10^{-20} cm^{-1}/(molecule.cm-2) was used for interference-free HONO detection. A minimum detection limit (MDL) of 100 ppbv HONO was achieved at 70 mbar using a laser output power of 50 mW and a lock-in time constant of 1 s. The corresponding power normalized MDL is 5 ppbW.

A further improvement in photoacoustic detection sensitivity could be realized by using higher exciting laser power at ~W level [6] in combination with intracavity enhanced QEPAS [7], which could allow detection of HONO at the ~ pptv level. This work demonstrates the potential of using QEPAS for the detection of highly reactive HONO species in ambient air, which enables an improved insight into atmospheric chemical processes related to HONO.

Acknowledgments. This work is mainly supported by the IRENI program of the Région Nord-Pas de Calais. The financial supports from the French national research agency (ANR) under the NexCILAS (ANR-11-NS09-0002) and the CaPPA (ANR-10-LABX-005) contracts are acknowledged.

[1] K. STEMMLER, M. AMMANN, C. DONDERS, J. KLEFFMANN, AND C. GEORGE, "PHOTOSENSITIZED REDUCTION OF NITROGEN DIOXIDE ON HUMIC ACID AS SOURCE OF NITROUS ACID", NATURE 440 (2006) 195–198

[2] X. ZHOU, N. ZHANG, M. TERAVEST, D. TANG, J. HOU, S. BERTMAN, M. ALAGHMAND, P. B. SHEPSON, M. A. CARROLL, ET AL., "NITRIC ACID PHOTOLYSIS ON FOREST CANOPY SURFACE AS A SOURCE FOR TROPOSPHERIC NITROUS ACID", NATURE GEOSCI. 4 (2011) 440–443

[3] H. SU, Y. CHENG, R. OSWALD, T. BEHRENDT, I. TREBS, F. X. MEIXNER, M. O. ANDREAE, P. CHENG, Y. ZHANG, AND U. PÖSCHL, "SOIL NITRITE AS A SOURCE OF ATMOSPHERIC HONO AND OH RADICALS", SCIENCE 333 (2011) 1616–1618

[4] H. YI, K. LIU, W. CHEN, T. TAN, L. WANG, AND X. GAO, "APPLICATION OF A BROADBAND BLUE LASER DIODE TO TRACE NO2 DETECTION USING OFF-BEAM QUARTZ-ENHANCED PHOTOACOUSTIC SPECTROSCOPY", OPT. LETT. 36 (2011) 481-483

[5] K.H. BECKER, J. KLEFFMANN, R. KURTENBACH, P. WIESEN, "LINE STRENGTH MEASUREMENTS OF TRANS-HONO NEAR 1255 CM-1 BY TUNABLE DIODE LASER SPECTROMETRY", GEOPHYS. RES. LETT. 22 (1995) 2485-2488

[6] Y. MA, R. LEWICKI, M. RAZEGHI, AND F.K. TITTEL, "QEPAS BASED PPB-LEVEL DETECTION OF CO AND N2O USING A HIGH POWER CW DFB-QCL", OPT. EXPRESS 21 (2013) 1008–1019

[7] S. BORRI, P. PATIMISCO, I. GALLI, D. MAZZOTTI, G. GIUSFREDI, G. SCAMARCIO, P. DE NATALE, AND V. SPAGNOLO, "INTRACAVITY QUARTZ-ENHANCED PHOTOACOUSTIC SENSOR", APPL. PHYS. LETT. 104 (2014) 091114

30% improved direct absorption spectroscopy detectivity by detuned loading of a quantum cascade laser

*Florian Michel[1], Carsten Juretzka[1], Matthieu Carras[2], and Wolfgang Elsäßer[1,3],**

[1]Institute for Applied Physics, Technische Universität Darmstadt, Schlossgartenstr. 7, 64289 Darmstadt, Germany
[2]III-V Lab, Campus Polytechnique, F-91767 Palaiseau Cedex, France
[3]Center of Smart Interfaces, Technische Universität Darmstadt, Germany
*corresponding author: elsaesser@physik.tu-darmstadt.de

20 years after their first realization in 1994 [1], quantum cascade lasers (QCLs) have reached a maturity which enables them to enter numerous application fields, as e.g., spectroscopic gas sensing via either direct absorption spectroscopy (DAS) [2, 3] or by more sophisticated techniques as wavelength modulation, cavity ring down, cavity enhanced or photoacoustic spectroscopy [4, 5]. Besides this application-oriented face, QCLs exhibit particularly interesting fundamental noise and fluctuation properties, both in intensity [6, 7] and frequency noise [8, 9] being unique for QCLs. We have recently demonstrated that a reduction of the intensity noise of a DFB-QCL by -9.5 dB can be achieved by applying self-injection via a short phase-sensitive optical cavity [10], an approach which is due to manipulation of the linewidth enhancement factor or alpha parameter and which is termed as the concept of detuned loading [11, 12]. Here, we perform now a direct absorption experiment (Fig. 1) at an absorption line at 2193 cm^{-1} of CO (880ppm in a 10cm long gas cell).

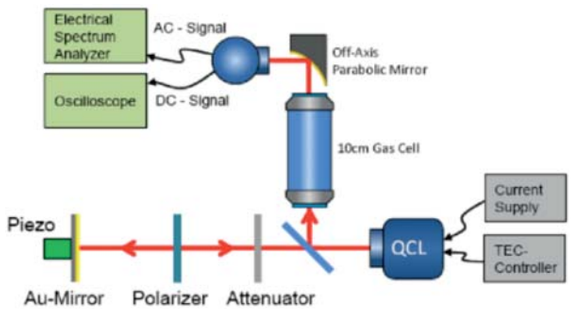

Fig. 1. Experimental setup for the direct absorption experiment with a DFB-QCL under detuned loading conditions with the piezo-translated phase-sensitive short cavity feedback for detuned loading operation, the 10cm long gas cell filled with 880ppm CO, and the detection branch with an MCT detector subsequently followed by an oscilloscope and an electrical spectrum analyzer, respectively.

We demonstrate how the improvement in intensity noise of a detuned loaded DFB quantum cascade laser (λ@4.56 µm) is directly transferred into an improvement in gas sensing detectivity by comparing the ultimate detectivity limits with and without detuned loading. Under optimum intensity noise reduction conditions we achieve an improved standard deviation for the absorption line (Fig. 2) yielding an improvement in signal-to-noise ratio (SNR) from 733 to 1048 which transfers into a detection limit improvement from 1.2 ppm to 840 ppb.

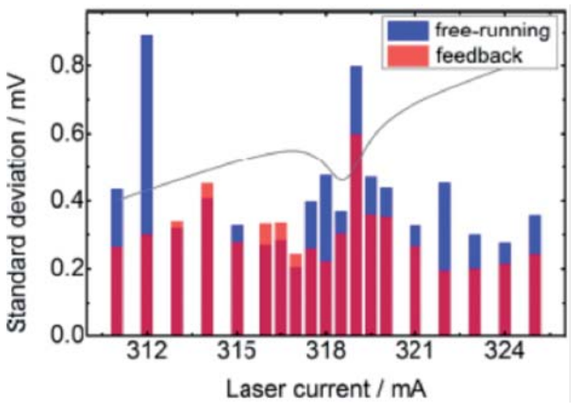

Fig. 2. Calculated standard deviation of the measured absorption signal when current-tuned across the absorption line at 2193cm^{-1} for the laser under detuned loading feedback (red) and without feedback (blue).

Therefore, we achieve a 30% lower detection limit with the intensity noise reduced light by detuned loading in comparison to the free-running case.

This work was supported by the European Communities 7th Frame-work Programme FP7/2007-2013 under Grant 288304 (CLARITY)

[1] J. FAIST, F. CAPASSO, D.L. SIVCO, C. SIRTORI, A.L. HUTCHINSON, A.Y. CHO, SCIENCE 264, 553 (1994)
[2] A. A. KOSTEREV, ET. AL., APPL. OPT. 39, 4425 (2000)
[3] D. WEIDMANN, ET. AL., APPL. PHYS. B 79, 907 (2004)
[4] Z. BOZOKI, ET. AL., APPL. SPECTROCSCOPY 56, 715 (2002)
[5] M. L. HAMILTON, ET. AL., APPL. PHYS. B 97, 715 (2009)
[6] T. GENSTY, W. ELSAESSER AND C. MANN, OPT. EXP. 13, 2032 (2005)
[7] T. GENSTY AND W. ELSAESSER, OPT. COMMUN. 256, 171 (2005)
[8] S. BARTALINI, ET. AL., PHYS. REV. LETT. 104, 083904 (2010).
[9] L. TOMBEZ, ET. AL., OPT. LETT. 36, 3109 (2011)
[10] C. JURETZKA, S. BREUER, L. DRZEWIETZKI, F. SCHAD, M. CARRAS AND W. ELSAESSER, ELECTRON. LETT. 49, 1548 (2013)
[11] K. VAHALA AND A. YARIV, APPL. PHYS. LETT. 45, 501 (1984)
[12] M.A. NEWKIRK AND K.J. VAHALA, IEEE J. QUANTUM ELECTRON. QE-27, 13 (1991)

Tuesday, 7 October

Tu-D

Mid-IR Photo-detectors I

16:20-18:30

InAs Avalanche Photodiodes with negligible excess noise (invited)

Chee Hing Tan[1], John David[1], Ian Sandall[1], Jo Shien Ng[1] and Ben White[1]*

[1]Department of Electronic and Electrical Engineering, The University Of Sheffield, Mappin Building, Mappin Street, Sheffield, S1 3JD, U.K.
*corresponding author: c.h.tan@sheffield.ac.uk

InAs electron-avalanche photodiodes (e-APDs) with "ideal" avalanche multiplication properties of excess noise factor F~1.5, unlimited gain-bandwidth product and high avalanche gain have been developed.

InAs has long been used as photodetectors for wavelengths up to 3.6 µm. Since InAs only covers a fraction of the important midwave infrared window of 3.0-5.0 µm, it has not been the most popular detector technology. However, recently we demonstrated that InAs has a band structure that makes it an excellent material to achieve "ideal" avalanche multiplication properties. The combination of small electron effective mass, large conduction band intervalley separation and small bandgap enables electron to gain energy rapidly in the low scattering environment of the Gamma valley such that there exist an electric field range where only electron can initiate impact ionization. The absence of hole impact ionization therefore leads to negligible excess noise of F~1.5 independent of temperature and gain [1, 2], unlimited gain-bandwidth products [3] and very high avalanche gain.

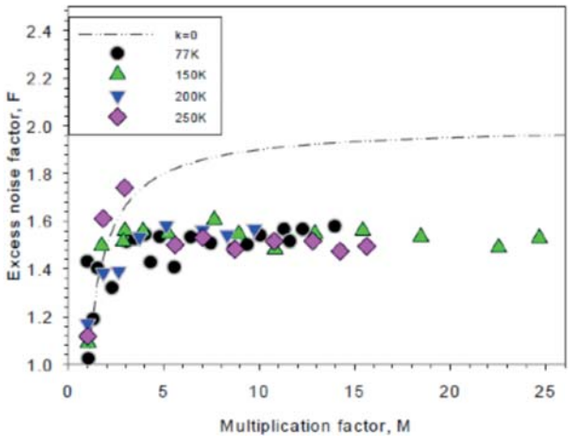

Fig.1. Measured excess noise factor in InAs e-APDs across temperatures of 77 to 250 K.

Key developments in InAs e-APDs will be presented in this paper. Achievements in device fabrication will be described. This will be followed by results obtained from a wide range of InAs diodes that confirm the low excess noise, shown in fig.1 and high gain bandwidth. Temperature dependence of gain and excess noise in InAs e-APDs showed that they can be excellent detection solution for sensing and imaging at wavelengths between 1.55 to 3.6 µm.

More recent work demonstrated uniformity of InAs e-APD array and very high gain exceeding 10,000 at an operating temperature of 200 K. Preliminary results from planar APD work also show great promise of fabrication of InAs planar e-APDs.

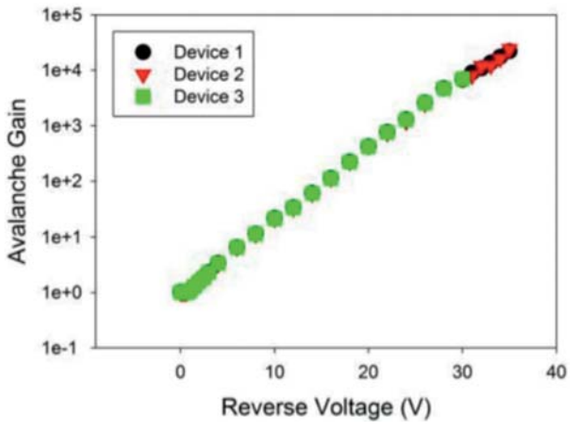

Fig.2. InAs e-APDs with high avalanche gain at an operating temperature of 200 K.

[1] ANDREW R. J. MARSHALL, PETER VINES, PIN JERN KER, JOHN P. R. DAVID, AND CHEE HING TAN, IEEE J. QUANTUM ELECTRON. VOL. 47, NO. 6, PP. 858-864 (2011)
[2] PIN JERN KER, JOHN P. R. DAVID, AND CHEE HING TAN, OPT. EXPRESS, VOL. 20, NO. 28, PP. 29568-29576 (2012).
[3] ANDREW R. J. MARSHALL, PIN JERN KER, ANDREY KRYSA, JOHN P. R. DAVID, AND CHEE HING TAN, OPT. EXPRESS, VOL. 19, ISSUE 23, PP. 23341-23349 (2011).

New separate absorption and multiplication APDs using a hetero-lattice interface to link an AlGaAs multiplication region and a GaSb absorber

A. R. J. Marshall[1], A. P. Craig[1], C. J. Reyner[2] and D. L. Huffaker[2,3]*

[1]Physics Department, Lancaster University, Lancaster, LA1 4YB, UK
[2]Department of Electrical Engineering, UCLA, Los Angeles, California 90095, USA
[3]California NanoSystems Institute, UCLA, Los Angeles, California 90095, USA
*corresponding author: a.r.marshall@lancaster.ac.uk

Development of APDs with cut-off wavelengths beyond 1.7 µm has proven challenging. In this work a novel approach is taken, building a separate absorption and multiplication (SAM) APD structure for these extended wavelengths. The structure combines a GaSb absorber with a desirable AlGaAs multiplication region, using an interface misfit (IMF) array to accommodate the lattice mismatch and additionally act as a charge sheet. The GaSb absorber could in the future be substituted for a GaSb-matched alloy or superlattice, facilitating absorption from the NIR to the LWIR. An initial proof of concept and experimental characterisation is presented here.

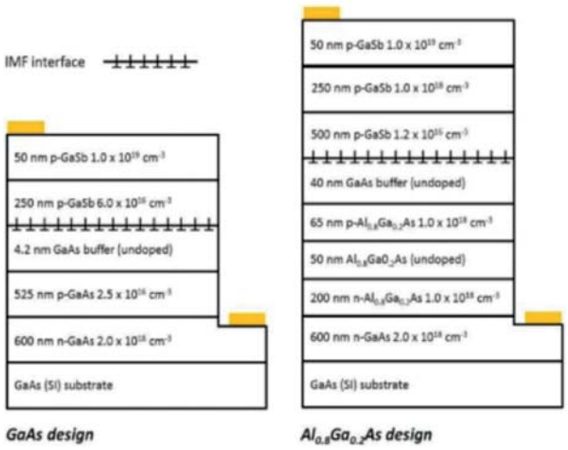

Fig.1. Shows the cross-sectional schematic of the two structures. Left: GaAs design, Right: AlGaAs design.

The two structures shown in Figure 1, were grown using a Veeco Gen930 MBE reactor. The GaAs design tests the simplest possible SAM APD concept, using the hetero-lattice interface, while the AlGaAs design adds low leakage currents and disparate ionisation coefficients, bringing commensurate low noise. As usual a charge sheet strongly confines the high electric field within the multiplication region. For the GaAs design, the charge associated with the IMF array itself serves this function. Following growth and fabrication, devices were extensively characterised using capacitance-voltage, current-voltage, photomultiplication and excess noise measurements. Figure 2 shows the dark current and photocurrent data obtained. A 1.55 µm laser was used to ensure that photocurrent was generated within the GaSb absorber alone. It is evident that the photogenerated carriers can travel from the GaSb, across the IMF hetero-lattice interface and into the multiplication region, where they undergo avalanche multiplication. The AlGaAs design in particular has a desirable characteristic with a low dark current density, of 5 µAcm^{-2} at 90% of the breakdown voltage, and gains in excess of 1000 recorded. Excess noise was measured using a calibrated HP 8970B noise figure meter. The excess noise factors obtained from the two multiplication regions were found to be in good agreement with the literature, confirming impact ionisation was confined within them.

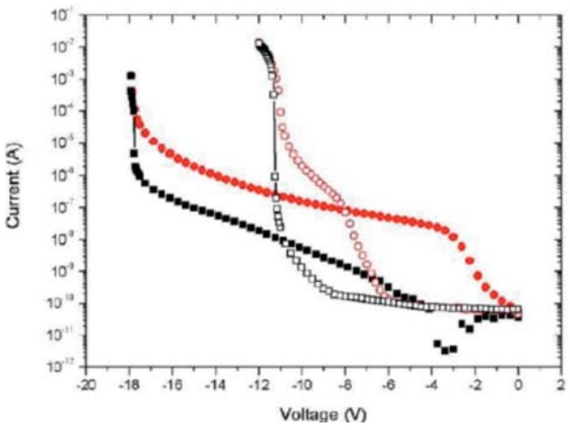

Fig.2. Shows IV data for 200 µm diameter mesas. Closed symbols: GaAs design, Open symbols: AlGaAs design, Black squares: dark current, Red circles: current under illumination from 1.55 µm laser. The solid lines are guides to the eye.

There remain challenges with this novel structure, in particular a low quantum efficiency in these initial proof of concept devices. However it has been shown that high gain, low noise APDs can be realised and indeed single photon sensitivity might be achievable. Future work will target the substitution of a longer wavelength absorber lattice-matched to GaSb.

Suppression of dark current density and enhancement in peak detectivity for quaternary (InAlGaAs) alloy capped InGaAs/GaAs QDIPs implanted with high energy protons

*S. Upadhyay[1], A. Mandal[2], H. Ghadi[2], D. Pal[2], N. B. V. Subrahmanyam[3], P. Singh[3] and S. Chakrabarti[2]**

[1]Center for Research in Nanotechnology and Science, Indian Institute of Technology Bombay, Mumbai-400076, India
[2]Center for Nanoelectronics, Department of Electrical Engineering, Indian Institute of Technology Bombay, Mumbai-400076, India
[3]Ion Accelerator Development Division, Bhabha Atomic Research Center, Mumbai-400085, India
*corresponding author: subhanandachakrabarti@gmail.com

Due to three dimensional carrier confinement, self-assembled In(Ga)As/GaAs quantum dot infrared photodetectors (QDIPs) have its promising applications in the field of night vision, medical diagnosis, environmental monitoring from space etc. $In_{0.50}Ga_{0.50}As$/GaAs based n-i-n QDIPs were grown over semi-insulating GaAs (100) substrates by solid source molecular beam epitaxy (SSMBE); 7.0 monolayer (ML) QDs were capped with a combination of 30Å quaternary ($In_{0.21}Al_{0.21}Ga_{0.58}As$) and 500Å GaAs layers (Fig. 1).

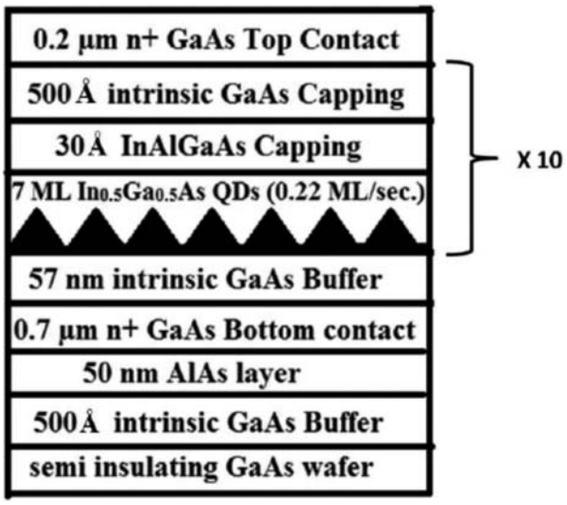

Fig.1. 10-layer n-i-n InGaAs/GaAs QDIP heterostructure used for proton implantation study.

Both the QD and combination capping were repeated for ten periods. With the purpose of improving the device performances of the InGaAs/GaAs QDIPs, the heterostructures were further implanted with 3 MeV protons of fluence varying between 2.0 x 10^{12} to 1.0 x 10^{13} ions/cm^2. A. Mandal et al. had already showed better device performances for In(Ga)As/GaAs QDIPs implanted with low energy hydrogen ions [1]. The present study is a further extension of the previous study with high energy protons. Both as-grown and implanted devices of 400 µm diameters were fabricated by conventional photolithography, wet etching and metal evaporation technique. At 77 K and at a bias of -0.75 V, the dark current density was reduced by three orders from ~7.0 × 10^{-4} A/cm^2 for as-grown device to ~2.0 × 10^{-7} A/cm^2 for device implanted with highest fluence (Fig. 2).

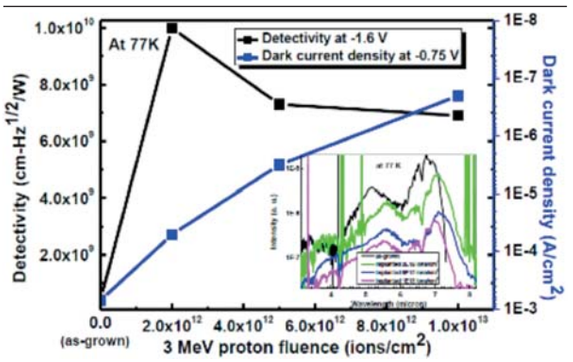

Fig.2. At 77 K, variation of dark current density and detectivity with fluence for as-grown and proton implanted devices; there was an enhancement in detectivity and reduction in dark current density for the devices implanted with high energy protons. Inset shows the spectral responses from as-grown and implanted devices at 77 K.

Suppression of field-assisted tunneling process of carriers was responsible for dark current reduction in implanted devices [2]. All the devices exhibited two colour spectral responses around 7.0 and 5.5 µm wavelengths at 77 K (inset of Fig. 2). At 77 K, increment in peak detectivity (D*) up to two orders of magnitude from 3.9 x10^8 to 1.0 × 10^{10} cm-Hz$^{1/2}$/W was obtained from the implanted devices at a bias of -1.6 V (Fig. 2). This is probably the first report about the effects of high energy proton implantations on the device performances of InGaAs/GaAs QDIPs. Riber, France and DST, India is acknowledged.

[1] A. MANDAL, A. AGARWAL, H. GHADI ET AL., APPL. PHYS. LETT. 102, 051105 (2013).
[2] A. D. STIFF-ROBERTS, X. H. SU, S. CHAKRABARTI, AND P. BHATTACHARYA, IEEE PHOTON. TECH. LETT. 16, 867 (2004).

Modelling of Intraband Absorption in Quantum-Dot-in-Well Mid-IR Photodetectors

Boon Hon Hong[1], Sergey I. Rybchenko[1], Igor E. Itskevich[1], Stephanie K. Haywood[1], Chee Hing Tan[2], Peter Vines[2], Maxime Hugues[3]*

[1]Dept. of Engineering, University of Hull, Cottingham Road, Hull, HU6 7RX, UK
[2]Dept. of Electronic & Elec Eng., University of Sheffield, Sheffield, S1 3JD, UK
[3]CRHEA-CNRS, Rue Bernard Grégory, 06560 Valbonne, FRANCE
*corresponding author: s.k.haywood@hull.ac.uk

Quantum-dot-in-well (DWELL) photodetectors offer benefits such as sensitivity to normal-incidence radiation, low dark current, gain and wide spectral range (3-12 µm for InGaAs/GaAs DWELLs). However, DWELL systems present a challenge for modelling of the electronic structure, because they combine discrete levels in the zero-dimensional QDs with continuous energy spectra in the 2D QWs. The Green's function method, often used for such problems, has a very high computational cost. Here, we use a simplified approach, simulating the 2D band structure in the QW by discrete levels in a large 3D 'quantum box'. We employ the finite element method within the effective-mass approximation with parameters taken from ref [1]. Perhaps the most useful result is that the composition of the InGaAs/GaAs dots - a parameter not readily available from other methods - can determined by comparison with simple PL spectra. The low computational cost means that intraband absorption spectra can be calculated for a wide range of compositions and shapes of QDs. Hence routine modeling can provide an efficient predictive tool for design of multispectral DWELL photodetectors.

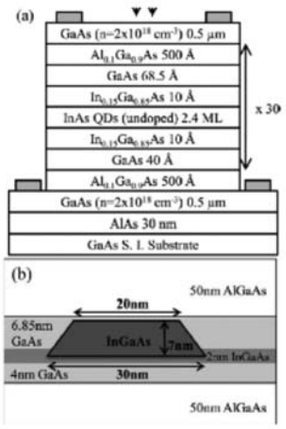

Fig 1: (a) the DWELL structure and geometry used for modeling.

For comparison with experiment, we used the InAs/GaAs/AlGaAs DWELL structure shown in Fig. 1(a).[2] The geometrical parameters of the QDs determined from TEM are given in Fig 1(b). TEM cannot distinguish between truncated cone (TC) or truncated pyramid (TP) QD shape; Hence we modelled both. Experimental PL spectra at 77K from the DWELL sample show a peak at 1.06 eV and a shoulder at ≈ 1.115 eV. The peak corresponds to a transition between the electron and hole ground states in the dot, while the shoulder corresponds to a transition between the first excited states. Regardless of TC or TP shape, the PL spectra could be fitted by an average In content in the dots of 73-75%.

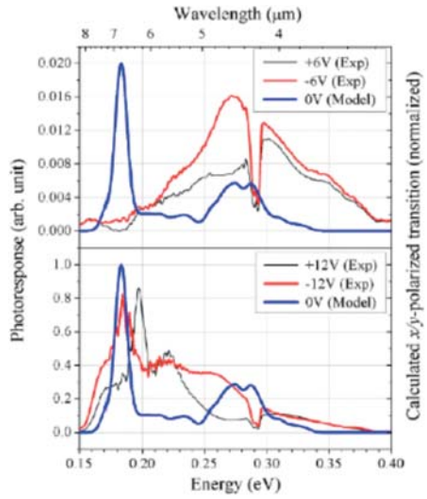

Fig 2: Photocurrent spectra obtained at (b) the 77 K under (a) low bias and (b) high bias.

The intraband absorption spectra were calculated for an $In_{0.75}Ga_{0.25}As$ QD of TC shape. The results are shown in Fig. 2. Absorption spectra were simulated and normal-incidence photocurrent measurements used for comparison (these correspond to in-plane (x/y) polarized light.) Fig. 3 shows the experimental spectra and modelled in-plane polarized absorption for 3-8 µm (0.12-0.4 eV) at 6V and 12V.

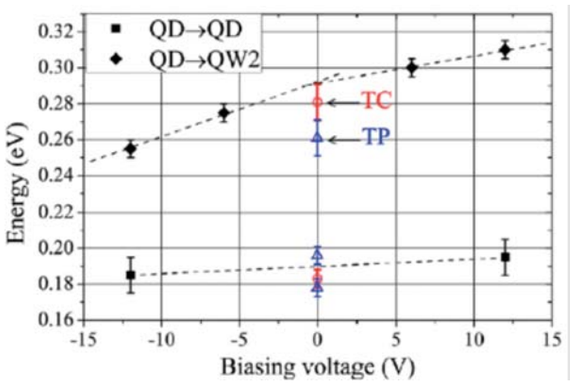

Fig 3: Peak energies as a function of bias. For non-zero voltages, experimental data are shown; for zero bias modelling, results are shown for In0.75Ga0.25As dots of both TC and TP shapes.

Fig.3 shows good agreement of the modelling results with the experimental data. In addition the energy of the experimental QD → QW2 peak strongly indicates TC shape of the dots, a parameter not readily obtained from other methods.

[1] I. VURGAFTMAN, J. R. MEYER, AND L. R. RAM-MOHAN, J. APPL. PHYS. 89, 5815 (2001).
[2] C.H.TAN, P.VINES, M.HOBBS, B.ANDERSON, M.HUGUES & J.P.R.DAVID, INFRARED PHYS.TECH. 54, 228 (2011)

High-temperature (~200K) Operation of p-i-p InAs/GaAs Quantum Dot Infrared Photodetectors

*M. S. Park[1], J. D. Song[1], H. S. Kim[1], S. H. Kim[1], H. Pettersson[2,3], Q. Wang[4], and W. J. Choi[1]**

[1]Center for Opto-electronic Convergence Systems, Korea Institute of Science and Technology (KIST), Hwarang-ro 14-gil 5, Seongbuk-gu, Seoul, 136-791, South Korea
[2]Center for Applied Mathematics and Physics, Halmstad University, P.O. Box 823, S-30118 Halmstad, Sweden
[3]Solid State Physics and the Nanometer Structure Consortium, Lund University, P.O. Box 118, S-22100 Lund, Sweden
[4]Acreo AB, Electrum 236, S-16440 Kista, Sweden
*corresponding author: wjchoi@kist.re.kr

InAs/GaAs quantum dot infrared photodetectors (QDIPs) have been extensively studied for photodetection in the mid-wavelength infrared (MWIR) and long-wavelength infrared (LWIR) ranges due to their distinctive properties arising from the three-dimensional carrier confinement [1-3]. Advantageous properties such as sensitivity to normal incident infrared radiation and the weak thermionic coupling between the ground state and excited states can be enjoyed by candidates for the next generation of infrared photodetectors (IPs). In the past few years, the intersubband photoresponses from n-type quantum dots structures have been the subject of intense research. However, hole transports originated from the intra-valence band transition in p-type QDIPs have recently attracted much attention due to not only the intermixing of heavy hole and light hole states enhancing the normal incidence absorption, but also the higher effective mass of holes lowering the dark current. These interesting properties make them suitable for realizing the high-temperature operating QDIPs, comparing to the n-type counterpart [3].

In this work, we successfully demonstrated high-temperature operating performances of p-i-p QDIPs composed of ten layers of self-assembled InAs dots embedded in $In_{0.15}Ga_{0.85}As$ asymmetric-well grown on GaAs substrate. Dark current of the fabricated p-i-p QDIPs can be suppressed by taking advantage of the dots-in-a-well (DWELL) structure and AlGaAs/GaAs superlattice layers. In order to improve the photoresponse of the devices, free carriers are introduced by inserting a p-type GaAs modulation doping layers in the vicinity of QDs. The photovoltaic behavior of the devices can be observed at MWIR region up to 200 K due to the built-in electric field by the strong asymmetric heterostructures.

Acknowledgement: This work was supported by the Agency for Defense Development (ADD) of Republic Korea and the KIST internal program.

[1] S. D. Gunapala, S. V. Bandara, C. J. Hill, at al., IEEE J. Quantum. Electron. 43, 230 (2007)
[2] L. HÖGLUND, K. F. KARLSSON, P. O. HOLTZ, H. PETTERSSON, AT AL., PHYS. REV. B 82, 035314 (2010)
[3] Y. F. LAO, S. WOLDE, A. G. U. PERERA, AT AL., APPL. PHYS. LETT. 103, 241115 (2013).

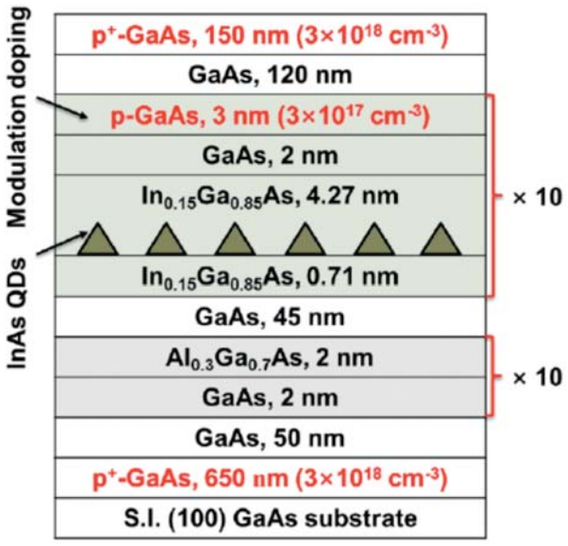

Fig.1. Schematic diagram of p-i-p type InAs/GaAs QDIP structure grown by molecular beam epitaxy (MBE)

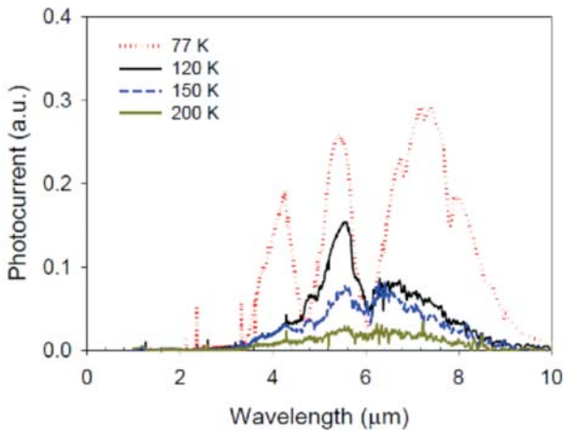

Fig.2. Temperature-dependent photo-responses of p-i-p type QDIP operating at photovoltaic-mode by utilizing Fourier transform infrared (FTIR) spectrometer system equipped with cryostat.

Enhancement in detectivity and temperature of operation in quaternary capped strain-coupled quantum dot infrared detectors by rapid thermal annealing

*H. Ghadi[1], S. Adhikary[1], S. Shetty[1], A. Balgarkashi[1], A. Manohar[1], and S. Chakrabarti[1]**

[1]Department of Electrical Engineering Indian Institute of Technology Bombay, Mumbai-400076, Maharashtra, India
*corresponding author: subho@ee.iitb.ac.in

InAs/GaAs based quantum dots infrared photodetectors (QDIPs) and focal plane array cameras have numerous applications in the field of military, astronomy and medical science. A multilayer detector structure in which strain coupling is present among the layers is known as coupled QDIP structure. Relatively thin spacer layer is used between the dot layers to make it vertically coupled. Also post growth rapid thermal annealing treatment is used to remove the as-grown defects, to check for the thermal stability in emission peak and to enhance the device performances.

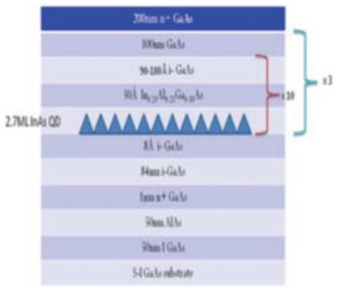

Fig. 1. 30 layer strain coupled quantum dot Heterostructures

In this paper we have reported a detailed investigation on the optical, electrical and spectral properties of annealed coupled QDIP heterostructure. The 30 layer strain coupled QDIP structures are grown by molecular beam epitaxy consists of 2.7 ML InAs QDs along with a combination of 30Å quaternary ($In_{0.21}Al_{0.21}Ga_{0.58}As$) and 120Å GaAs capping. Then the sample was subjected to rapid thermal annealing for 30 sec at four different temperatures – 650, 700, 750 and 800°C.

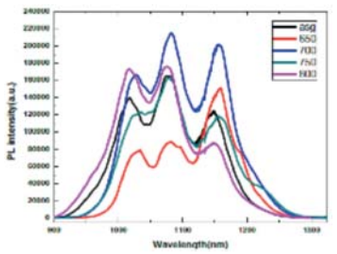

Fig. 2 Low temperature PL shows multimodal distribution of QDs

Low temperature PL spectra exhibit a multimodal distribution of the QDs in the as-grown as well as the annealed samples. Most importantly, with annealing there was no significant PL peak shift observed, indicating high thermal stability for coupled samples which is useful for laser applications. The n-i-n detector was fabricated by using two step photolithography, wet etching and metal evaporation technique with these samples. Dark current densities were measured at low temperature (80K) and were found to be minimum in 750°C annealed QDIP. The peak spectral response was observed at ~ 6.8 µm for all the devices. But most significantly, 5 times enhancement in photocurrent is observed for 750°C annealed QDIP compared to the as-grown, indicating improvement in device performance due to annealing.

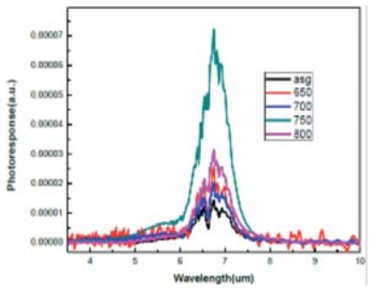

Fig. 3. Spectral response of all the samples measured at 80 K. 750°C annealed QDIP shows 5 times enhancement.

Maximum temperature of operation was 100K for as-grown sample but with annealing, increase in temperature of operation was also observed and for 750°C annealed QDIP a maximum operating temperature of 140K is attained.

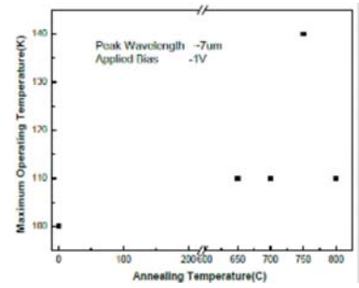

Fig. 4 Maximum operating temperature vs annealing temp of the coupled QDIP

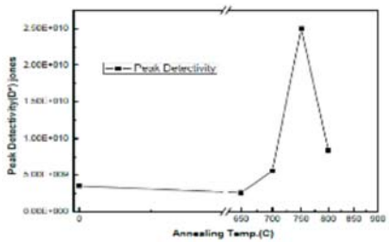

Fig. 5. Peak detectivity of as-grown and annealed QDIP. One order enhancement in D* is observed 750°C annealed QDIP.

One order enhancement in peak detectivity was observed for 750°C annealed QDIP compared to the as-grown and the measured value was ~$2.5E^{10}$ Jones. The as-grown defects and the trap states were probably minimized at optimized 750°C annealed temperature, which causes the improvement in device performance. *This is probably the first report where by using coupled structure, we have observed stability in PL peak and also enhancement in QDIP performance due to post growth annealing treatment.* DST, India and Riber, France are acknowledged.

Wednesday, 8 October

We-A

Materials

8:20-10:10

Designer Plasmonic Materials for Mid-Infrared Devices (invited)

S. Law[1,2], R. Liu[2], L. Yu[2], C. Roberts[3], V. Podolskiy[3], and D. Wasserman[2]*

[1]Department of Materials Science and Engineering, University of Delaware, 201 DuPont Hall, Newark, DE 19716 USA

[2]Micro and Nano Technology Lab, University of Illinois Urbana-Champaign, 208 North Wright Street, Urbana, IL 61801 USA

[3]Department of Physics and Applied Physics, University of Massachusetts Lowell, Lowell, MA 01854 USA

*corresponding author: slaw2@illinois.edu

The field of plasmonics has seen significant growth in recent years due to the interest in confining light to subwavelength volumes for applications such as enhanced sensing and nanoscale optoelectronics, which rely on the excitation of localized surface plasmon (LSP) and propagating surface plasmon polariton (SPP) modes. Much of this work has been done in the visible spectral range using traditional metals such as gold and silver. However, the mid-infrared spectral range offers much in the way of applied research in health, security, defense, and sensing. Unfortunately, traditional metals have extremely large and negative permittivities in the mid-IR, making excitation of LSPs and SPPs difficult or impossible [1]. Doped semiconductors offer an alternative [2,3]. The combination of small effective masses and high doping densities in materials such as InAs lead to tunable plasma wavelengths in the mid-infrared and enable plasmonic excitations [4]. In Fig. 1(a), the real part of the permittivity for silicon-doped InAs films is shown. The plasma wavelength (the point at which the real part becomes negative) can be tuned from 5.5 µm to 17 µm by changing the doping density. These materials can be grown using molecular beam epitaxy (MBE), resulting in high crystal quality, as demonstrated in Fig. 1(b), where the imaginary part of the permittivity is shown at the plasma frequency. These losses are comparable or better than those observed in traditional metal films at their plasma frequencies. Growth by MBE also enables the monolithic integration of semiconductor optoelectronics with infrared plasmonic structures.

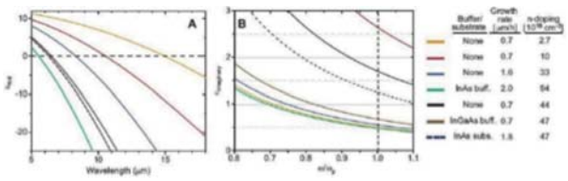

Fig. 1. (a) Real and (b) imaginary parts of the permittivity for silicon-doped InAs films grown with various doping densities, growth rates, and buffer layers, as indicated in the legend. The real part demonstrates the ability to tune the plasma wavelength from 5.5µm to beyond 17µm, while the imaginary part shows low losses as the plasma frequency for the correct choice of growth parameters. Figure from [1].

One example of a plasmonic device made from doped InAs is shown in Fig. 2. Nanoantennas of height ~200 nm and tunable radii from 160 nm- 210 nm were fabricated from Si:InAs films [5]. In Fig. 2(a), reflection from nanoantenna arrays fabricated from films with two different plasma wavelengths (A=5.5µm; B=6.2µm; C is undoped) is shown for both uncoated antennas and antennas coated with polymethylmethacrylate (PMMA). A clear antenna response is observed which depends on plasma wavelength and which shifts when the PMMA is applied, due to the difference in refractive index between PMMA and air. As shown in Fig. 2(c), when the nanoantenna resonance is spectrally aligned with molecular absorption lines in the PMMA, the molecular absorption is much more easily observed, due to the enhancement of the E-field around the antennas. This is one example of the way in which this materials system opens the door to improved mid-IR plasmonic architectures, which can be integrated with existing semiconductor optoelectronic devices.

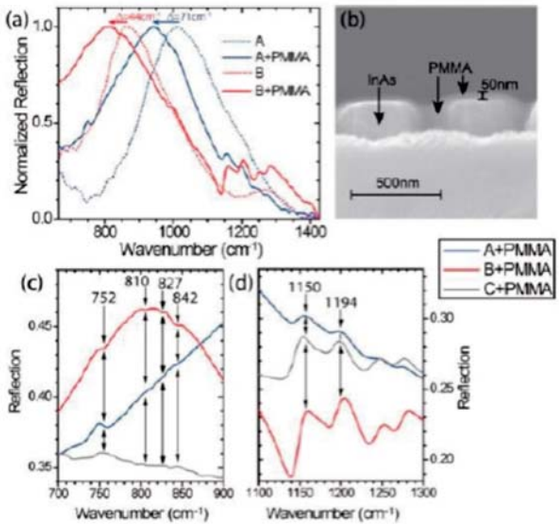

Fig. 2. a) Normalized reflection spectra for 200nm radius nanoantenna samples with two differing plasma wavelengths (A=5.5µm and B=6.2µm) before (dotted) and after (solid) coating with polymethylmethacrylate (PMMA). (b) Cross-sectional scanning electron microscope image of the PMMA-coated nanoantennas. Reflection spectra for nanoantenna samples coated with PMMA (c) in the range of nanoantenna resonance for sample B and (d) far from any nanoantenna resonance. The black arrows indicate the positions of the PMMA molecular absorption lines. The spectrum of sample C (nanoantennas fabricated from an undoped film) has been shifted vertically in panels (c) and (d) to aid in viewing. Figure from [5].

[1] S. LAW, V. PODOLSKIY, AND D. WASSERMAN, NANO PHOTONICS, 2, 103 (2013).
[2] J. C. GINN, R. L. JARECKI, E. A. SHANER, AND P. S. DAVIDS, J. APPL. PHYS. 110, 043110 (2011).
[3] M. SHAHZAD, G. MEDHI, R. E. PEALE, ET. AL., J. APPL. PHYS. 110, 123105 (2011).
[4] S. LAW, D. C. ADAMS, A. M. TAYLOR, AND D. WASSERMAN, OP. EX. 20, 12155 (2012).
[5] S. LAW, L. YU, A. ROSENBERG, AND D. WASSERMAN, NANO LETT. 13, 4560 (2013).

Mid-Infrared intersubband polaritons in dispersive metal-insulator-metal resonators

J-M. Manceau[1,], T. Ongarello[1], S. Zanotto[2], A. Tredicucci[2], G. Biasiol[3] and R. Colombelli[1]*

[1]Institut d'Electronique Fondamentale, Université Paris Sud, UMR8622 CNRS, 91405 Orsay, France
[2]NEST, Istituto Nanoscienze–CNR and Scuola Normale Superiore, Piazza S. Silvestro 12, I-56127 Pisa, Italy
[3]Laboratorio TASC, CNR-IOM, Area Science Park, Trieste I-34149, Italy
*corresponding author: jean-michel.manceau@u-psud.fr

In this work, we demonstrate room-temperature strong-coupling between a mid-infrared (λ=9.9 µm) intersubband transition and the fundamental cavity mode of a metal-insulator-metal resonator, as depicted in Figure 1a. This patterning of the resonator surface enables surface-coupling and introduces an energy dispersion which is probed with a Fourier transform infrared spectrometer over a large bandwidth (200 to 2000 cm^{-1}) and a wide angular range (13° < θ < 73°). The band-structure of a device with a grating period Λ of 3.83 µm in Figure 1(b). The lower dispersive branch of the transverse magnetic (TM) mode folded in the first Brillion zone is clearly observable. Importantly, the upper branch is now divided in two dispersive branches which correspond to the lower and upper polariton modes. The experimental results can be predicted using rigorous coupled wave analysis simulations (RCWA). Figure 1(c) shows the simulated polariton dispersion (continuous lines) superimposed onto the reflectivity minima as extracted from the experimental data (dots). Theory and experiment are in excellent agreement and - most importantly – the dispersion presents an energy minimum at *k//=0*.

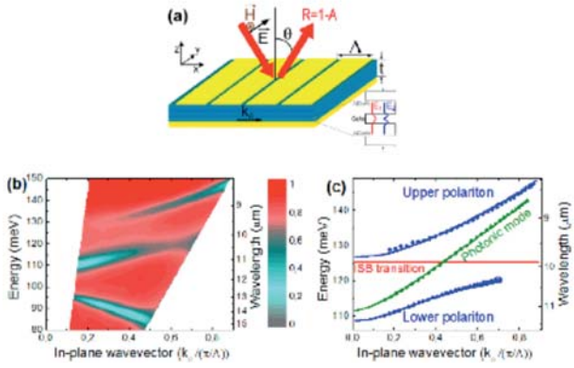

Figure 1: (a) Schematic representation of the mid-infrared quantum wells embedded in the dispersive metal-insulator-metal resonator. Λ is the period of the grating (3.83 µm) and t is the thickness of the active region equal to 1um. (b) Experimental band-diagram of the device (doping $n_{2d}=7.10^{11}$ cm^{-2}) with the apparition of the two polaritonic branch. (c) Dots are the extracted minimum reflectivity of the experimental data. A similar sample without doping was measured in order to get the photonic mode dispersion Solid lines are the modes dispersions simulated with the RCWA code.

This result is of particular importance since the polaritons could potentially accumulate at this minimum energy, which in turn could lead to stimulated scattering mechanisms as their excitonic counterparts [1] and the implementation of an inversionless laser [2].

We also show that it is possible to maximize the coupling of photons into the polaritonic states and - simultaneously – to engineer the position of the minimum Rabi splitting at a desired value of the in-plane wavevector as presented in Figure 2 (a,b).

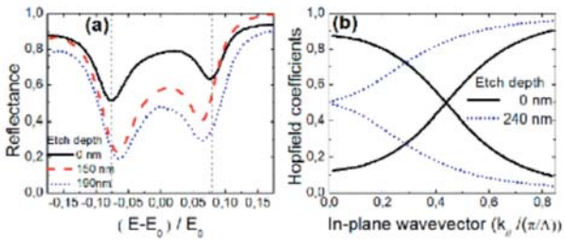

Figure 2: (a) Reflectance at the minimum splitting value for different etching depths. As expected from coupled mode theory the resonator which is initially under-coupled gets more and more light coupled within the polariton branch (the x-axis is renormalized by the ISB transition energy). (b) Hopfield coefficients of the polaritons as function of the in-plane wavevector. These coefficients gauged the weight of the photon/matter within the polaritons branch. The wavevector at which the evenly mixed polaritons occur can be brought to the dispersion minimum energy at k//=0.

This can be precisely accomplished via a simple post-processing technique based on the etching between the metallic fingers of the resonator grating [3]. The results are confirmed using the temporal couple mode theory formalism and their significance in the context of the concept of critical strong coupling will be highlighted. In conclusion, these results constitute an important step for future developments of long wavelength optically or electrically pumped polaritonic light emitting devices.

[1] H. DENG, G. WEIHS, ET AL., SCIENCE 298, 199 (OCT, 2002).
[2] S. DE LIBERATO, C. CIUTI, PHYS.REV.LETT. 102, 136403 (2009).
[3] J. M. MANCEAU, S. ZANOTTO, ET AL, APPL. PHYS. LETT. 103, 091110 (2013).

Superliner and High-Temperature Electroluminescence due to Impact Ionization in GaSb-based Heterostructures with a High Potential Barrier

Yu.P. Yakovlev[1], B.E. Zhurtanov[1], A.A. Petykhov[1], K.V. Kalinina[1], N.D. Stoyanov[1], H.M. Salikhov[1] and M.P. Mikhailova[1]*

[1]Ioffe Physico-Technical Institute, St. Petersburg, 194024, Russia
*corresponding author: Yakovlev@iropto.ioffe.ru

Heterostructures based on InGaAsSb solid solution are used to develop light-emitting diodes (LEDs) and photodiodes for the Mid-IR spectral range.

This work reports on a study of the electroluminescent properties(EL)of an anisotype n-GaSb/n-InGaAsSb/p-AlGaAsSb heterostructures in which the conduction-band offset at the n-GaSb/n-InGaAsSb heterointerface exceeds the threshold ionization energy of carrier in the InGaAsSb active region atthe high temperature range T=290-480K.

Heterostructure samples were fabricated by liquid-phase epitaxy an n-GaSb(100) substrate. The wide-gap-AlGaAsSb layer (Eg=1.28eV, T=300K) had a thickness of 0.5μm.The band offset ΔEc at the heteroboundary between n-GaSb and narrow gap n-InGaAsSb is equal to 0.79 eV, which several times exceeds the band gap of the narrow-gap layer (Eg~0.284 eV, T=300 K) (Fig.1).

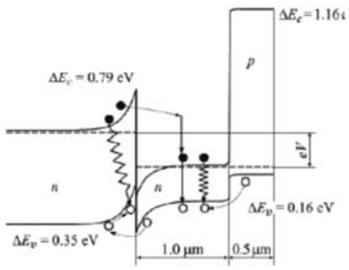

Fig.1. Energy-banddiagram of the isotype n-GaSb/ n-InGaAsSb/p-AlGaAsSb heterostructure.

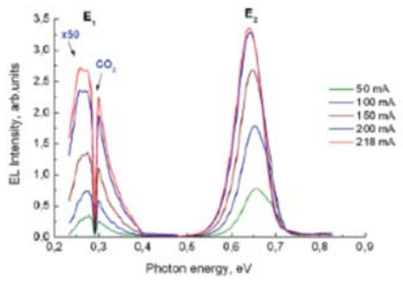

Fig.2. Electroluminescence spectra under forward bias.

Two peaks (Fig.2) are observed in the electroluminescence spectra of the anisotype structure at T=300 K. One peak is broad and is located in the longwavelength region at 0.28eV (E1)and the other peak (E2) is located at shorter wavelengths at 0.64eV. At room temperature, the optical power of the emission P=A*IB for band E2increased almost linearly with current (B=0.88), whereas the power of the band E1 increased superlinearly with the exponent B=1.54 (Fig.3).

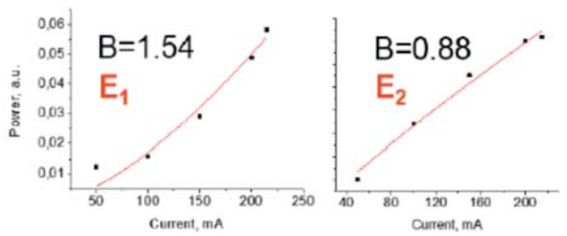

Fig.3. The dependences of the electroluminescenceunder forward bias.

The superliner dependence of the band E1can be explained as a result of impact ionization by hot electrons in the narrow gap of active layer (Fig.1). The impact ionization effect can be used to raise the quantum efficiency of Mid IR LEDs. Therefore, it is of interest to study the EL from LEDs based on type-II heterostructures with large conduction-band offsets, especially at elevated temperatures. In the structure under study the emission power P of the long-wavelength band increases with increasing temperature in the range of 290-350K (Fig.4, Fig.5). Further heating leads to linear rising of the emission power of E1 band.

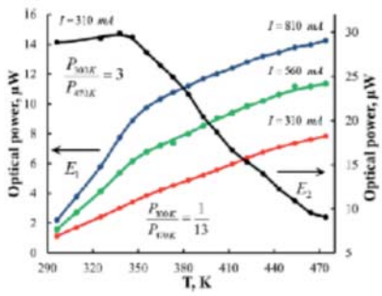

Fig. 4. Temperature dependence of the emission power P1 of the long-wavelength band at currents and that of the emission power P2 of the short-wavelength band at a current of 310 mA.

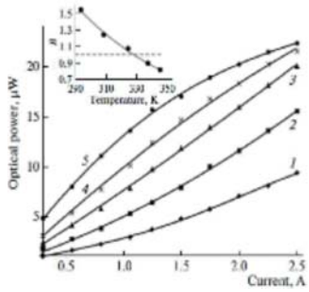

Fig. 5 Dependences of the emission power P1 of the long wavelength band on the pump current at temperature T = (1)294, (2)309, 53)325, (4)338, and (5)383 K. The inset shows the temperature dependence of the exponent B in approximation of the light-current characteristic of the long-wavelength band E1 with the power function PI = AIB.

It is shown that a superlinear increase of the output optical power with increasing temperature is caused by a decrease in the threshold energy of the impact ionization due to narrowing of the band gap of the active region. Firstly, we observed the transformation of impact ionization of carriers in radiative recombination at the heterostructure with a high potential barrier in the conduction band.

This work was supported by the project of the Presidium RAS №24 and contract No. 11705.004.11.001.

[1] N.D.STOYANOV, B.E.ZHURTANOV, A.P.ASTAKHOVA, A.N.IMENKOV AND YU.P.YAKOVLEV, SEMICONDUCTORS, 37, 878 (2003)

Emission Efficiency Enhancement in Mid-infrared In(AsN) by Rapid Thermal Annealing and Hydrogenation

M. Kesaria[1], A. Krier[1], Q. Zhuang[1], A.R. Marshall[1], A .V. Velichko[2], A. Patanè[2], S. Birindelli[3], M. De Luca[3], A. Polimeni[3] and M. Capizzi[3]*

[1]Physics Department, Lancaster University, Lancaster, LA1 4YB, UK
[2]School of Physics and Astronomy, University of Nottingham, Nottingham NG7 2RD, UK
[3]Dipartimento di Fisica and CNISM, Sapienza Università di Roma, Piazzale A. Moro 2, 00185 Roma, Italy
*corresponding author: a.krier@lancaster.ac.uk

The design and fabrication of optoelectronic devices operating in the mid-infrared spectral region requires a detailed knowledge and optimization of the structural and electronic properties of narrow-energy-gap semiconductors. Considerable attention has been paid to III-V dilute nitrides whose structural (lattice parameter) and electronic (carrier effective mass, energy gap, conduction band non-parabolicity, etc.) properties may be strongly tuned by the substitution of small percentages of group V atoms with N atoms [1-3].

In this work we report on substantial increases in the photoluminescence emission efficiency of In(AsN) dilute nitride alloys grown on both InAs and GaAs substrates in response to rapid thermal annealing and post-growth hydrogenation treatments.

In response to rapid thermal annealing, the photoluminescence emission efficiency at 4 K increased by 25 times (Fig. 1) due to a reduction in non-radiative Shockley-Read-Hall recombination originating from point defects. Rapid thermal annealing produced a small increase (of a few meV) in the 4 K bandgap with a negligible change in the photoluminescence linewidth. The activation energy for thermal quenching increased by a factor of three, but there was no change in the residual electron concentration or mobility for annealing temperatures up to 500°C. Temperature dependent photoluminescence together with X-ray diffraction measurements revealed an improvement in compositional uniformity.

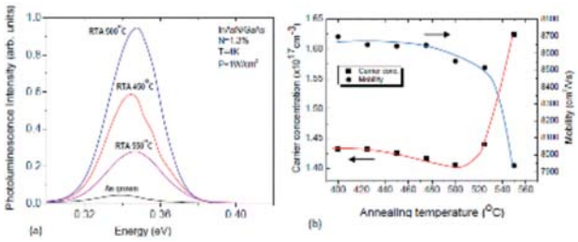

Fig.1. (a) The 4 K PL spectra of as grown and RTA In(AsN)/GaAs at different temperatures; (b) The variation in residual electron carrier concentration (left-axis) and mobility (right-axis) for In(AsN) in response to RTA treatments from 450-550°C in steps of 25°C.

Hydrogenation produced an increase in the PL intensity by almost two orders of magnitude in samples containing 1.1% of nitrogen atoms (Fig. 2). However, hydrogen does not seem to passivate the electronic activity of nitrogen. No recovery of the band-gap energy has been observed upon hydrogenation, contrary to what is found in other dilute nitrides such as Ga(PN), Ga(AsN), and (InGa)(AsN). However, hydrogen does passivate non-radiative recombination centers by forming complexes that are stable at temperatures as high as 300°C. These significant improvements in the optical efficiency should foster theoretical and experimental investigations of hydrogenated In(AsN), and the subsequent exploitation of this mid-infrared alloy.

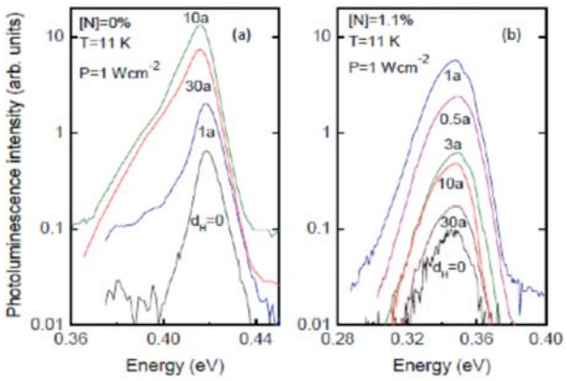

Fig.2. Low-temperature photoluminescence spectra at increasing H doses, *d*H, for (a): N-free InAs; (b) In(AsN) with [N]=1.1%. *d*H=1a=1×10[16] impinging ions/cm2. Note the semi-logarithmic scale.

Acknowledgments: This work was supported by EPSRC under grant EP/J015849/1 and by COST Action MP0805, EU (under grant agreement N° PIEF-GA-2010-272612) and Italian MIUR (under FIRB project DeLIGHTeD, Prot. RBFR12RS1W).

[1] E.P. O'REILLY ET AL., SEMICOND. SCI. TECHNOL., 24, 033001. (2009)
[2] N.V. KOSLOVA ET AL, PHYS. REV. B., 87, 65207, (2013)
[3] M. LATKOWSKA ET AL., APPL. PHYS . LETT., 102, 122109 (2013)

Nanostructures with InSb quantum dots/dashes in the n-InAs unipolar matrix

K. Moiseev[1], V. Romanov[1], P. Dement'ev[1], V. Nevedomsky[1], N. Bert[1], E. Ivanov[1]*

[1]Ioffe Institute, Politekhnicheskaya 26, St. Petersburg, 194021, Russia
*corresponding author: mkd@iropt2.ioffe.ru

The self-assembled InSb quantum dots (QDs) and quantum dashes (Q-dashes) were obtained on InAs(001) substrate by metalorganic vapour epitaxy. Bimodal distribution in a size of the InSb nanoobjects, low-density (5×10^7 cm^{-2}) large QDs with 20-40 nm in a height and high-density (7×10^9 cm^{-2}) small QDs with an average height of 4 nm, was observed [1]. Coherent small QDs with convex lens-like shape were found to be dislocation-free without any extended defects. The implications of these observations on a possible universal description of the Stranski–Krastanow growth mode are discussed with respect to obtained calculation results. Existence of striking similarities was revealed that extend even to the nature of island precursors and to the islands that form when depositing on binary InAs or quaternary InAsSbP surface of the matrix. Use of the InAsSbP matrix layers lattice-matched with InAs substrate resulted in the uniform distribution in a height of the InSb QDs under Stranski-Krastanow mode due to a considerable change of a surface chemistry [2]. The wetting layer thickness was dependent on matrix: 2 nm for the InAs surface and 1.3 nm for the InAsSbP one [3]. Transformation of the large QDs from a truncated pyramid formed by (111) planes and confined by (011) plane at the top to a multifaceted dome formed by (111) and (443) planes with octagon base was found out in dependence of matrix surface chemistry. The dome clusters with aspect ratio of 0.3 had flat top formed by (233) and (113) planes. A drastic change of the nano-objects geometry from QDs to Q-dashes in dependence on III/V ratio was observed [4]. The InSb Q-dashes with density of 2.5×10^9 cm^{-2} were self-oriented by 500 nm length along [110] direction. Heterostructures with the InSb QDs(Q-dashes) buried into the n-InAs unipolar matrix exhibited intense electroluminescence (3.34 μm at 77 K and 3.62 μm at 300 K) under both forward and reversed bias [5]. The blue shift of the EL peak from 3.34 to 3.22 μm with increasing of a drive current was observed at low temperatures. The interface-induced luminescence dominated for the nano-heterostructures and was comparable in intensity with interband EL in the n-InAs bulk (3.46 μm) at room temperature. Energy band diagram of the type II broken-gap InSb/InAs nano-heterostructure with localised states will be proposed and discussed. The heterostructures with the InSb QDs and Q-dashes buried into InAs-rich matrix are promising for emitters and detectors operating in the wavelength range of 3–5 μm that is important for mid-IR device engineering and biological applications.

This work was in part supported by the RBRF (grant #14-02-01102).

[1] N.A. BERT, V.N. NEVEDOMSKY, P.A. DEMENT`EV, K.D. MOISEEV, APPL. SURF. SCI. 267, 77 (2013).
[2] K. MOISEEV, V. ROMANOV, P. DEMENT'EV, M. MIKHAILOVA, J. CRYST. GROWTH 318, 379 (2011).
[3] K.D. MOISEEV, YA.A. PARKHOMENKO, V.N. NEVEDOMSKY, THIN SOLID FILMS 543, 74 (2013).
[4] V.V. ROMANOV, P.A. DEMENT'EV, K.D. MOISEEV, // SEMICOND. 47, 443 (2013).
[5] V.V. ROMANOV, E.V. IVANOV, K.D. MOISEEV SEMICOND. 48, 732 (2014).

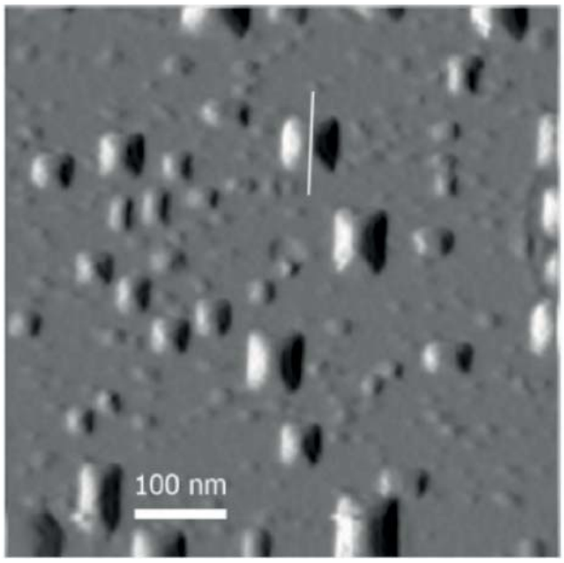

FIG.1. AFM topography images of 1x1 μm square surface of the samples with InSb QDs grown on the InAsSbP epilayer lattice-matched to InAs(001) substrate.

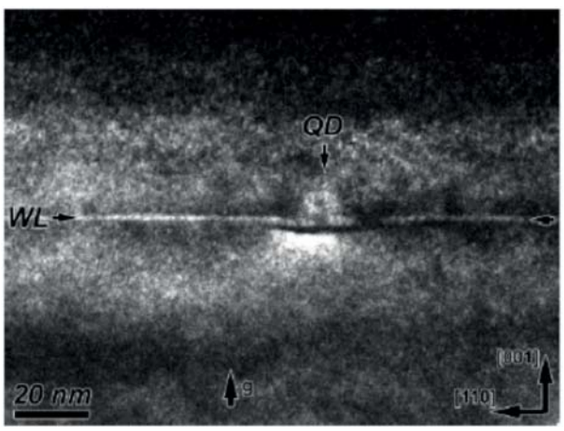

Fig.2. TEM dark-field image of (1-10) cross-section of the InAs/InAsSbP/InSb-QDs/InAsSbP heterostructure obtained under two-beam conditions with diffraction vector g=(002). Horizontal arrow indicates the position of the wetting layer at the heterointerface.

Wednesday, 8 October

We-B

Mid-IR Photo-detectors II

10:40-12:30

Mid-infrared Materials and Devices for Next Generation Neurophotonic Systems

*Sanjay Krishna[1]**

[1]Director, Center for High Technology Materials Professor and Regents' Lecturer, Department of Electrical and Computer Engineering, University of New Mexico, Albuquerque NM
*corresponding author: skrishna@chtm.unm.edu

Infrared imaging (3-25μm) has been an important technological tool for the past sixty years since the first report of infrared detectors in 1950s. The ability to detect the temperature of a scene from the blackbody radiation that it emits has spawned applications in a wide variety of fields ranging from defense and security to non-invasive medical diagnostics and remote sensing. However, IR imaging landscape has dramatically changed in the past decade. Firstly, the cost of lower end imagers has been steadily declining (30% every year since 2005) enabling them to be mounted on dashboards of automobiles including Audis and BMWs. Secondly, advent of novel antimonide based semiconductor technology has dramatically improved the performance of higher end imagers that are used for military, defense and security applications. Our group (www.chtm.unm.edu/kind) has been involved with the development of next generation infrared detectors and is one of two university laboratories that can undertake "Epi to Camera" research and realize focal plane arrays. Our research is currently focused along two directions. The first involves the fundamental investigation into quantum confined detectors and concepts such as metamaterials and plasmonics to realize the next generation of infrared detectors. The second involves the application of these detectors for biomedical diagnostics. In this talk, I will emphasize these two aspects of our research. Using the concept of a bio-inspired infrared retina[1], I will make a case for an enhanced functionality in the pixel. The key idea is to engineer the pixel such that it not only has the ability to sense multimodal data such as color, polarization, dynamic range and phase but also the intelligence to transmit a reduced data set to the central processing unit (Neurophotonics). I will use two material systems, which are emerging as promising infrared detector technologies as prototypes to highlight this approach. These are (i) InAs/InGaAs self assembled quantum dots in well (DWELL) hetereostructure and InAs/(In,Ga)Sb strain layer superlattices (SLS) Detectors. Various approaches for realizing the infrared retina, such as plasmonic resonators[2], will be discussed. I will also highlight the role of infrared imaging in non-invasive medical diagnostics. In particular, I will highlight some work on using infrared imaging in the early detection of skin cancer and the use of IR imaging for detection of flow in cerebral shunts.

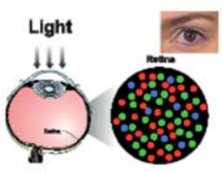

Acknowledgements: I wish to acknowledge my collaborators (Profs. Brueck/Hayat/Zarkesh Ha group at UNM, Dr. Ali Javey's group at Berkeley, Dr. Levan/Cardimona RVS group at AFRL, Prof. Painter's group at Caltech, Dr. Toni Taylor, Rohit Prasankumar, Aaron Gin at Center for Integrated Nanotechnology (CINT), Prof. Lin's group at RPI, Dr. S.K. Noh and Dr. S.J. Lee from Korean Research Institute of Standards and Science (KRISS), Dr. Ed Smith and Advanced Technology Group at Raytheon Vision Systems. This work would not have been possible with out the hard working members of the research group (Dr. E. Plis, Dr. Z.B.Tian, DDr. Greg von Winckel, Dr. Tom Rotter, Dr. J.O. Kim, J. Montoya, B. Klein, T. Sandy-Schuler, S. Godoy, M. Zamiri, A. Kazemi, L. Acosta, E. Dughie, T. Garwood, C. Kadlec, and F. Santiago). Work supported by AFRL, AFOSR, MDA, and NSF Biography of the Speaker:

[1] KRISHNA ET AL, INFRARED RETINA, US PATENT 8071945, 2011.
[2] S.J. LEE ET AL, NATURE COMMUNICATIONS, 2: 286 2011

Sanjay Krishna is the Director of the Center for High Technology Materials and Professor and Regents in the Department of Electrical and Computer Engineering at the University of New Mexico. Sanjay received his M.S. from IIT, Madras, MS in Electrical Engineering in 1999 and PhD in Applied Physics in 2001 from the University of Michigan. He joined UNM as a tenure track faculty member in 2001. He currently heads a group of 20 researchers involved with the development of next generation infrared imagers. Sanjay received the Gold Medal from IIT, Madras, Ralph Powe Junior Faculty Award, IEEE Outstanding Engineering Award, ECE Department Outstanding Researcher Award, School of Engineering Jr Faculty Teaching Excellence Award, NCMR-DIA Chief Scientist Award for Excellence, the NAMBE Young Investigator Award, IEEE-NTC and SPIE Early Career Achievement Award. He was recently awarded the UNM Teacher of the Year and the UNM Regents Lecturer award. Sanjay has more than 200 peer-reviewed journal articles (h-index=35), two book chapters and six issued patents and has recently been elected as an SPIE Fellow. He is the co-founder and CTO of SKINfrared, a UNM start-up involved with the use of IR imaging for non-invasive medical diagnostics including early detection of skin cancer. He is a fellow of IEEE and SPIE.

TCAD modeling and characterization of InAs/GaSb superlattice photodiode device for MWIR detection

M. Delmas[1,2], J. B. Rodriguez[1,2], P. Christol[1,2], J. Imbert[3,4], V. Trinité[3], J. Jaeck[4], S. Derelle[4], E. Giard[4], I. Ribet-Mohamed[4]*

[1]Univ. Montpellier, IES, UMR 5214, F – 34000, Montpellier, France
[2]CNRS, IES, UMR 5214, F – 34000, Montpellier, France
[3]III-VLab, 1 avenue Auguste Fresnel Campus Polytechnique, Palaiseau France
[4]Onera, Chemin de la Hunière et des Joncherettes , Palaiseau France
*corresponding author : marie.delmas@ies.univ-montp2.fr

Considering the significant progress achieved the last past years, the InAs/GaSb superlattice (SL) photodetector appears as an emerging infrared (IR) technology suitable for high performance imaging. However, up to now, their performances do not reach their theoretical capabilities. Consequently, for a better understanding of their current performances, it is necessary to develop accurate modeling of SL photodiode with realistic parameters deduced from characterizations performed on dedicated samples.

This communication is focused on the electrical performance analysis of InAs-rich SL photodiode, well suited for the midwave infrared (MWIR) domain [1]. To do that, the MWIR InAs-rich SL device has been modeled and simulated using ATLAS software from SILVACO. ATLAS is a commercially available device simulation software often used in the development of advanced semiconductor devices based on traditional material of the electronic industry. For the SL material, that is a periodic nanostructure comparable to a bulk material, the electronic and optical properties are strongly dependent of the InAs/GaSb period. Consequently, for a given SL period, it is necessary to define all the parameters used in the simulator. Some material parameters, such as effective masses, intrinsic carrier concentration or density of states, can be determined from accurate electronic band structure calculations. Another parameters, such as energy bandgap, absorption coefficient, carrier lifetime or residual doping of the active zone can be extracted from measurements.

The simulated InAs-rich SL structure is shown in Figure 1. The active zone is made of 7 monolayers (MLs) of InAs and 4 MLs of GaSb. The photodiode exhibits at 77K, a cut-off wavelength at around 5µm.

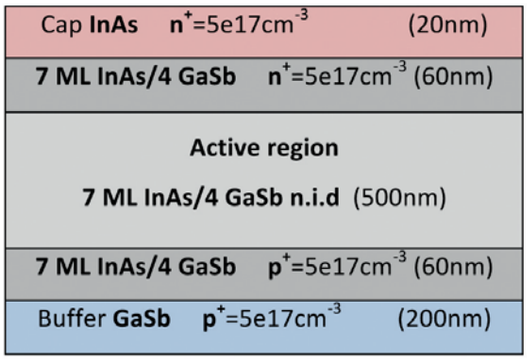

Figure 1 Simulated SL pin structure

In order to validate the parameters useful for the simulation, a set of four InAs-rich SL samples has been fabricated by molecular beam epitaxy (MBE) with an average period composition close to the one depicted in figure 1. The structures show slightly different bandgaps and the background carrier concentrations, measured by capacitance-voltage on diodes, are between $2x10^{15}$ cm^{-3} and $6x10^{15}cm^{-3}$. The carrier lifetime value at 77K was taken equal to 100 ns [2] for the four MWIR samples.

Figure 2 reports comparison between experimental current-voltage (J-V) characteristics and simulated J-V curves obtained by using the most appropriate input values for trap energy level (Etrap) and tunneling mass (mt).

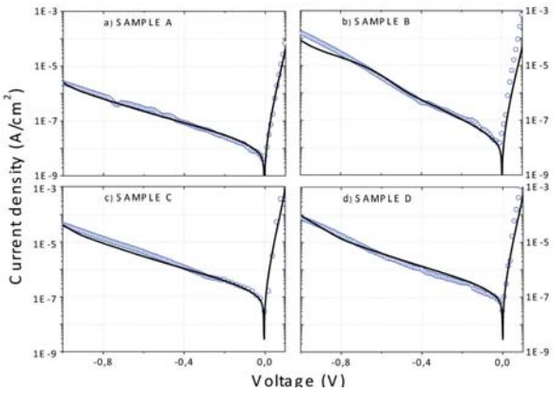

Figure 2 : Simulated (solid line) and experimental (open circle) J-V curves at T=77K for different MWIR SL samples

Next, the simulation of J-V curves at different temperatures was made for one sample (sample A) and compared to the measurements. mt and Etrap were kept constant while the lifetime was adjusted to fit the experimental curves. The simulated current density at -50mV are plotted in Figure 3. Lifetime values between 100ns and 50ns are obtained in the temperature range [77K-230K]. The variation of the lifetime follows a $T^{-1/2}$ law, which is the signature of SRH limitation [3].

In conclusion, TCAD simulation helps us to understand and analyze the electrical performances of the InAs-rich SL diodes.

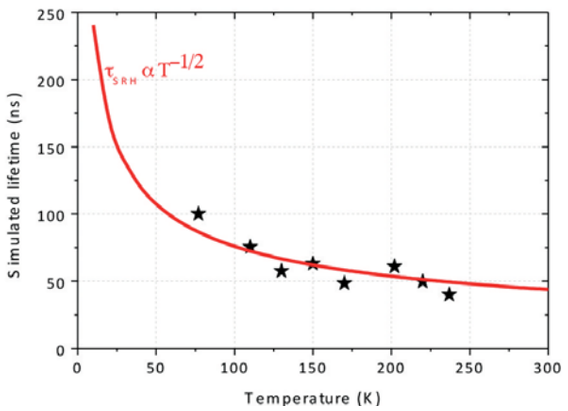

Figure 3 Simulated lifetime as a function of temperature (stars) and the T-1/2 law (solid line)

Acknowledgements : work supported by the french DGA

[1] R. Taalat et al J. Phys. D **47**, 015101 (2014).
[2] Svenson et al. J. Crystal Growth **334**, 103–107 (2011).
[3] B. C. Connelly et al Appl. Phys. Lett. **97**, 251117, (2010).

Mid-infrared InAsSb-based nBn photodetectors with AlGaAsSb barrier layers – grown on GaAs, using an interfacial misfit array, and on native GaSb

A. P. Craig[1], A. R. J. Marshall[1], Z.-B. Tian[2] and S. Krishna[2]*

[1]Physics Department, Lancaster University, Lancaster, LA1 4YB, UK
[2]Center for High Technology Materials, Department of Electrical and Computer Engineering, University of New Mexico, Albuquerque, New Mexico 87106, USA
*corresponding author: a.craig1@lancaster.ac.uk

nBn photodetectors virtually eliminate the Shockley Read Hall (SRH) and surface currents observed in p-i-n photodiodes. [1] The nBn bandstructure allows free passage to photogenerated holes, whilst preventing the flow of majority carriers, and hence suppressing the dark currents. An nBn detector structure was grown on GaAs, using an interfacial misfit (IMF) array, [2] and on native GaSb. At -0.1 V bias, 200 K dark current densities of $1.4x10^{-5}$ Acm^{-2} (GaAs) and $4.8x10^{-6}$ Acm^{-2} (GaSb), and D* figures of $1.2x10^{10}$ Jones (GaAs) and $7.2x10^{10}$ (GaSb) Jones, were calculated. These devices could support FPAs operating at 200 K, using cost-effective thermoelectric coolers.

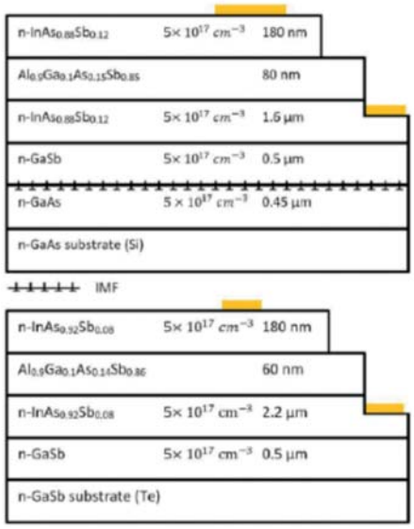

Fig.1. Layer structures for the two samples. Upper figure: detector grown on GaAs, using an IMF array, lower figure: detector grown on native GaSb.

The common layer profile is shown in Figure 1. The composition of the AlGaAsSb barrier layers allows for valence band offsets with the absorption and contact layers of ~20 meV, but a conduction band offset of > 1eV. The shunt resistance associated with the surface states is greatly increased through the processing, where the barrier layer is left unetched. Dark current measurements were carried out using a Lakeshore low-temperature probe station. D* figures were calculated based on temperature dependent responsivity measurements, taken on a custom-built low temperature probe station using fibre-coupled 1.55 µm laser. Arrhenius plots of the dark currents were made, as shown in Figure 2, and activation energies of 0.36 eV and 0.41 eV were calculated. These values are close to the bandgap of the absorption layers (0.32 – 0.35 eV), indicating diffusion limited dark currents and small valence band offsets. It is observed that the substitution of a GaAs substrate for a native GaSb substrate results in a similar level of performance. This may be explained in terms of the suppression of SRH currents by the nBn design; any remaining threading dislocations under the IMF growth mode then have little impact on the dark currents. Growth on GaAs is also cost-effective and, since GaAs is optically transparent in the mid-wave infrared, could allow for flip-chip mounted focal plane arrays supporting higher operating temperatures (HOTs).

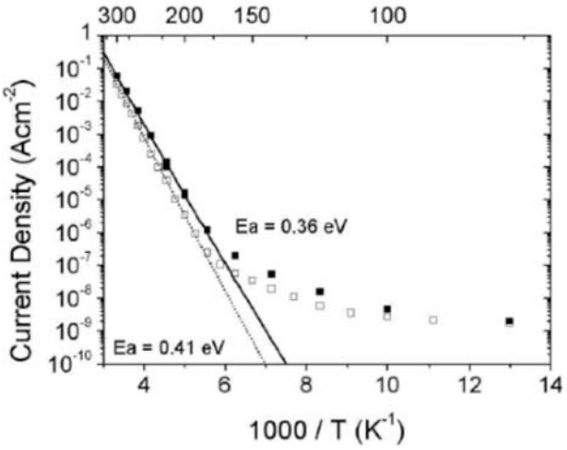

Fig.2. Arrhenius plots of the dark current density, (■) GaAs substrate, (L) native GaSb substrate. The activation energies were calculated (as shown) to be close to the bandgap of the absorption layers (0.32 – 0.35 eV).

[1] A. P. CRAIG, A. R. J. MARSHALL, Z.-B. TIAN, S. KRISHNA AND A. KRIER, APPL. PHYS. LETT. 103, 253502 (2013).
[2]] S. H. HUANG, G. BALAKRISHNAN, A. KHOSHAKHLAGH, A. JALLIPALLI, L. R. DAWSON, AND D. L. HUFFAKER, APPL. PHYS. LETT. 88, 131911 (2006).

Ultrafast (bandwidth 2-10 GHz) photodiodes for the 1.3-3.8 micron spectral range

I. Andreev[1], O. Yu. Serebrennikova[1], G. S. Sokolovskii1, E. V. Kunitsyna[1], V. V. Dudelev[1], G. G. Konovalov[1], N. D. Ilynskaya[1], M. P. Mikhailova[1], Yu. P. Yakovlev[1]

[1]Ioffe Physical-Technical Institute RAS, 194021, Politekhnicheskaya 26, St-Petersburg, Russia
*corresponding author: igor@iropt9.ioffe.ru

High-efficiency, broad bandwidth (2-10 GHz) GaInAsSb/GaAlAsSb and InAsSbP/InAs/ InAsSbP p-i-n photodiodes with air-brigde frontal contact operating in the 1.2-2.4 and 2.0-3.8 μm spectral range at room temperature have been developed for the first time. The broad bandwidth photodiodes make it possible to study fast processes in laser physics, nuclear physics, and physics of cosmic rays. These devices are also of great interest for long distance ranging, the free-space optical link, medicine.

A reproducible technique for the creation of the broad bandwidth photodiodes has been developed. The distinguishing feature of photodiodes with air-brigde frontal contact is separation of photosensitive and contact areas. A 50 μm diameter sensitive area of the photodiode and contact area as a 50× 70 μm rectangle was formed by wet etching. Thermal evaporated Cr-Au 2200 Å thick and CrAuNiAu ohmic contacts were applied to the p-GaAlAsSb top of each mesa and to the back of n-GaSb substrate, respectively. Frontal ohmic contact was as “air-bridge” form contact with 20 μm width and 85 μm length (Figure 1). This contact was added 3-6 μm thick galvanic Au. “Air-bridge” contact was isolated from contact area by Si3N4 dielectric layer. The best results on value capacity and reverse dark current were obtained for photodiodes with dielectic layer under frontal contact at contact mesa. The GaInAsSb/GaAlAsSb photodiodes demonstrated the capacitance as low as C=2.0-3.0 pF at reverse bias U= 0 V and C=0.8-1.0 pF at U=−(1-3) V, respectively.

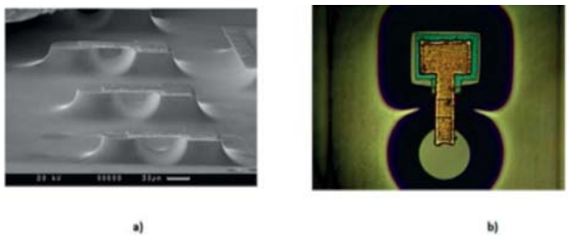

a) b)

Fig.1. a) Scanning electron microscope image of the photodiode with air- bridge frontal contact. b) Front view foto of the photodiode.

We have studied the spectral response characteristics of GaSb/GaInAsSb/GaAlAsSb photodiodes. The response current (ampere–watt) monochromatic sensitivity at λ = 2.1 μm amounted to Sλ = 0.9–1.15 A/W, which corresponded to a quantum efficiency of 0.6–0.7. The response speed of the p-i-n photodiodes was studied under conditions of their excitation by radiation pulses of a semiconductor laser operating at λ = 1.3 μm with a pulse full width at half maximum (FWHM) of 25 ps. Figure 2 shows the typical photoresponse waveform, from which it is seen that the output signal has a FWHM of about 220 ps. The photodiode response time is estimated at $t_{0.1-0.9}$=90–150 ps. The photodiode bandwidth of 2-10 GHz was reached. The photodiodes are characterized by low level of the reverse dark current (200-1500 nA at U=-(0.5-3.0) V), high monochromatic current sensitivity (1.10-1.15 A/W at λ=2.0-2.2 μm).

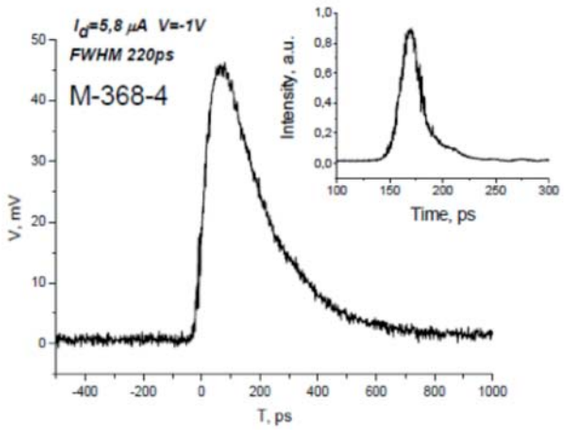

Fig.2. Responce of the GaInAsSb/ GaAlAsSb p–i–n photodiode irradiated by a laser pulse λ =1.3 μm (in the inset).

InAsSbP/InAs/InAsSbP p-i-n photodiodes are characterized by low level of the reverse dark current (10-30 μA at U=-(0.2-0.4) V), small value of the capacity (2-5 pF at U=-(0.2-0.4) V), high monochromatic current sensitivity (1.20-1.35 A/W at λ=3.0-3.3 μm). The response time of InAsSbP/InAs/InAsSbP p-i-n photodiodes will be measured in the coming months.

MidWave Infrared InSb Avalanche Photodiodes

J. Abautret[1,2,4], A. Evirgen[1,2,4], J.P. Perez[1,2], P. Christol[1,2], J. Rothman[3], R. Cluzel[4], A. Cordat[4]*

[1]Univ. Montpellier, IES, UMR 5214, F – 34000, Montpellier, France
[2]CNRS, IES, UMR 5214, F – 34000, Montpellier, France
[3]CEA-LETI, 17 rue des Martyrs, 38054 Grenoble Cedex 9, France
[4]SOFRADIR, BP 21, 38113 Veurey-Voroize, France
*corresponding author: johan.abautret@ies.univ-montp2.fr

InSb is the emblematic material for MWIR imaging applications. This material is particularly attractive for large format Focal Plane Array (FPA) fabrication due to a very good homogeneity on large substrates commercially available. It is also one of the most used MWIR detector technologies thanks to the stability of its performances. The next generation of IR FPA has to integrate new functionalities allowing high performance passive and active imaging for specific military applications. Among the new features, one can cite MWIR avalanche photodiodes (APD).

Currently, only two technologies have been reported for MWIR APD operation. The most successful is the HgCdTe II-VI material. It was the first technology showing a single carrier multiplication (SCM) allowing the possibility to obtain high gain without excess noise (F(M)<2), in the case of a multiplication process only initiated by the electrons (e-APD)[1]. These impressive results make this technology well suited for integration into next generation of FPA. More recently, it has been demonstrated the same behavior on InAs III-V material, with gain value higher than 10 without excess noise [2]. The cut-off wavelength of 3.05µm at 77K makes the InAs material as an alternative to the HgCdTe technology for active imaging applications.

This communication is focused on the InSb potentiality for the realization of APD devices. Firstly, we used a TCAD model, well adapted with experimental measurements, in order to explore the InSb PiN behavior (Fig.1) and define some designs favorable to the avalanche process in InSb photodiodes [3].

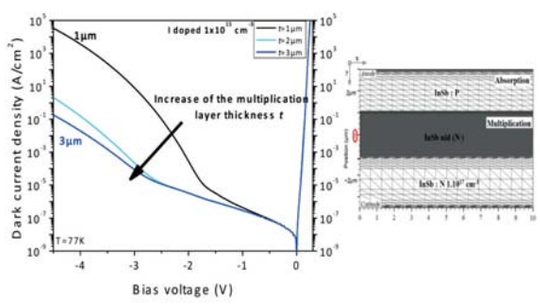

Figure 2. Simulated dark current density at 77K in function of the multiplication layer thickness t.

Then, we have fabricated SAM e-APD structures, by Molecular Beam Epitaxy (MBE) growth, with different multiplication layer thicknesses and characterized them both in dark conditions and under illuminations. State of the art dark current densities of 13nA/cm² was measured at 77K (Fig.2), signature of high material quality.

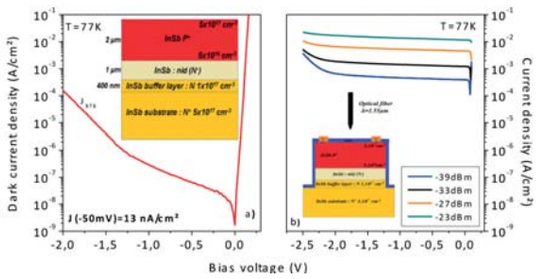

Figure 3. Current density in dark conditions (a) & under different illuminations (b) on InSb SAM e-APD (W=1.3µm) at 77K.

Illuminating the structures under different intensities at a wavelength of 1.5µm, useful gain values from 1.5 at -2V to 2.8 at -3V was extracted, increasing with the efficient multiplication layer thickness W from 1.3µm to 1.6µm (Fig.3). Those gain values at low bias voltage are compared with HgCdTe and InAs technologies (Table.1), demonstrating the potentiality of InSb as APD device.

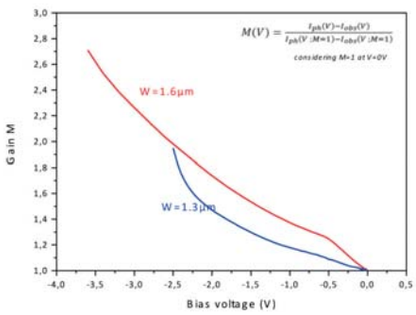

Figure 4. Gain measurement for two different multiplication layer thicknesses.

Material	InAs	HgCdTe	InSb
Cut-off wavelength λ(µm) at 77K	3.05	5	5.4
Efficient multiplication layer thickness W (µm)	2	1.5	1.6
Gain M(-3.5V)	2.2	4	2.8
Gain M(-5V)	3.6	10	

Table 1. Gain comparison between InAs, HgCdTe and InSb for identical multiplication layer thickness.

Several improvements have to be considered to enhance the gain value, in particular concerning the reduction of tunneling current at reverse bias. It will be the subject of further investigations on the way to use InSb technology as efficient system for active or dual mode IR imaging.

[1] G. Perrais, J. Rothman, G. Destefanis, J.P. Chamonal, Journal of Electronic Mat. 37, 1261 (2008).
[2] P.J. Ker, A.R.J. Marshall, A.B. Krysa, J.P.R. David et C.H. Tan, IEEE J. Quantum Electron. 47, 1123 (2011).
[3] J. Abautret, J.P. Perez, A. Evirgen, F. Martinez, P. Christol, et al, J. Appl. Phys. 113, 183716 (2013).

Wednesday, 8 October

We-C

New sources

13:30-15:40

Phase-Locked Multi-Terahertz High-Harmonic Generation by Dynamical Bloch Oscillations (invited)

M. Hohenleutner[1], O. Schubert[1], F. Langer[1], C. Lange[1], U. Huttner[2], D. Golde[2], T. Meier[3], M. Kira[2], S. W. Koch[2], and R. Huber[1]*

[1]Department of Physics, University of Regensburg, 93040 Regensburg, Germany
[2]Department of Physics, University of Marburg, 35032 Marburg, Germany
[3]Department of Physics, University of Paderborn, 33098 Paderborn, Germany
*corresponding author: matthias.hohenleutner@physik.uni-regensburg.de

Atomically strong multi-THz pulses with stable carrier-envelope phase (CEP) drive coherent interband polarization and dynamical Bloch oscillations in a bulk solid, resulting in the emission of a record-bandwidth, all-coherent high-order harmonic frequency comb. The spectrum continuously covers 12.7 optical octaves ranging from the microwave to the ultraviolet regime. Precise field shaping via amplitude and phase of the driving waveform allows for sensitive control of the microscopic dynamics and the shape of the high-harmonic spectra, as explained by a quantum many-body theory. The founding fathers of modern solid state physics pointed out that the quantum wave nature of crystal electrons should cause an intriguing quiver motion when the crystal is biased by a strong electric field [1,2]. Observing these so-called Bloch oscillations in bulk solids has been hampered by ultrafast carrier scattering and dielectric breakdown. Recently, high-harmonic (HH) generation after optical excitation has been attributed to a dynamical version of Bloch oscillations [3]. Here, electromagnetic waveforms with adjustable CEP and atomically strong fields [4] serve as a tailorable femtosecond bias for coherent high-field transport far beyond d.c. breakdown thresholds. Few-cycle transients centered at a frequency of 30 THz with peak fields of 72 MV/cm (Fig. 1a) off-resonantly drive coherent interband polarization and dynamical Bloch oscillations in undoped gallium selenide (GaSe) [5]. The transmitted waveform (Fig. 1b) reveals low-frequency as well as second harmonic components centered at 1 THz and 60 THz, respectively. The entire phase-stable HH-frequency comb contains intense harmonics up to the 22nd order, even exceeding the bandgap of GaSe (Fig. 1c). Our full quantum many-body theory based on Ref. 6 reproduces the measured spectra very well (Fig. 1c) and identifies Bloch oscillations in combination with coherent interband polarization as the microscopic origin of HH generation. Quantum interference of inter- and intraband dynamics via different carrier excitation pathways enables sensitive control of the emitted spectra (Fig. 1d, e) via amplitude and phase of the driving fields, in-line with the microscopic calculations [5]. Our results set a new record for ultrabroadband CEP-stable light sources in a previously elusive spectral range and may pave the way towards novel electronics at optical clock rates.

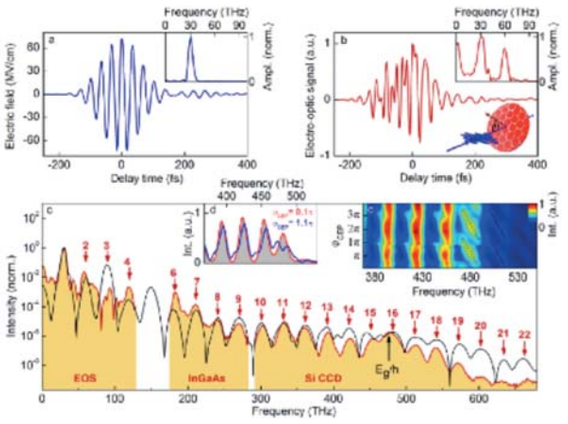

Fig. 1. a Electro-optically detected multi-THz transient with peak fields of 72 MV/cm in air, centered at 30 THz (inset). b Electromagnetic waveform generated in a 220 µm thick GaSe sample (θ = 70°) by the pulse shown in panel a, consisting of a superposition of fundamental, optically rectified and second harmonic components (insets: corresponding spectrum and experimental geometry defining the angle of incidence θ). c Phase-stable HH intensity spectrum (red curve) as detected by electro-optic sampling (EOS), an InGaAs and a Si detector array, respectively. The black line shows the calculated HH intensity obtained by a quantum-mechanical five-band model. (Eg: band gap energy of GaSe). d Measured HH intensity spectra generated by driving waveforms with carrier-envelope phases of ϕCEP = 0.1π (red) and 1.1π (blue). e Systematic dependence of HH spectra on the CEP of the transient. HH peaks of order n ≥ 15 shift in frequency with a slope of -2.5 THz rad-1 (indicated by the black dashed line), whereas lower orders are only slightly affected.

[1] F. BLOCH, Z. PHYS. 52, 555–600 (1928).
[2] C. ZENER, PROC. R. SOC. A 137, 696–702 (1932).
[3] S. GHIMIRE, A. D. DICHIARA, E. SISTRUNK ET AL., NATURE PHYS. 7, 138–141 (2010).
[4] A. SELL, A. LEITENSTORFER AND R. HUBER, OPT. LETT. 33, 2767–2769 (2008).
[5] O. SCHUBERT, M. HOHENLEUTNER, F. LANGER ET AL., NATURE PHOTON. 8, 119-123 (2014).
[6] D. GOLDE, M. KIRA, T. MEIER ET AL., PHYS. STATUS SOLIDI B 248, 863-866 (2011).

First Experimental Observations of External Optical Feedback Regimes in Mid-Infrared Quantum Cascade Lasers

L. Jumpertz[1,2], M. Carras[2], and F. Grillot[1]*

[1]Telecom ParisTech, Ecole Nationale Supérieure des Télécommunications, CNRS LTCI, 46 rue Barrault, 75013 Paris, France
[2]Alcatel Thales III-V Lab, Campus de Polytechnique, 1 avenue Augustin Fresnel, 91767 Palaiseau, France
*corresponding author: louise.jumpertz@telecom-paristech.fr

Optical feedback is studied experimentally in mid-infrared quantum cascade lasers. The response in those structures exhibits dynamical features as those observed in interband lasers. The light current curves present a clear threshold reduction and an enhancement of the output power with the feedback rate. Moreover, the optical spectra prove that the laser undergoes five distinct regimes depending on the phase and amplitude of the delayed field. Only the so-called coherence collapse regime differs from interband lasers. Its narrow range of observation combined with the absence of relaxation oscillations make quantum cascade lasers much more resistant against optical feedback.

Since they were invented twenty years ago [1], quantum cascade lasers (QCLs) developed quickly due to the large range of accessible wavelengths and to their numerous applications such as free space communications or gas spectroscopy. One of the main challenges is therefore to obtain a narrow linewidth to detect one single gas in small quantities. Optical feedback, ie. reinjection of the light emitted by the laser after reflection on a mirror or a fiber tip has been deeply studied in interband lasers [2], but there are few reports of this phenomenon in QCLs, mostly theoretical [3, 4]. Although this nonlinear effect can provide a stable, narrow linewidth source, it can also strongly alter the laser performances. The aim of this study is to provide first experimental observations of the dynamical regimes of optical feedback in a mid-infrared distributed feedback (DFB) QCL.

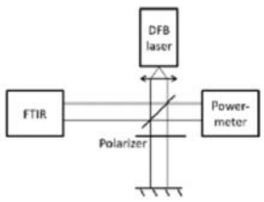

Fig.1. Experimental set-up for optical feedback. The external cavity can be tuned from 10 to 50 cm.

The QCL used for the experiments is a mid-infrared AlInAs/GaInAs DFB laser emitting at 5.6 µm. The active region consists in 30 periods and single-mode operation is obtained with a top metal grating. The chosen coupling efficiency is κ=4 cm^{-1} over a length of 2 mm, for a width of 9 µm. Anti-reflective and high-reflectivity coatings enable continuous-wave emission at room temperature. The experimental set-up is described in Figure 1. The laser light is split in a reinjection branch and a detection branch, where it is analyzed by a Fourier transform infrared spectrometer (FTIR) to obtain the optical spectra, with a 40 nm resolution. The feedback rate, ie. the ratio between reijected and emitted power, is tuned using a polarizer. Figure 2 shows the L(I) curves of the laser for several feedback rates. We observe a clear diminution of the threshold current, up to 4%, and a significant increase of the output power with the feedback ratio. The optical spectra were measured for different values of feedback rates. As shown in Figure 3, five regimes of optical feedback relatively similar to those observed in interband lasers can be identified. When increasing the feedback strength, the laser first remains on the DFB wavelength with an optical power and linewidth fluctuating with the phase of the delayed field. Then we observe a beating between the DFB mode and the first side-mode until the laser becomes locked on this side-mode. The next regime corresponds to coherence collapse. Although we did not observe a fully developed coherence collapse regime because of the limited FTIR resolution, this dynamical regime was associated to a substantial increase of the noise and apparition of side-modes. However, as opposed to interband lasers, the coherence collapse was observed on a very narrow window of operation beyond which the laser enters rapidly into the extended cavity regime and becomes single-mode again, with a very high optical power.

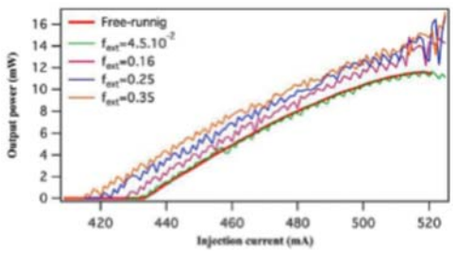

Fig.2. L(I) curve for several feedback levels fext, with a 13 cm long external cavity.

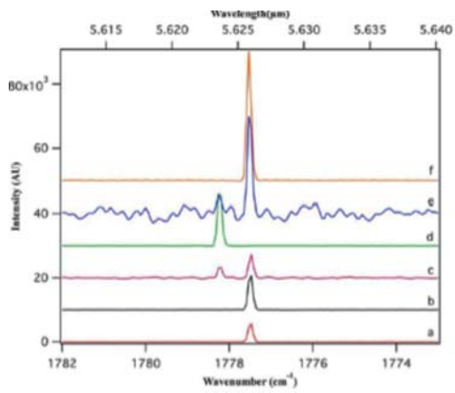

Fig. 3. Optical spectra for several feedback levels. The measurements were done for an external cavity length of 13 cm and an injection current of 435 mA: a) Free-running case. b) Regime 1, fext = 1.3×10^{-3}. c) Regime 2, fext = 2.2×10^{-3}. d) Regime 3, fext = 4.5×10^{-2}. e) Regime 4, fext = 0.18. f) Regime 5, fext = 0.35.

In conclusion, we have shown that a mid-infrared DFB QCL operating at room-temperature in continuous-wave does exhibit sensitivity to optical feedback and undergoes five regimes very similar to the ones observed in interband lasers. *Acknowledgments*: This work is supported by the French defense ministry (DGA).

[1] J. FAIST, F. CAPASSO, D. L. SIVCO ET AL., SCIENCE 264, 553 (1994)
[2] K. PETERMANN, JOURNAL OF SELECTED TOPICS IN QUANTUM ELECTRONICS VOL. 1, NO. 2, 480 (1995)
[3] F. P. MEZZAPESA, L. L. COLUMBO, M. BRAMBILLA ET AL., OPTICS EXPRESS VOL. 21, NO. 11, 13749 (2013)
[4] L. L. COLUMBO AND M. BRAMBILLA, OPTICS EXPRESS VOL. 22, NO. 9, 10105 (2014)

Robust dual-frequency laser for THz generation

R. Paquet[1,2], M. Sellahi[1,2], S. Blin[1,2], M. Myara[1,2], I. Sagnes[3], A. Garnache[1,2]*

[1]Univ. Montpellier, IES, UMR 5214, F-34000 Montpellier, France
[2]CNRS, IES, UMR 5214, F-34000 Montpellier, France
[3]Laboratoire de Photonique et de Nanostructures, UPR 20 CNRS, 91460 Marcoussis, France
*corresponding author: Stephane.Blin@univ-montp2.fr

Terahertz (THz) systems are attractive for many applications such as spectroscopy, communications, security or industrial monitoring. However, the advent of real systems is limited by the lack of adequate components, THz sources in particular. Indeed, coherent, tunable, and compact THz sources that deliver a significant power in a continuous-wave operation at room temperature are still not available. The photo-mixing of two laser lines using a non linear crystal, a uni-travelling-carrier photodiode or a photo-conductive switch is among the most adequate solution to ensure a coherent and tunable THz emission. If one can operate a single laser cavity at two frequencies, the stability of the THz beat note would be dramatically increased, as the two lines would share the same frequency noise. However, robust and stable operation of a dual-frequency laser is challenging due to the difficulty to manage laser dynamics, such as gain competition in a homogeneous-gain medium. Nevertheless, successful dual-frequency laser operations were reported, e.g. using two polarization modes [1], using two optical axis combined with spectral filtering [2], or by controlling the power of the two laser lines of a crystal by tilting one of the cavity mirrors [3]. We propose and demonstrate a new laser design based on a Vertical-external-Cavity Surface-Emitting Laser (VeCSEL), thus taking advantage of its inherent coherence (spatial, spectral, polarization) and possibly high output power [4]. Robust dual-frequency operation is reported in the sub-THz range by stabilizing two Laguerre-Gauss (LG) transverse modes using an integrated metallic mask [5] that adds spatially dependent losses. A diode-pumped GaAs-based quantum-wells VeCSEL presents a stable dual-frequency operation for the LG_{00} and LG_{02} modes, with a frequency difference of 162 GHz. The laser operates at room temperature at a wavelength around 1 µm with an output power of 35 mW for a pumping power of 325 mW. Both transverse modes coexist and operate on a single longitudinal mode. We show that spatial coupling of the two orthogonal modes is possible by injecting the laser beam in an offsetted single-mode optical fiber, with a beat efficiency that can exceed 20%. This work was supported by the French ANR *Micphir* program, and the French RENATECH network.

[1] A. ROLLAND ET AL., OPTICS EXPRESS 19(19), PP. 17944–17950 (2011).
[2] M. WICHMANN ET AL., PROC. SPIE 89660N (2014).
[3] F. PALLAS ET AL., APPLIED PHYSICS LETTERS 99, 241113 (2011)
[4] A. LAURAIN ET AL., OPTICS EXPRESS 14, 14631 (2010).
[5] M. SELLAHI ET AL., PROC. SPIE 89660U (2014).

Power scaling of high-brightness 2.X µm VECSEL

M. Rattunde[1], S. Kaspar[1], S. Adler[1], P. Holl[1], A. Bächle[1], C. Manz[1], R. Aidam[1], J. Wagner[1]*

[1]Fraunhofer-Institut for Applied Solid-State Physics, Tullastrasse 72, 79108 Freiburg, Germany
*corresponding author: marcel.rattunde@iaf.fraunhofer.de

Optically pumped vertical-external-cavity surface-emitting lasers (VECSEL, also known as semiconductor disk lasers, SDL) are attractive laser sources for many applications, as they simultaneously offer a multiple-Watt output power and an excellent beam quality [1]. The (AlGaIn)(AsSb) semiconductor materials system has been shown to be ideally suited to realize VECSELs for the 2-3 µm wavelength range [2,3]. Room-temperature multiple-Watt output powers have been demonstrated, making this laser source very attractive for applications such as medical therapy, materials processing and the use as pump laser for Ho-based solid state or OPO laser systems. For these applications, continuous-wave (CW) output powers in the 5-10 W regime are required from the 2.X µm VECSEL source.

In this contribution, we will present different strands for power scaling of the VECSEL devices and discuss the physics of the underlying limiting loss mechanisms.

An increase in output power and power efficiency was achieved recently by using a GaSb-based VECSEL structure with a reduced quantum deficit between pump-laser and VECSEL photon energy. The VECSEL structure was optimized for 1.5 µm barrier-pumping (compared to 980 nm pump light used before) which resulted in a maximum output power of over 7 W CW at 20°C and over 10 W CW at -10°C heatsink temperature for a single-chip linear cavity. In addition, the differential power efficiency reaches 30 % at 20 °C.

Besides thermal rollover, we could show that lateral lasing perpendicular to the vertical laser emission can occur as an unwanted optical loss mechanism that limits the maximum output power. The cleaved side facets of the VECSEL chip can form an optical cavity and provide optical feedback for amplifying the laterally spontaneous emission. We investigated the conditions for which lateral lasing occurs and demonstrate an effective means to suppress this unwanted phenomenon even for small VECSEL chip sizes.

Further power scaling, while conserving the good beam quality of the single-chip VECSEL, can be achieved by using multiple-chip VECSEL resonator setups. We have realized two- and three-chip cavities and have compared the resulting increase in modal gain on the one hand and in optical losses on the other. With these results we can explain the benefits but also the limits for this power scaling strand.

[1] M. KUZNETSOV ET AL., IEEE J. SEL. TOPICS IN QUANTUM ELECTRON. 5, 561 (1999).
[2] B. RÖSENER ET AL., IN „SEMICONDUCTOR DISK LASERS", ED. O. OKHOTNIKOV (WILEY-VCH, WEINHEIM, 2010), P. 143.
[3] A. OUVRARD ET AL., IEEE PHOTON. TECHNOL. LETT. 17, 2020 (2005).

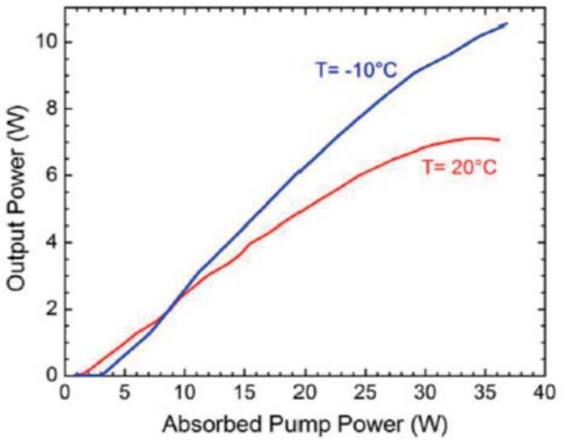

Fig.1. Output power characteristics of a 2.0 µm VECSEL at two different heatsink temperatures. The structure was designed for barrier-pumping at 1.5 µm, leading to a reduced quantum deficit (compared to 980nm pumping) and thus an increased power efficiency and output power of over 7 W at room temperature (10 W at -10°C) for a single-chip VECSEL resonator.

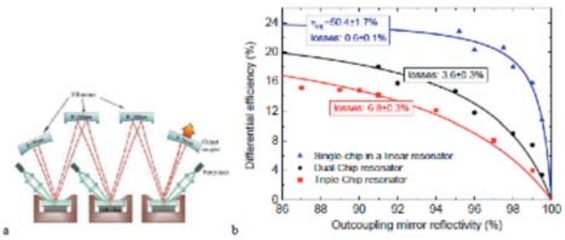

Fig.2. a) Schematic view of the multiple-chip VECSEL resonator for further power scaling. b) Differential efficiency vs. outcoupling mirror reflectivity for a single- double- and triple chip resonator. With this data, the internal losses and internal efficiency of the different setups can be deduced.

Tunable narrow-band CW MIR generator based on the difference frequency generation in KTP crystal

P. Honzatko[1], Y. Baravets[1], F. Todorov[1], P. Gladkov[1]*

[1]Institute of Photonics and Electronics, Academy of Sciences CR, Chaberska 57, 18251 Prague 8, Czech Republic
*corresponding author: honzatko@ufe.cz

We have developed a narrow-band CW MIR generator based on a difference frequency generation in a periodically poled KTP crystal. The crystal is used to mix the beams from high power master-oscillator power-amplifier (MOPA) systems working at 1060nm and 1550nm bands (Fig. 1), respectively. The generator operates in the range of 3150-3450 nm.

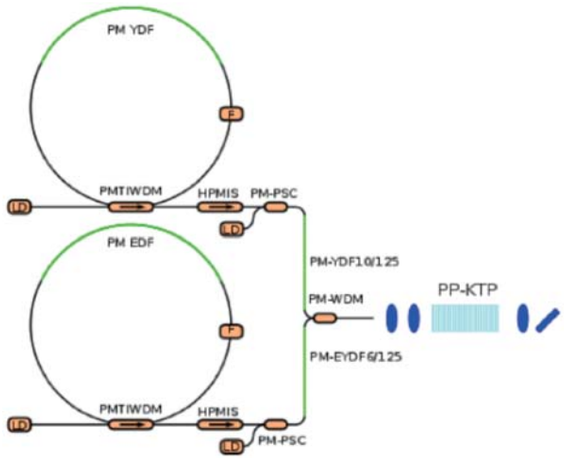

Fig.1. Experimental setup of the MIR generator.

The master-oscillators utilize a fiber ring configuration built of polarization maintaining (PM) components and fibers in order to achieve high stability and well defined polarization. Each of fiber lasers consists of an active fiber, a computer driven narrow band tunable filter and a hybrid fiber pigtailed optical component that integrates a WDM coupler, a polarizing isolator and an output coupler. The active fibers of master oscillators are core-pumped by laser diodes working at wavelengths of 976nm and 980nm, respectively. The master-oscillators are tunable in the spectral range of 1020-1089 and 1510-1590nm, respectively and their line-width is less than 0.03nm.

The signals at fundamental wavelengths are amplified in high-power amplifiers based on double-clad fibers pumped by multimode laser diodes by means of pump signal combiners. The pump is amplified in a PM ytterbium-doped double-clad fiber with geometry 10/125µm up to a power of 2W, while the signal is amplified by a PM erbium-ytterbium-doped double-clad fiber with geometry 6/125µm up to a power of 0.5W. The pump and the signal are combined in a fused biconic taper wavelength division multiplexer. The output pigtail of the multiplexer is equipped with an angle-polished connector to suppress the reflections from the end-facet of the fiber.

The z-axis polarized light from the output pigtail of the multiplexer is collimated by an antireflection-coated achromatic lens with an effective focal length of 4mm and then it is focused on the (y,z) face of the periodically-poled KTP crystal using an antireflection-coated achromatic doublet with a focal length of 75mm. The periodically-poled KTP crystal has a length of 16.5mm and is 1mm thick. The length of the periodically-poled pattern is 15mm. The unabsorbed pump at the output of the crystal is filtered by a germanium window. The generated signal is collimated by CaF_2 lens and detected by PbSe detector. The master-oscillators are synchronously tuned to achieve the targeted mid-infrared frequency while the phase-matching is maintained (Fig.2a). The tuning curves correspond well to the calculated values (Fig. 2b).

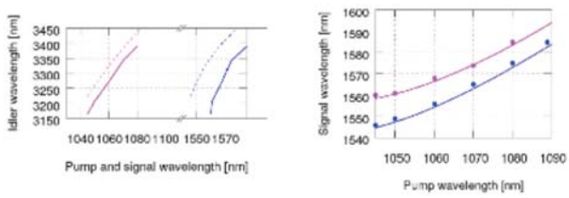

Fig.2. a) Dependence of the output wavelength on the pump and signal wavelength for PP- KTP crystal with a period of 36.1µm (solid line) and 35.9µm (dashed line). b) Phase matching conditions for PP-KTP crystal with a period of 36.1µm (magenta) and 35.9µm (blue).

We gratefully acknowledge funding of this work by the Technology Agency of the Czech Republic under Grant No. TA02010825 and by Ministry of Education, Youth and Sports under Grant No. LD14112 in the frame of the COST Action MP1204.

Nonlinear Fiber Mid-IR Sources

L.B. Shaw[1], R.R. Gattass[1], V.Q. Nguyen[1], G.D. Chin[2], I.D. Aggarwal[3] and J.S. Sanghera[1]*

[1]Naval Research Laboratory, Code 5623, Washington, DC, USA 20375,
[2]University Research Foundation, Greenbelt, MD, 20770
[3]Sotera Defense Solutions, Crofton, MD 21114
*corresponding author: brandon.shaw@nrl.navy.mil

Nonlinear processes such as stimulated Raman scattering, self-phase modulation, and four wave mixing can occur in fiber and waveguides. With correct fiber or waveguide design, these nonlinear processes can be enhanced and exploited to create sources. In this paper, we review on our work on development of mid-IR sources based upon nonlinear interactions in IR transmitting chalcogenide fiber. Work on broadband mid-IR supercontinuum sources, mid-IR Raman amplifiers and parametric sources will be reported.

We have demonstrated an all fiber based mid-IR supercontinuum source from 1.5 to 5 µm based upon As_2S_3 fiber and pumped by a near-IR pulsed fiber laser operating around 2.0 µm [1]. Broadband output with a spectral flatness of 10 dB from 1.9 to 4.4 µm and 20 dB from 1.65 to 4.8 µm was demonstrated as shown in Figure 1(a). The output power was 565 mW but scalable by scaling the repetition rate of the pump laser. A compact supercontinuum source based upon selenide based photonic crystal fiber (PCF) pumped by a Nd:YAG microchip laser pumped PPLN OPA operating at 3.8 µm has also been demonstrated [2]. Output spectrum extended from 3.74 to 4.64 µm at -10 dB from the peak and 3.65 to 4.9 µm at -20 dB from the peak as shown in Figure 1(b). Power scaling and extension of these sources to longer and broader wavelength coverage will be reported.

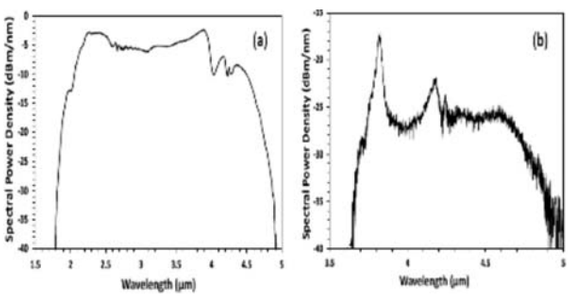

Fig.1. (a) Supercontinuum spectrum from 2 m length As_2S_3 fiber. Average output power was 565 mW (b) Measured output from 2 m length selenide based PCF pumped by PPLN OPA/Nd:YAG microchip laser. Average pump power was 5 mW.

Raman amplification in the mid-IR has also been demonstrated. In the Raman application process, lower wavelength pumps amplify longer wavelength signals for power scaling and wavelength conversion. With the availability of commercial quantum cascade and interband cascade lasers spanning the 4-12 µm as potential seed sources, we investigated the potential for seeded Raman amplification in the mid-IR at 4.6 µm. 15 dB of Raman amplification at 4.6 µm was demonstrated in an As_2S_3 fiber pumped by a PPLN OPO source as shown in Figure 2 below. Work on power scaling and high efficiency cascaded mid-IR Raman amplification will be reported.

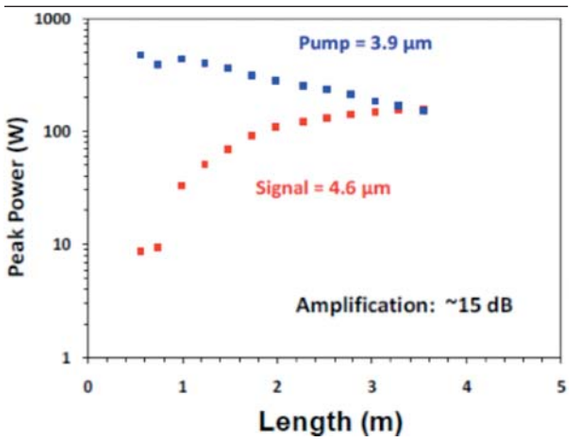

Fig.2. Peak power vs fiber length for pump (λ = 3.9 µm) and amplified signal (λ = 4.6 µm)

Parametric sources require precise control of the dispersion of the fiber to enable efficient four wave mixing. We have designed PCF fiber structures with engineered dispersion profiles to enable broadly tunable sources and frequency combs covering the mid-IR and long-wave-IR under near-IR laser pumping (Figure 3). Modeling and fabrication of these fiber and waveguide structures to enable these parametric sources will be reported.

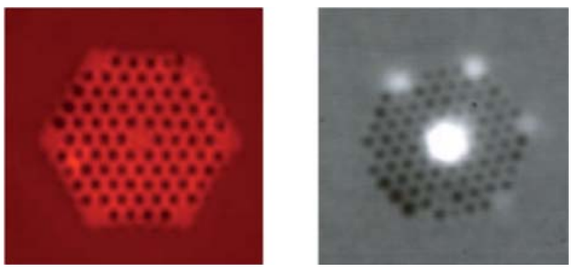

Fig. 3. As2S3 photonic crystal fiber structure

[1] R.R. GATTASS, L.B. SHAW, J.S. SANGHERA, ET. AL., OPT. FIBER. TECH, 18, 345 (2012)
[2] R.R. GATTASS, L.B. SHAW, J.S. SANGHERA., IN PRESS OPT. LETT, (20

AUTHORS